AFRL-RH-WP-TR-2017-0079

JET FUEL EXACERBATED NOISE-INDUCED HEARING LOSS: FOCUS ON PREDICTION OF CENTRAL AUDITORY PROCESSING DYSFUNCTION

Teresa R. Sterner
Peter J. Robinson
C. Eric Hack
Lining Qi
Latha Narayanan
Sarah T. Law
Henry M. Jackson Foundation
for the Advancement of Military Medicine
Bioeffects Division
Molecular Bioeffects Branch
Wright-Patterson AFB OH

Tammie R. Covington
Henry M. Jackson Foundation
for the Advancement of Military Medicine
Aeromedical Research Department
United States Air Force School of Aerospace Medicine
Wright-Patterson AFB OH

Elaine A. Merrill
Nadja Grobe
Dominique N. Brown
David R. Mattie
Bioeffects Division
Molecular Bioeffects Branch

September 2017

Final Report for Oct 2015 to Mar 2017

Air Force Research Laboratory
711th Human Performance Wing
Airman Systems Directorate
Bioeffects Division
Molecular Bioeffects Branch
Wright-Patterson AFB OH 45433-5707

NOTICE AND SIGNATURE PAGE

Using Government drawings, specifications, or other data included in this document for any purpose other than Government procurement does not in any way obligate the U.S. Government. The fact that the Government formulated or supplied the drawings, specifications, or other data does not license the holder or any other person or corporation; or convey any rights or permission to manufacture, use, or sell any patented invention that may relate to them.

This report was cleared for public release by the 88th ABW Public Affairs Office and is available to the general public, including foreign nationals. Copies may be obtained from the Defense Technical Information Center (DTIC) (http://www.dtic.mil).

Jet Fuel Exacerbated Noise Induced Hearing Loss: Focus on Prediction of Central Auditory Processing Dysfunction

(AFRL-RH-WP-TR-2017-0079) has been reviewed and is approved for publication in accordance with assigned distribution statement.

MATTIE.DAVID.R.1230101880
Digitally signed by MATTIE.DAVID.R.1230101880
Date: 2017.12.05 12:26:12 -05'00'

DAVID R. MATTIE
Work Unit Manager
Molecular Bioeffects Branch

MILLER.STEPHANIE.A.1230536283
Digitally signed by MILLER.STEPHANIE.A.1230536283
Date: 2017.12.05 18:36:27 -06'00'

STEPHANIE A. MILLER, DR-IV, DAF
Chief, Bioeffects Division
Airman Systems Directorate
711th Human Performance Wing
Air Force Research Laboratory

This report is published in the interest of scientific and technical information exchange, and its publication does not constitute the Government's approval or disapproval of its ideas or findings.

REPORT DOCUMENTATION PAGE

Form Approved
OMB No. 0704-0188

1. REPORT DATE *(DD-MM-YYYY)*	2. REPORT TYPE	3. DATES COVERED *(From - To)*
30-09-2017	Final	10/2015 – 03/2017

4. TITLE AND SUBTITLE
Jet Fuel Exacerbated Noise Induced Hearing Loss: Focus on Prediction of Central Auditory Processing Dysfunction

5a. CONTRACT NUMBER
FA8650-15-2-6608

5b. GRANT NUMBER
NA

5c. PROGRAM ELEMENT NUMBER
62202F

6. AUTHOR(S)
Sterner, Teresa R.[1]; Robinson, Peter J.[1]; Hack, C. Eric.[1]; Qi, Lining[1]; Narayanan, Latha[1]; Law, Sarah T.[1]; Covington, Tammie R.[2]; Merrill, Elaine A.*; Grobe, Nadja*; Brown, Dominique N.*; Mattie, David R.*

5d. PROJECT NUMBER
H0FS

5e. TASK NUMBER
H0

5f. WORK UNIT NUMBER
H0FS3003

7. PERFORMING ORGANIZATION NAME(S) AND ADDRESS(ES)
[1]HJF, 2728 Q St, Bldg 837, WPAFB OH 45433-5707
[2]HJF, 2510 Fifth Street, Bldg 840, WPAFB OH 45433-7951
*711 HPW/RHDJ, 2728 Q St, Bldg 837, WPAFB OH 45433-5707

8. PERFORMING ORGANIZATION REPORT NUMBER

9. SPONSORING/MONITORING AGENCY NAME(S) AND ADDRESS(ES)
Air Force Materiel Command*
Air Force Research Laboratory
711th Human Performance Wing
Airman Systems Directorate
Bioeffects Division
Molecular Bioeffects Branch
Wright-Patterson AFB OH 45433-5707

10. SPONSOR/MONITOR'S ACRONYM(S)
711 HPW/RHDJ

11. SPONSORING/MONITORING AGENCY REPORT NUMBER
AFRL-RH-WP-TR-2017-0079

12. DISTRIBUTION AVAILABILITY STATEMENT
Distribution A: Approved for public release; distribution unlimited. (PA Case No 88ABW-2017-6190, 11 Dec 2017)

13. SUPPLEMENTARY NOTES

14. ABSTRACT
Multiple laboratory rat studies link JP-8 jet fuel exposure to enhanced noise induced hearing loss (NIHL). Further, JP-8 jet fuel exposure, with and without noise, has been found to result in central auditory system dysfunctions in rats. Aircraft pilots, technicians and maintenance crews have frequently shown increased hearing loss. The overall objective of this project was to develop a multi-scale model, together with relevant supporting experimental data, to describe jet fuel exacerbated noise induced hearing loss. *In vitro* experiments were used to measure oxidative stress in cell lines representative of the auditory pathway. A novel mixtures exposure physiologically-based pharmacokinetic (PBPK) array model was designed to describe hearing loss target tissues along the peripheral and central auditory pathways. Partition coefficients (PC) were measured for five JP-8 jet fuel hydrocarbon components in cochlea, brain stem and temporal lobe tissues. Tissue composition (water, protein, fat types) was characterized for hearing target tissues. A mathematical model of a simple neuronal circuit in the dorsal cochlear nucleus was developed and a model of synaptic neurotransmitter kinetics was designed. These models may be linked together in future efforts to describe a JP-8 component exposure resulting in neurotransmission alterations.

15. SUBJECT TERMS
pharmacokinetic, pharmacodynamics, models, hearing loss, JP-8, jet fuel, exposure

16. SECURITY CLASSIFICATION OF:			17. LIMITATION OF ABSTRACT	18. NUMBER OF PAGES	19a. NAME OF RESPONSIBLE PERSON
					D. R. Mattie
a. REPORT	b. ABSTRACT	c. THIS PAGE			19b. TELEPONE NUMBER (*Include area code)*
U	U	U	SAR	128	NA

Standard Form 298 (Rev. 8-98)
Prescribed by ANSI-Std Z39-18

THIS PAGE INTENTIONALLY LEFT BLANK.

TABLE OF CONTENTS

LIST OF FIGURES

LIST OF TABLES

THIS PAGE INTENTIONALLY LEFT BLANK.

PREFACE

Primary funding for this project was provided through the Air Force Office of Scientific Research (AFOSR) Laboratory Research Initiation Request (LRIR) 14RH09COR, under the program management of Pat Bradshaw, PhD (AFOSR/RTB). Partial funding was also provided by the Aerospace Toxicology Program in the Air Force Research Laboratory, 711th Human Performance Wing, Airman Systems Directorate, Bioeffects Division, Molecular Bioeffects Branch (711 HPW/RHDJ).

This research was conducted under contract FA8650-10-2-6062 with the Henry M. Jackson Foundation for the Advancement of Military Medicine (HJF). The program manager for the HJF contract was David R. Mattie, PhD (711 HPW/RHDJ), who was also the technical manager for this project.

The study "Fischer 344 Rat (*Rattus norvegicus*) Pilot Pharmacokinetic Study for Jet Fuel in the Hearing Pathways" was approved by the Wright-Patterson Air Force Base (AFB) Installation Animal Care and Use Committee (IACUC) as protocol number F-WA-2015-0159-A. The study was conducted in a facility accredited by the Association for the Assessment and Accreditation of Laboratory Animal Care (AAALAC), International, in accordance with the Guide for the Care and Use of Laboratory Animals (NRC, 2011). The study was performed in compliance with DODI 3216.1.

The authors would like to acknowledge LTC Karyn Armstrong (Attending Veterinarian) and the Wright-Patterson AFB Vivarium staff of the U.S. Air Force 711 Human Performance Wing (711 HPW/RHDV), who provided the daily efforts necessary for animal husbandry.

THIS PAGE INTENTIONALLY LEFT BLANK.

1.0 SUMMARY

Multiple laboratory rat studies have supported JP-8 jet fuel's role in enhancing noise-induced hearing loss. JP-8 jet fuel exposure, with and without noise, has been found to result in central auditory system dysfunctions in rats. Across the world, aircraft pilots, technicians and maintenance crews have frequently shown increased hearing loss, often assumed to be the product of noise alone. However, a preliminary epidemiology study found that jet fuel exposure apparently resulted in increased hearing loss in military workers, as compared to military exposure to noise alone.

The overall objective of this project was to develop a multi-scale model, together with relevant supporting experimental data, to describe jet fuel exacerbated noise-induced hearing loss. Such hearing loss has been attributed to the effects of oxidative stress as well as disruption of signaling along the auditory pathway. The efforts toward completion of this objective can be broken down into three goals. The first goal was to utilize *in vitro* experiments to measure oxidative stress in cell lines representative of the auditory pathway. Second, the goal was to develop a physiologically-based pharmacokinetic (PBPK) model capable of describing the tissue dose of JP-8 components along the peripheral and central auditory pathways. The third goal was to design a cellular network model that focuses on disruption of the excitatory and inhibitory synaptic connections along the auditory pathway.

Goal 1: Three cochlear cell lines demonstrate sensitivity to JP-8 induced lipid peroxidation and glutathione depletion. However, a clear dose response for lipid peroxidation and glutathione depletion in any of the three cell line cultures was not evident. The lack of consistent dose/response relationships may be indicative of a problem with delivery of volatile chemicals to the cells.

Goal 2: To facilitate building a PBPK model to describe five JP-8 key hydrocarbons, partition coefficients (PCs) for hearing pathway target tissues were measured. Further, to allow for future prediction of Air Force relevant chemicals in the PBPK model, tissue composition (water, protein, fat types) was characterized for hearing target tissues. This composition information can be utilized to calculate PCs without animal use.

Using these data and literature values, an existing PBPK model was expanded and parameterized to include cochlea, brainstem and temporal lobe compartments. In order to streamline the addition of these tissues, the model was first re-written in an array format, allowing the addition of only one set of code per tissue, instead of five sets of code corresponding to each key hydrocarbon per tissue added. The parameterized model was then utilized to estimate concentrations of the key hydrocarbons in cochlea, brain stem, temporal lobe, and the remaining brain tissue for an inhalation exposure to 1000 mg/m^3 JP-8. These predictions indicate the anticipated levels of detection needed to measure the key hydrocarbons in these tissues in a pharmacokinetic experiment using this exposure scenario.

Goal 3: A mathematical model of a simple neuronal circuit in the dorsal cochlear nucleus was developed. The dorsal cochlear nucleus is located on the dorso-lateral surface of the brainstem and is the site of the first synapse for the auditory nerve fibers after transmission from the

cochleae. The model includes the following attributes: frequency coding of signal intensity, saturation of receptors at high signal intensities, and longer term alterations in signal processing mediated by changes in receptor densities at the synapse. Additionally, a model of synaptic neurotransmitter kinetics was designed. The resulting pre-synaptic neuron input signal intensity can be linked with neurotransmitter levels at its axonal output. Using receptor occupancy modeling, this neurotransmitter level then determines the response of the post-synaptic neuron, and signal transmission along the central auditory pathway.

Models from Goals 2 and 3 may be further validated and linked together in future efforts. This composite model would describe a JP-8 component exposure resulting in neurotransmission alterations at the dorsal cochlear nucleus.

2.0 INTRODUCTION

Excessive noise is known to induce hearing loss through hair cell functional deficits and death in the cochlea. Hair cell loss has been associated with oxidative stress in several publications (Fechter, 2005; Henderson *et al.*, 2006; Poirrier *et al.*, 2010). Similarly, multiple laboratory studies have supported JP-8 jet fuel's role in enhancing noise-induced hearing loss (NIHL) (Fechter *et al.*, 2007, 2010, 2012). The initial hypothesis that JP-8 jet fuel and noise exposure both produce oxidative stress in cochlear tissues, resulting in hearing loss when the oxidative stress exceeds glutathione reserves, was explored with the use of a mathematical model (Robinson *et al.*, 2013, 2015).

Recent work by Guthrie *et al.* (2014) indicated that JP-8 jet fuel exposure, with and without noise, resulted in minimal effects on peripheral auditory systems. However, this publication showed clear central auditory processing dysfunctions from JP-8 exposure, both with and without co-exposure at regulatory settings of safe levels of noise (85 dBA). *In vitro* studies published in Robinson *et al.* (2015) mirrored the relative lack of JP-8 toxicity in cochlear cells. Therefore, it was concluded that peripheral auditory system deficits are not the most sensitive outcome with JP-8 exposure even when combined with noise, particularly for relatively short term and low concentration exposures. Focus then turned to the diminished brain stem signaling findings as a likely more sensitive toxicological endpoint involving central auditory processing dysfunction.

The jet fuel JP-8 is a kerosene-range petroleum fuel currently utilized as the single fuel for land-based operations by the U.S. Armed Forces (Stucker *et al.*, 1994) and NATO forces (Work, 2011). Across the world, aircraft pilots, technicians and maintenance crews have frequently shown increased hearing loss; often assumed to be the product of noise exposures within their work environment alone. Swedish commercial aircraft technicians and mechanics develop hearing loss at relatively young ages, when compared to reference populations (Smedje, 2011). In France, military fighter, transport and helicopter pilots were all found to be at higher risk for developing hearing loss; helicopter pilots were more likely to experience losses at frequencies that compromise verbal communication (Raynal *et al.*, 2006). Similarly, 32 to 47 percent of Thai helicopter pilots, aircrew, aircraft technicians and mechanics have all been found to have persistent hearing loss. Noise, measured at 91 to 110 dBA in cockpit and around the helicopter, is consistently a hazard near these aircraft (Jaruchinda *et al.*, 2005).

However, a preliminary epidemiology study found that fuel exposure (JP-8 or its predecessor, JP-4) apparently resulted in increased hearing loss in military workers, as compared to military exposure to noise alone. The fuel exposures were determined to be under each respective jet fuel occupational exposure limit (OEL) and noise ranged from under the action level (<85 dBA, time weighted average (TWA)), under the OEL (85 to 89.99 dBA TWA) and higher than occupational limits (90 to 94.99 or 95 and over dBA) (Kaufman *et al.*, 2005). Noise, fuel and additional chemical exposures go hand in hand for many military personnel who work around aircraft. Royal Australian Air Force F-111 fuel tank maintenance workers exposed to fuel, solvents and noise were found by Guest *et al.* (2010) to have higher hearing thresholds compared to published data from otologically normal age-matched populations.

2.1 Jet Fuel, Noise, and Hearing Loss

OELs are generally based on exposure to a single agent; much less is known about combined exposures such as jet fuel and noise. Animal studies concur with Kaufman *et al.* (2005) in that jet fuels promote hearing loss caused by noise. Fechter *et al.* (2007) were the first to show that exposure to high concentrations of JP-8 followed by exposure to damaging noise levels resulted in loss of hair cell sensitivity, as shown by suppression of distortion product otoacoustic emissions (DPOAE), and cochlear outer hair cell loss in Long-Evans rats; the effects were greater with jet fuel exposure as compared to the effects of noise alone. Additional studies with high JP-8 concentrations resulted in similar findings (Fechter *et al.*, 2010 and 2012).

Hypotheses for hair cell toxicity mechanisms have ranged from disruption of intracellular calcium homeostasis (Liu and Fechter, 1997), to disruption of membrane fluidity (Campo *et al.*, 2001; Liu *et al.*, 1997), and disruption of efferent pathways synapsing at the cochlea (Lataye *et al.*, 2000). Free radical generation resulting in oxidative stress was a pathway investigated by Fechter (1999) and Rao and Fechter (2000). Oxidative stress was found to be the mechanism resulting in hearing loss following exposure to carbon monoxide and acrylonitrile, but only with concurrent noise exposure (Fechter, 2005). Therefore, as jet fuel exposures can increase free radical production and oxidative stress at the cellular level, jet fuel exposure would be expected to enhance hair cell dysfunction and loss. This assumption was substantiated by the finding that JP-8 reduced cellular glutathione (GSH) levels by approximately 40 percent in rat lung epithelial cells after only one hour of exposure (Boulares *et al.*, 2002).

However, data in Guthrie *et al.* (2014) suggest that central auditory processing dysfunction (CAPD) is more likely to be an early manifestation of JP-8 induced ototoxicity, especially at more occupationally relevant fuel exposure levels. In their study with Long-Evans rats, Guthrie *et al.* showed that exposure to somewhat lower levels of JP-8 (1000 mg/m^3) than previous studies did not induce peripheral hearing loss. Instead, a CAPD, measured as impaired brainstem encoding of stimulus intensity, was shown to exist at four weeks after the exposure. This impairment in stimulus encoding was exacerbated by a concurrent low level (non-damaging) noise (8 kHz octave band at 85 dBA sound pressure level) exposure. Therefore, CAPDs may play early, critical roles in hearing loss among military involved with aircraft.

For humans, CAPD may be an early biomarker of brain alteration (Bamiou *et al.*, 2000). Aging characteristically alters brainstem function in auditory brainstem response (ABR) measurements (Boettcher *et al.*, 1993; Popelar *et al.*, 2006; Zhou *et al.*, 2006). A potential mechanism for age induced changes in ABR is altered membrane fluidity, which would lead to potential impairments of vesicular transport and/or fusion at the synapses within the auditory brainstem. Membrane fluidity is known to be affected by solvent/anesthetic exposure (Bamiou *et al.*, 2000).

2.2 Objectives

The overall objective of this project was to develop a multi-scale model, together with relevant supporting experimental data, to describe jet fuel exacerbated NIHL. Herein we describe the efforts toward completion of this objective as broken down into three goals. The first goal was

to utilize *in vitro* experiments to measure oxidative stress in cell lines representative of the auditory pathway. Second, the goal was to develop a mixtures pharmacokinetic model capable of describing the tissue dose of JP-8 components along the peripheral and central auditory pathways. The third goal was to design a cellular network model that focuses on disruption of the excitatory and inhibitory synaptic connections along the auditory pathway.

3.0 *IN VITRO* STUDIES

Previous *in vitro* studies have been used to explore the effect of JP-8, key hydrocarbons, and an ototoxic noise surrogate (oligomycin) on cellular function and viability. Robinson *et al.* (2015) detailed a 24-hour proteomic study of cochlear epithelial cells exposed to JP-8. JP-8 was found to have marginal cytotoxic effects on House Ear Institute-Organ of Corti 1 (HEI-OC1) auditory cells at the highest dose of 500 ppm. Proteomics analyses indicated upregulation of histones involved in chromatin remodeling as a result of oxidative stress at this dose level. It has been shown that oxidative stress and pro-inflammatory mediators can alter nuclear histone acetylation and deacetylation (Rahman, 2003). Although effects were not dramatic, a dose-response effect was apparent with increasing concentrations. The purpose of the proteomic study was to identify potentially novel biomarkers of JP-8 toxicity in a cochlear cell line, focusing on biomarkers of oxidative stress and lipid peroxidation. Novel biomarker identification could not be made due to the mild response.

Overall, little toxicity in HEI-OC1 cells was seen from JP-8. An initial increase in live/dead ratios suggests that early induction of protective cellular mechanisms may explain the lack of cytotoxic effects at the two-hour time point. Apoptosis and necrosis induced by JP-8 components (toluene, ethylbenzene, xylene, nonane, and decane) were enhanced by the presence of oligomycin; however, the hydrocarbon component mixture alone showed little impact. Collectively, these findings support the proteomic results in demonstrating JP-8 had minimal effects on cochlear hair (HEI-OC1) cells (Robinson *et al.*, 2015).

To complete the investigation of JP-8 effects on auditory cells *in vitro*, dose response studies to monitor oxidative stress and viability in three cell lines were tested. These studies were intended to correlate JP-8 exposure, reactive oxygen species production, GSH depletion, and cytotoxicity (from Robinson *et al.*, 2015) to provide a broader picture of the JP-8 effect on cochlear cells.

3.1 Cell Lines

Three cell lines were used in these studies. Conditionally immortalized HEI-OC1 auditory cells, isolated from the Organ of Corti, were provided by Federico Kalinec, PhD (David Geffen School of Medicine, Department of Head and Neck Surgery, University of California, Los Angeles CA). The development and characterization of the HEI-OC1 cells is described in Kalinec *et al.* (2003). This cell line is a recognized *in vitro* system to investigate the cellular and molecular mechanisms involved in ototoxicity, and for screening of the potential ototoxic properties of jet fuel components and other chemical stressors.

The neuroblast cell line, VOT-N33, and the otic epithelial cell line, VOT-E36, were originally derived from similar regions of the ventral otocyst of the Immortomouse© at embryonic day 10.5 (Lawoko-Kerali *et al.*, 2004). These cells were kindly provided by Dr. Matthew C. Holley (Department of Biomedical Science, University of Sheffield, England). As experimental models, the VOT-E36 and VOT-N33 cell lines express a number of sensory epithelia and spiral ganglion specific markers making them useful tools for the *in vitro* study of the influence and the mechanism of ototoxic agent on auditory cells. A description of the source, timing and derivation of these cell lines is reviewed by Rivolta and Holley (2002).

3.2 Cell Culture and Exposure Methods

The HEI-OCI cells were grown in high glucose Dulbecco's modified Eagle's medium (DMEM) with 10 percent fetal bovine serum (FBS). VOT-E36 and VOT-N33 cells were cultured in minimal essential medium (MEM) with Glutamax, 10 percent FBS, and 50 Units/mL gamma-interferon. The cells were allowed to proliferate in an incubator with 5 percent CO_2 at 33°C to approximately 80 percent confluency before being harvested for assays. Assays were conducted in Falcon™ black-walled, clear-flat bottom 96-well or clear flat bottom 24-well tissue culture plates (BD Biosciences, San Jose CA) in either 200 or 1000 µL of their respective culture media. Seeding cell densities were optimized at 15,000 and 50,000 cells/well for 96- and 24-well plates, respectively. These conditions were selected by seeding plates at various densitites and identifying the density resulting in the greatest viability after 24-hour incubation at 33°C and 5 percent CO_2. Viability was measured using the (3-(4,5-dimethylthiazol-2-yl)-5-(3-carboxymethoxyphenyl)-2-(4-sulfophenyl)-2H-tetrazolium (MTS) cell proliferation assay (abcam, Cambridge MA).

JP-8 cytotoxicity was measured by MTS, using varying concentration of either dimethyl sulfoxide (DMSO) or ethanol as carriers, to optimize dose delivery. In addition, the impact of serum content in exposure media on JP-8 dose/response was assessed (0, 1 or 10 percent FBS). Following seeding and a 24-hour incubation, media was replaced with fresh media, with or without FBS, plus JP-8, ranging from 0 to 5000 ppm. The MTS assay was conducted as described by the abcam protocol ab197010.

JP-8 induced lipid peroxidation was assessed using an Image-iT® Lipid Peroxidation Kit (Thermo Fisher Scientific, Waltham MA). Following exposures, Lipid Peroxidation Sensor (Component A), was added to each well at a final concentration of 10 µM and incubated for 30 minutes at 37°C. The media containing the sensor was then removed, cells were washed three times with phosphate buffered saline (PBS), and fluorescence was read at excitation and emission peaks of 581 and 591 nm, respectively.

Glutathione depletion induced by JP-8, with and without oligomycin was measured. Oligomycin inhibits the production of adenosine triphosphate (ATP) and was used in previous studies as an *in vitro* surrogate for noise (Robinson *et al.*, 2015). In these studies, JP-8 was delivered in the presence of 1 percent fetal bovine serum and 0.4 percent DMSO. Immediately after, the plate was sealed and incubated for 24-hour. Glutathione depletion was measured using Invitrogen™ ThiolTracker Violet dye. Following JP-8 exposure, the incubation medium was removed from

the wells and cells in each well were rinsed with 100 µL Dulbecco's PBS (D-PBS), which was removed each time. Prewarmed 100 µL aliquots of ThiolTracker™ Violet dye (Thermo Fischer Scientific, Waltham MA) working solution (20 µM) in D-PBS was added to each well and allowed to incubate at 33˚C for 30 minutes. At that time the dye solution was replaced with D-PBS and cells were imaged using fluorescence excitation and emission peaks of 404 and 526 nm, respectively.

3.3 *In Vitro* Results and Discussion

The effect of carriers, dimethyl sulfoxide or ethanol, on JP-8 and toluene cytotoxicity was assessed using the MTS assay. Both DMSO and ethanol are amphiphilic compounds whose miscibility with water and ability to dissolve lipophilic compounds like JP-8, make them useful solvents for *in vitro* studies involving insoluble compounds. A clear dose response to JP-8 and toluene was not achieved in 96-well plates with either solvent, suggesting that dose delivery of these volatile compounds was not consistent. However, the assay was repeated in 24-well plates using DMSO as a carrier, resulting in improved dose/response relationships (Figure 1), suggesting less loss of volatile components during preparation of larger volumes. The use of ethanol as a carrier was not attempted in 24-well plates.

Based upon the cell proliferation assay, MTS, little difference was seen in JP-8 toxicity when the exposure media contained 0, 1 or 10 percent FBS. The clearest dose response curve was obtained in the presence of 1.0 percent FBS, which was subsequently used in all other assays.

All three cell lines demonstrated sensitivity to JP-8 induced lipid peroxidation and glutathione depletion induced by cumene hydroperoxide, a positive control, with the neural line VOT-N33 being more sensitive than the epithelial cell lines. However, in the presence of JP-8 concentrations ranging from 10 to 3000 ppm for 4 and 24 hours, with either 0.5 percent dimethyl sulfoxide or 0.5 percent ethanol, a clear dose response for lipid peroxidation was not evident (data not shown). A slight, but not significant, trend in increasing lipid peroxidation with JP-8 concentration was seen in the HEI-OC1 cells, whereas a slight trend in the opposite direction was seen in both VOT cell lines.

Glutathione depletion induced by JP-8, with and without oligomycin, resulted in opposite trends in VOT-E36 and VOT-N33 cells. JP-8 was delivered in the presence of 1 percent fetal bovine serum and 0.4 percent DMSO. VOT-E36 demonstrated slight but insignificant glutathione depletion in the presence of JP-8. However, in the presence of JP-8 and 100 µM oligomycin, a significant increase in glutathione was seen (Figure 2). The trend was reversed in the neuroblast culture. In the VOT-N33 cell line, relative glutathione increased in the presence of JP-8 at lower doses up to 1000 ppm, but in the presence of both JP-8 and oligomycin, relative glutathione remained near control values. The negative glutathione value seen at the lowest combined JP-8 and oligomycin dose may possibly be an artifact of cell death, as normalization to cell number was not performed with this assay (Figure 2). There was a slight but insignificant difference between controls (0 ppm JP-8) and 100 µM oligomycin in both cells lines.

Much of the data collected suggest a protective effect from the combination of JP-8 with either DMSO or ethanol. However, the lack of consistent dose/response relationships is indicative of a problem with delivery of volatile chemicals to the cells. Dose/response studies in the three cell lines with DMSO alone indicated a slight decline in viability at a concentration of 1 percent. Aviation jet fuels used for civil and military aircrafts are a kerosene type. To avoid peroxide production after the refinery process, a specific antioxidant is added. The antioxidants generally used are hindered phenols in a concentration range of 10 to 20 µg/mL (Bernabei *et al.*, 2000). It is possible that the antioxidants in JP-8 are protective against lipid peroxidation and glutathione depletion. In addition, antioxidant properties of DMSO and ethanol have been reported (Bonnefont-Rousselot *et al.*, 2001; Sanmartín-Suárez *et al.*, 2011). Our results raise doubts about the use of these solvents in the evaluation of potential oxidative or antioxidant properties of immiscible hydrocarbons. Plates were tightly sealed immediately after dosing, allowing the volatile portion to come to equilibrium with the media. However, JP-8 appears to dissociate and component concentrations reaching the cells may not be representative of the mixture concentrations used. Binding to serum may serve as a carrier to deliver compounds to cells, given the on/off rate of binding is rapid. In our studies the percent of serum used had little effect on dose/response; however, its effect may have been masked by a significant loss of volatiles in the exposure system. In addition, because the plates were tightly sealed and no buffer was used, an increase in medium pH may have affected cell viability.

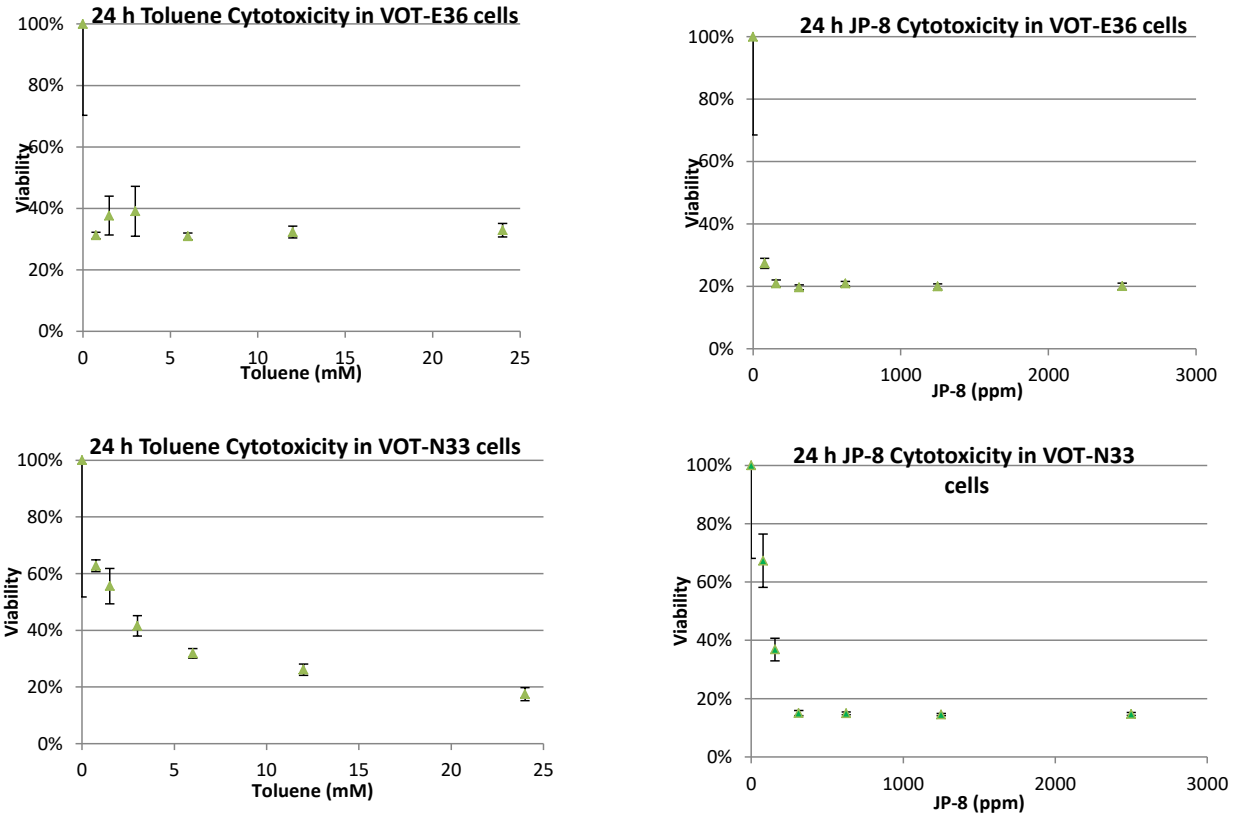

Figure 1. Cytotoxicity in VOT-E36 and VOT-N33 cell lines exposed to toluene or JP-8 in 24-well plates. Media contained 1 percent FBS and 0.5 percent DMSO for 24 hours.

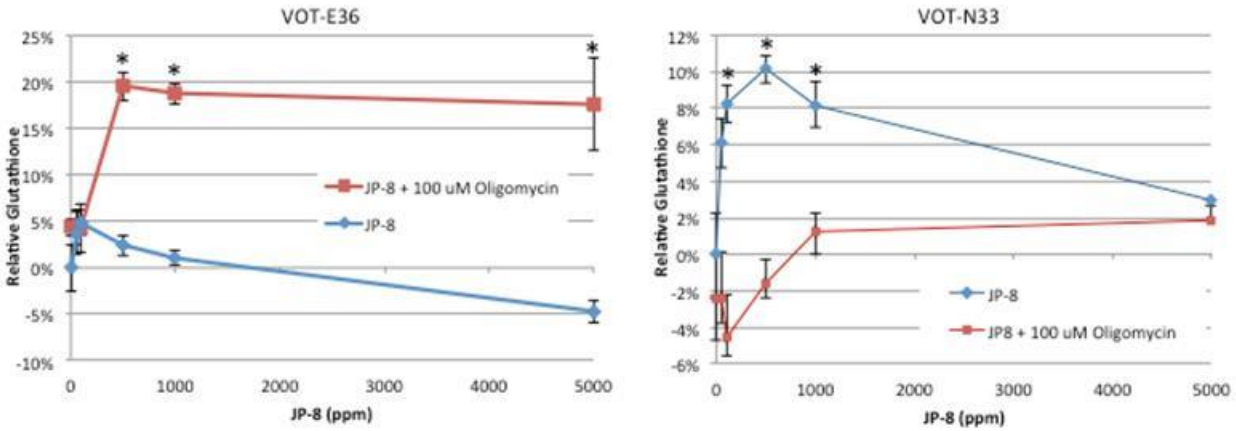

Figure 2. Glutathione relative to controls following 24-hour exposure to JP-8 with and without 100 µM oligomycin in VOT-E36 and VOT-N33 cells. Exposure media contained 0.5 percent DMSO, 1 percent FBS. *p <0.05 (n=3)

4.0 JET FUEL PBPK MODEL AND PARAMETER DEVELOPMENT

A pharmacokinetic study to measure JP-8 components in the cochlea and other major tissues is needed to inform a physiologically-based pharmacokinetic/pharmacodynamic (PBPK/PD) model to predict the impact of JP-8 concentrations on noise-induced hearing loss. *In vivo* studies in rats (Fechter *et al.*, 2012) have shown that exposure to 1500 mg/m^3 JP-8 in combination with non-damaging noise levels may induce low levels of peripheral (cochlear) hearing loss, while exposure to non-damaging noise combined with lower (1000 mg/m^3) JP-8 atmospheres results in central auditory pathway damage to hearing without peripheral changes (Guthrie *et al.*, 2014). Fechter *et al.* (2012) did not monitor the central auditory pathway for changes. A PBPK/PD model of the process will help in predicting the thresholds of damage when exposed to both jet fuels and noise.

JP-8 is a mixture of thousands of components that fluctuate depending on the source of the crude oil from which it is refined (Shafer *et al.*, 2006). The key hydrocarbons in this proposal are common constituents of JP-8 well-known for ototoxicity, including the aromatics toluene, ethylbenzene, p-xylene (Johnson and Morata, 2010). Also included are nonane and decane, components of white spirits, which are known to affect the central auditory pathway (Lund *et al.*, 1996; SCOEL, 2007).

Hearing physiology is commonly broken into two segments, the peripheral hearing pathway, which includes all portions of the ear, and the central auditory pathway, which includes the nerves and nuclei signaling hearing reception into the brain. Therefore, the cochlea and its hair cells, which make up the peripheral auditory pathway, are not the only tissues of interest in a PBPK/PD model. Portions of the brain containing the central auditory pathway include the brainstem and the temporal lobe, which houses the auditory cortex.

Given that these tissues of interest have not been characterized in such a way as to facilitate a PBPK/PD model, *ex vivo* rat studies were performed to develop these data. First, tissue to air

partition coefficients for each of the key hydrocarbons were measured in the tissues. Second, target tissue composition was characterized. Water, fats (neutral lipids, neutral phospholipids, and acidic phospholipids), and protein content were measured for use in quantitative structure-property relationship (QSPR) algorithms designed to mathematically predict chemical-specific tissue to air partition coefficients. This knowledge allows the PBPK/PD model to be adapted to additional chemicals of concern in the future.

4.1 Cochlea Harvesting and Relationship to Bodyweight

A common practice among PBPK modelers is to weigh a tissue/organ and calculate the fraction of the total body weight that the tissue represents. This approximation of the volume of the tissue provides a unitless factor that facilitates subsequent predictions of tissue concentration. The resulting value also allows for scaling of tissue volume for different sized animal models.

Two technicians from the Wright-Patterson Air Force Base (WPAFB) Vivarium (711HPW/RHDV) were sent to the laboratory of Richard J. Salvi, PhD (Department of Communicative Disorders and Sciences, University at Buffalo, The State University of New York, Buffalo NY) on February 11, 2015. The WPAFB technicians observed and learned the process of removing rat cochlea intact from the skull (Figure 3).

This capability has allowed dissection and removal of 177 individual cochleae from male Fischer 344 and Sprague-Dawley rats; cochlea were weighed and then stored at -80 °C. All cochlea were measured from rats used as part of this pilot study. Additionally, rat skulls were obtained through several tissue sharing agreements with other projects in 711 HPW/RHDJ and the Navy Medical Research Unit Dayton.

Figure 3. Photograph of Rat Cochlea Harvested at WPAFB. Magnification level was unspecified.

4.1.1 Results. Single cochlea weights were compared to male rat body weight from both strains of rats. Cochlea weight in general increases with body size, but is not adequately described as a percent of body weight due to the fact that cochlea are large among young rats and do not appreciably increase in size after the rat reaches maturation. Therefore, the typical description of a tissue as a fraction of bodyweight utilized in most PBPK models will not work for this tissue. Early in this cochlea comparison work, the cochlea was estimated to stay roughly the same size

across most body weights (0.025 g for one cochlea, see the red line in Figure 4A). This is a sufficient description of cochlea weight for a model, given the very small size of this tissue.

After 177 cochleae were gathered, a more accurate way to describe cochlea weight was found. This mathematical best fit line by linear regression is shown as the black line in Figure 4A. Visual inspection of cochlea weights by strain against the regression line indicate that the description is adequate for both strains of rat (graphs not shown).

Given that the model requires the weight be provided in kg for a pair of cochlea, the units were converted and the data points doubled, assuming that any given rat would have identical cochlea (by weight) on each side of their head (Figure 4B). The PBPK model in this study then calculates the paired cochlea size based on bodyweight of the simulated rat, using the equation in Figure 4B.

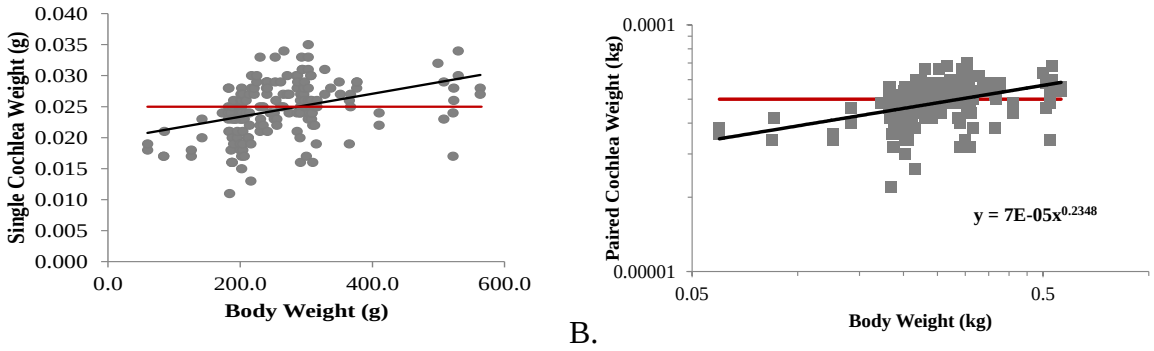

Figure 4. Cochlea Pair and Body Weight Comparisons. (A) Body weight is compared to 177 single cochlea weights. The red line shows an assumed constant cochlea weight of 0.025 g while the black line shows numerical best fit to the data. (B) Body weight is shown in kg compared to doubled cochlea weights in kg to determine the equation needed for model calculation of cochlea size based on body weight. The red line again shows a constant paired cochlea weight (0.00005 kg) and the black line shows the numerical best fit as described by the equation posted on the graph.

4.2 Rat Tissue Partition Coefficient Measurement

Cochlea and other harvested tissues from male Fischer 344 (F-344) rats were utilized to measure *in vitro* partition coefficients of JP-8 constituents. These methods were published by scientists from 711 HPW/RHDJ (under its former office symbols), most recently by Mahle *et al.* (2007).

4.2.1 Vial Evaluation. Vial optimization was performed with one key hydrocarbon, toluene. A 3 L DuPont Tedlar® bag (Sigma-Aldrich, St. Louis MO) of toluene gas was prepared by injecting the bag with 992 ppm toluene first, agitating the bag over a heat gun, allowing the bag to saturate overnight and, then emptying the bag. This preparation coats the bag's interior surface with toluene and prevents further absorption during the experiment. A known

concentration of toluene (992 ppm) was infused into the prepared bag and heated to volatilize any remaining liquid. Two vial and cap options with polytetrafluoroethylene (PTFE)/silicone septa were evaluated for leakage: 10 mL glass vials with magnetic screw thread caps (3.0 mm thick septa) and 20 mL glass vials with regular crimp caps (3.3 mm thick septa). All vials, caps and septa were purchased from Thermo Fisher Scientific (Rockwood TN).

Two injection methods were also evaluated: direct injection of toluene and injection of toluene after removing an equivalent volume of air from the vial, which theoretically reduces the strain of over-inflation on the seal. Following injection of 2.5 mL of 992 ppm toluene, the glass vials were incubated at 37 ˚C for 10 minutes, 3 hours, or 92 hours.

For analysis, one mL of headspace was extracted and then injected onto an Agilent G1540A gas chromatograph-flame ionization detector (GC-FID) system (Agilent, Santa Clara CA) fitted with an RTX-1 fused-silica column (30 m × 0.32 mm ID × 0.25 μm film) (Restek, Bellefonte PA). A Combi-Pal autosampler (CTC Analyticas, Carrboro NC) was used for automatic injections. A split injection mode (2:1) was applied after each 1 mL sample. The injector was set at a temperature of 250°C, and helium (constant pressure 10 psi, flow rate 2.1 mL/minute, average velocity 35 cm/second). Toluene loss was calculated for each time point.

The 10 mL glass vial with the magnetic screw cap lost less toluene after incubation at 37˚C for 3 or 92 hours (Table 1). This finding is likely due to better and consistent tightening of a screw cap versus a crimp. Further, the theoretical need to remove air in order to place a like volume of chemical inside the vial was found to be unnecessary as the vial septum is pierced twice in this method. Single injection vials (those from which no air is drawn before injecting the volatile) lost less toluene than vials pierced twice; any advantage in reducing intra-vial air pressure was negated.

Table 1. PC Vial and Cap Evaluation

Experimental Setup		Percent Toluene Loss	
		3 Hours	92 Hours
25 mL vial with crimp cap	no air draw out first	29.78	54.61
	draw 2.5 mL air out of vial before infusing 2.5 mL toluene into vial	19.20	43.20
10 mL vial with magnetic screw cap	no air draw out first	12.77	37.36
	draw 2.5 mL air out of vial before infusing 2.5 mL toluene into vial	21.51	46.81

4.2.2 PC Measurement Methods and Optimization. Mixed xylene isomers (o-, m-, p-isomers, 96 percent with 4 percent ethylbenzene) were used for this study; during analysis, the largest xylene isomer peak with the earliest retention time was utilized. Peaks from toluene, ethylbenzene, mixed xylenes, nonane, and decane mixture were verified by the single standards.

A 3 L Tedlar bag was saturated similarly to the procedure described above with a mixture of the five key hydrocarbons. Then the bag was prepared by installation of 32.6 mL (3000 ppm) toluene, 37.9 mL (3000 ppm) ethylbenzene, 37.7 mL (3000 ppm) mixed xylenes, 91.3 mL (5000 ppm) nonane, and 99 mL (5000 ppm) decane. The bag was allowed to equilibrate overnight and then reheated to ensure volatilization prior to PC vial preparation.

Partition coefficients were measured for rat blood, cochlea, fat, kidney, skull, and three brain sections: frontal lobe, brain stem and temporal lobe. Tissue samples (ranging from 15 to 100 mg) were weighed. Samples were then smeared on the interior walls of the vials (10 mL glass vials, magnetic screw thread caps, 3.0 mm thick PTFE/silicone septa) to maximize the contact surface of the tissue with the volatile compounds. Due to the bony nature of the skull and cochlea, these tissues were crushed inside the vial using a sterile aluminum rod in order to provide maximum surface area for absorption. The vials were capped securely and gas mixture (2.5 mL) from the Tedlar bag was then injected into the vial. Empty control vials were also injected with 2.5 mL of the gas mixture; these vials were designed to account for vapor loss through the septum and adherence of the chemicals to the glass vial walls.

Each type of tissue was optimized for best absorption time. Frozen samples (-80 ºC) from rats were utilized for optimization, while fresh samples excised from male F-344 rats were used for data collection. Results from the optimization stage indicated that all tissues should be incubated at 37˚C for 1 hour, except fat and brain samples, which were incubated for 2 hours prior to sampling (1 mL headspace gas) and analysis by GC-FID. Tissue:air partition coefficients were calculated using Equation 1 from Gargas *et al.* (1989):

$$P_{tiss} = \frac{C_{ref}(V_{vial}) - C_{tiss}(V_{vial} - V_{tiss})}{C_{tiss}(V_{tiss})}$$

Equation 1

…, where P_{tiss} is the partition coefficient for the tissue, C_{ref} is the concentration in the reference vial, C_{tiss} is the headspace concentration in the sample vial, V_{vial} is 10 mL and V_{tiss} is the volume of tissue where 1 mg is equivalent to 0.001 mL.

4.2.3 Results. PCs were measured during two efforts, the first in April of 2016 and the second in August of the same year. In April, six male F-344 rats were utilized for the experiment. Additional samples were required due to high variability. Low absorbance by a single pair of cochlea, equivalent to approximately 50 mg of bony tissue, was also an issue. In August, an additional 15 rats were used to improve the measurement of PCs. Cochleae from five rats were pooled, resulting in an experimental sample n of three.

Tissue:air partition coefficient measurements were calculated using Equation 1 and the results analyzed using R software version 3.1.3 (R Core Team, 2015). Visual inspection of the plots from the April and August collections showed consistency between the days, so the two sets were combined for further analysis, except for cochlea data, for which only the August data were used.

The data for each tissue and chemical were plotted to examine the skewness of the data and to identify potential outliers. Sample 1 of fat measured in April was very low relative to all other samples across all chemicals. The median, however, was not affected by this outlier, so the median PC value was used for further comparisons. A summary of the resulting tissue:air PC data is shown in Table 2. Tissue:blood PCs utilized in the model were computed by dividing the tissue:air values by the blood:air PC.

Table 2. Measured Tissue:Air Partition Coefficients

Chemical	Tissue	N	Mean	Median	SD	Minimum	Maximum
Decane	blood	11	8.6	7.9	5.0	-0.2	15.7
	brain frontal	9	26.7	16.9	24.7	0.6	78.5
	brain stem	9	24.5	15.0	33.8	-8.8	99.5
	brain temporal	9	14.6	11.2	13.9	-1.4	34.7
	cochlea	9	-1.3	-1.1	44.4	-60.5	89.2
	fat	6	2069.1	2037.1	217.7	1827.5	2459.7
	kidney	17	14.0	10.5	15.2	-8.2	36.9
	skull	6	13.2	14.7	8.7	3.3	23.9
Ethylbenzene	blood	11	46.3	41.1	13.0	33.0	72.8
	brain frontal	9	62.3	55.5	21.5	34.4	105.5
	brain stem	9	93.1	87.8	36.3	42.1	171.4
	brain temporal	9	60.7	65.7	12.4	41.4	73.5
	cochlea	9	18.5	15.4	12.6	5.7	45.0
	fat	6	2816.9	2747.7	545.6	1795.5	3300.2
	kidney	17	163.1	140.5	77.9	81.4	391.1
	skull	6	15.2	14.7	4.3	9.6	22.4
Nonane	blood	11	6.3	5.9	4.7	0.3	17.3
	brain frontal	9	13.0	9.5	19.3	-16.3	46.2
	brain stem	9	20.8	16.5	25.1	-14.1	78.1
	brain temporal	9	12.5	14.8	8.4	1.2	22.2
	cochlea	9	-2.8	-1.9	9.8	-16.0	12.5
	fat	6	848.2	799.2	154.4	714.6	1148.0
	kidney	17	13.7	14.5	12.1	-6.0	47.5
	skull	6	6.5	5.9	2.4	3.9	10.5

Table 2. (continued)

Chemical	Tissue	N	Mean	Median	SD	Minimum	Maximum
Toluene	blood	11	26.2	22.8	5.8	20.3	38.6
	brain frontal	9	39.5	34.8	18.0	24.4	83.4
	brain stem	9	54.0	49.7	22.8	17.0	91.6
	brain temporal	9	33.9	37.0	8.2	19.8	45.1
	cochlea	9	20.8	18.1	14.4	3.6	44.3
	fat	6	1283.5	1264.9	245.7	826.7	1481.3
	kidney	17	67.7	65.3	22.3	30.2	110.5
	skull	6	10.3	10.8	3.6	4.6	15.5
Xylene	blood	11	47.1	42.3	13.6	32.3	73.1
	brain frontal	9	69.3	62.4	23.0	39.9	115.3
	brain stem	9	106.9	104.1	38.1	53.2	188.2
	brain temporal	9	69.2	72.9	13.8	50.2	84.7
	cochlea	9	16.9	14.3	12.0	4.0	41.9
	fat	6	3273.8	3189.2	652.6	2068.9	3888.0
	kidney	17	148.0	130.5	67.7	81.2	355.1
	skull	6	16.3	16.0	4.7	10.4	23.9

4.3 Rat Tissue Composition Determinations and PC Predictions

Although PCs may be measured in target tissues such as cochlea or brain stem for a limited number of key JP-8 hydrocarbons, QSPR algorithms can be utilized to calculate PCs for additional chemicals that may affect hearing. QSPR algorithms require specific data on tissue composition in order to accurately predict PCs. Composition data needed include water, protein, neutral lipid, acidic phospholipid, and neutral phospholipid contents (Ruark *et al.*, 2014).

4.3.1 Tissue Water Content for Partition Coefficient Prediction. Water content data are required to better understand retention and partition of chemicals of interest in the different tissues of a living organism. To examine water content, fresh rat tissues (brain stem, temporal lobe and frontal lobe, skull, cochlea, kidney and fat) were obtained. Data were collected from 10 rats, in order to provide statistically relevant data for PBPK modeling.

In order to delineate the brainstem for excision, the following procedure was used. The first cut was made at Bregma line -9.9. The second cut was made as close as possible to Bregma line -12.6 to collect a slice of rat brainstem that contained the cochlear nuclei. The cerebellum was not saved. The slice of brainstem was within the regions shown in Plates 41 through 50 in Kruger *et al.* (1995) and may not have always included the regions in Plates 49 and/or 50. Although the cochlear nuclei can extend into the junction of the pons and medulla in humans, the slices collected would be in the caudal portion of the pons in the rat.

To determine water percentage, tissues were frozen at -80 ºC and then subjected to lyophilization using a Labconco FreeZone Freeze Dry System (Labconco, Kansas City MO). The lyophilization was performed at -40 ºC for 48 hours. Samples were brought up to ambient room temperature before filling the lyophilizer chamber with air. Water content was determined by weighing tissues before and after lyophilization.

Water content was calculated as a percentage of wet tissue weight for each rat and averaged over ten rats (Table 3, Figure 5). The mean (± SD) water content of cochlea and skull were similar: 29.90 (± 3.61) percent and 24.27 (± 3.88) percent, respectively. The brainstem, temporal lobe, and frontal lobe contained about 70.82 (± 3.43), 79.82 (± 0.49), and 79.25 (± 0.62) percent water, respectively. These values are similar to 77.4 percent, the value reported for the whole brain by Ruark *et al.* (2014). The kidney contained 75.01 (± 0.58) percent water, which is also similar to the reported value of 71.7 percent. Lyophilization of the left and right renal fat pads resulted in 5.75 (± 0.98) and 4.73 (± 1.03) percent water, respectively, which is less than a third of the value reported by Ruark *et al.* (2014), 17.5 percent. This result could be due to fat samples being from different regions of the rat.

Table 3. Tissue Water Content

Tissue	Water Content (% wet tissue weight)
Cochlea	29.90 (± 3.61)
Skull	24.27 (± 3.88)
Brainstem	70.82 (± 3.43)
Temporal Lobe	79.82 (± 0.49)
Frontal Lobe	79.25 (± 0.62)
Kidney	75.01 (± 0.58)
Left Renal Fat Pad	5.75 (± 0.98)
Right Renal Fat Pad	4.73 (± 1.03)

Note: Water content is given as average percent wet tissue weight.

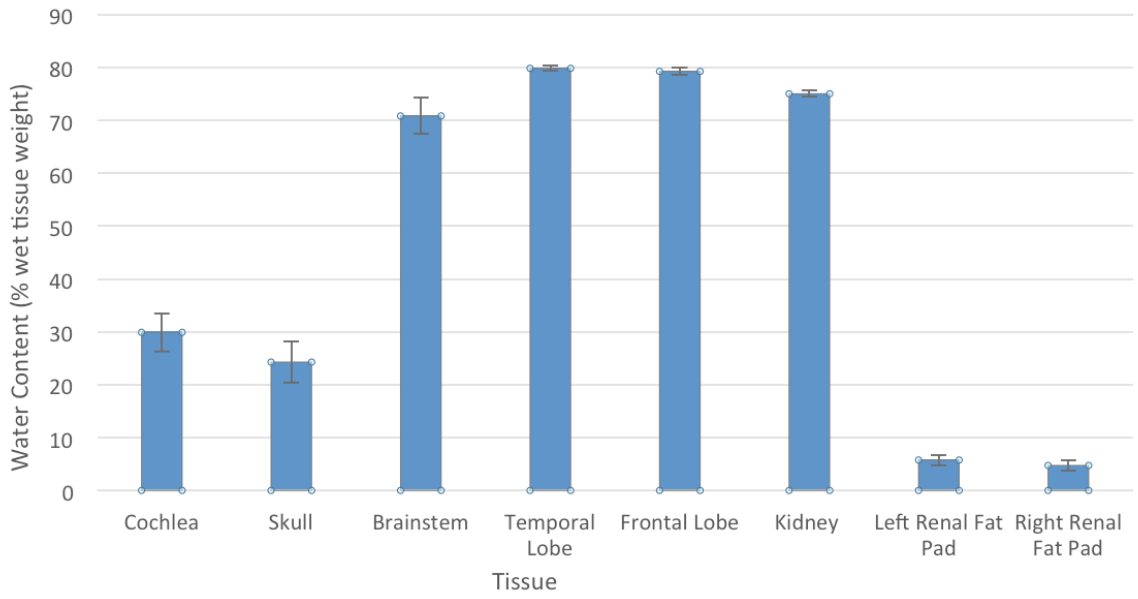

Figure 5. Water Content. The water content is given as an average percent (± 1 standard deviation) wet tissue weight from a sample size of ten rat tissues.

4.3.2 Protein Content for PC Prediction. The protein content fractions for rat kidney, renal fat pads, brainstem, temporal lobe, and frontal lobe were determined using freeze-dried tissues from the water content measurement. Tissues were homogenized with 1 percent Triton X-100 in PBS containing 1X protease inhibitors at a concentration of 1 mL per 150 mg of tissue in 5 mL glass homogenizing vials. The skull and cochlea samples were crushed over liquid nitrogen using a mortar and pestle before homogenizing. Following homogenization, kidney samples were diluted 1:80 with 1 percent Triton X-100 in PBS; renal fat pads and brain regions were diluted 1:10. Cochlea and skull homogenates were not diluted. All tissues were then analyzed using a bicinchoninic acid (BCA) assay (Thermo Scientific, Waltham MA). All tissues had a sample size of 10, except for the cochlea. Cochlea samples required pooling in order to obtain an absorbance reading within the standard curve using the BCA assay. Five cochlea pairs were pooled in order to achieve this. To increase the experimental n from 2 to 3, a pooled sample (five additional cochlea pairs) from Sprague-Dawley rats were added to the study.

Ten freeze-dried kidney homogenates had an average (± standard deviation) protein content of 0.188 (± 0.030) mg/mg tissue (Table 4 and Figure 6), which is close to the reported value of 0.18 by Ruark *et al.* (2014). The left and right renal fat pads contained 0.014 (± 0.006) and 0.023 (± 0.008) mg protein/mg tissue, respectively. This value falls below the reported value of 0.06 (mg/mg) from Ruark *et al.* (2014). This result could be due to taking fat samples from different regions of the rat. The brainstem, temporal lobe, and frontal lobe contained 0.100 (± 0.010), 0.095 (± 0.010), and 0.104 (± 0.005) mg protein/mg tissue, respectively. These particular regions had slightly higher protein content than the reported value of 0.08 for the whole brain by Ruark *et al.* 2014. The skull and cochlea had similar values of 0.007 (± 0.002) and 0.008 (± 0.002) mg protein/mg tissue, respectively. Cochlea from Fisher 344 and Sprague Dawley rats showed similar protein amounts with a percent standard error between 7.2 and 12.4 percent, as defined by standard deviation*100/average.

Table 4. Tissue Protein Content

Tissue	Protein Content (mg/mg tissue)
Kidney	0.188 (± 0.030)
Brainstem	0.100 (± 0.010)
Temporal Lobe	0.095 (± 0.010)
Frontal Lobe	0.104 (± 0.005)
Left Renal Fat Pad	0.014 (± 0.006)
Right Renal Fat Pad	0.023 (± 0.008)
Skull	0.007 (± 0.002)
Cochlea	0.008 (± 0.002)

Note: The protein content of the (wet weight) tissues is reported as an average (±1 standard deviation) of ten samples.

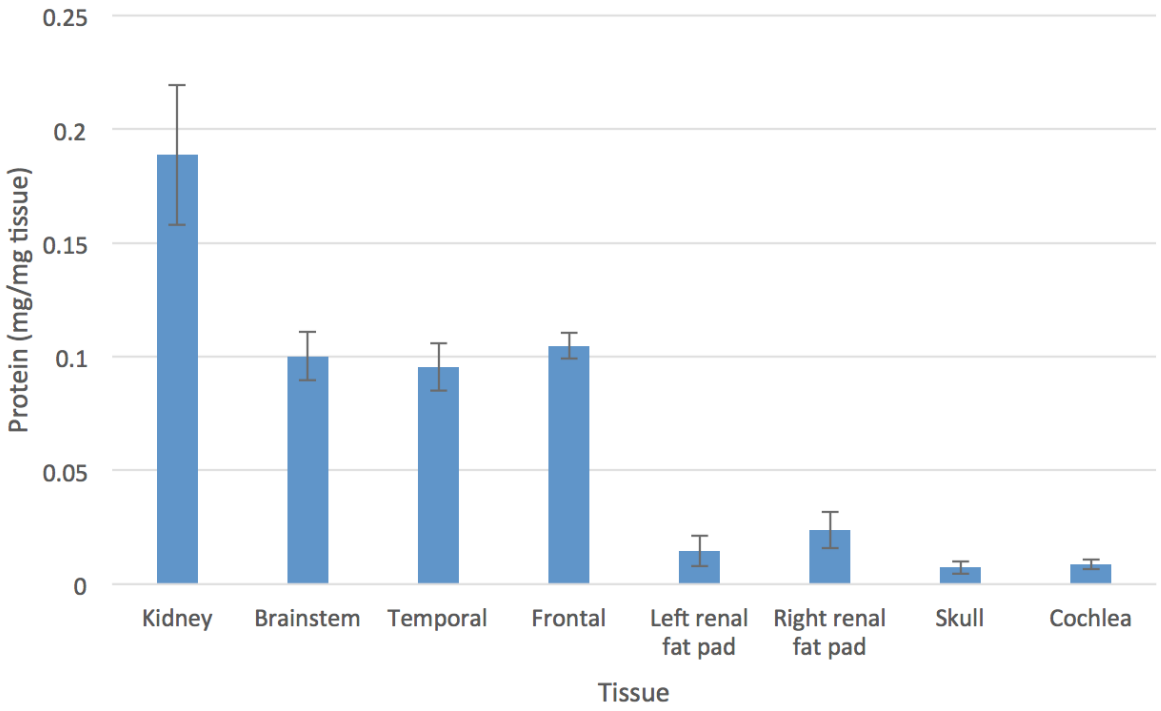

Figure 6. Protein Content. The reported values are the average protein content in mg/mg tissue from ten rat tissues (± 1 standard deviation).

4.3.3 Lipid Class Determination for Partition Coefficient Prediction. Research was conducted on methods to quantify different classes of lipids in tissues to aid in the development of modeling parameters. The three classes of lipids that hold importance in estimating partition coefficients for PBPK modeling are the neutral, neutral phospholipids and acidic phospholipids

(Ruark *et al.*, 2014). Multiple methodologies for quantitation of these lipids were discussed with solid phase extraction being the most viable and efficient.

The lipid content of the kidney, renal fat pads, brainstem, frontal lobe, temporal lobe, skull, and cochlea was determined by eluting four classes of lipids. Neutral lipids, free fatty acids, neutral phospholipids, and acidic phospholipids were eluted from the tissue using solid phase extraction. All tissues except the skull and cochlea were first homogenized in distilled water at a concentration of 1.67 μL/mg of tissue. An aliquot equivalent to 170 mg was used for the extraction. The skull and cochlea were ground over liquid nitrogen before homogenization in distilled water. A sample size of ten was used for the kidney, temporal lobe, and fat. However, samples had to be pooled to achieve the appropriate mass for the remaining tissues. The brainstem, frontal lobe, and skull samples were pooled into five groups of two, and the cochlea had two groups of ten pairs each.

In order to separate the total lipids from the homogenized tissue, the qualitative method of Bligh and Dyer was utilized (1959). For every 1 mL of homogenized tissue sample, 3.75 mL of 1:2 (volume:volume (v:v)) chloroform-methanol was added, followed by 1.25 mL chloroform ($CHCl_3$), and then 1.25 mL H_2O, vortexing vigorously for one minute between each step. The mixture was then centrifuged at 1000 rpm at room temperature for five minutes. This causes a separation between a water phase, an interphase, and an organic chloroform phase. The chloroform phase at the bottom of the vial was collected using a Pasteur pipette and 2.5 mL $CHCl_3$/mL sample was added to the remaining two phases. The mixture was vortexed for one minute and centrifuged as previously described. The new chloroform layer was collected and added to the original chloroform layer. The lipid-containing chloroform was evaporated under nitrogen until about 100 μL of the extract remained.

The procedure for separating lipid classes was modified from Kim and Salem (1990). A 500 mg, 3 mL Bond Elut aminopropyl column was used to elute the lipids. The column was placed on a vacuum manifold with pre-weighted glass test tubes underneath to separately collect the lipid fractions. The column was first equilibrated with two washes of hexane (3 mL each). The flow rate of the column was adjusted to approximately 3 mL per minute. The chloroform extract was then added to the column. Neutral lipids were eluted first using 3 mL $CHCl_3$-isopropanol (2:1). Free fatty acids were eluted next using 3 mL ethyl ether-acetic acid (100:2) and the neutral phospholipids were eluted using 3 mL methanol. Lastly, acidic phospholipids were eluted using 3 mL of hexane-isopropanol-ethanol-0.1 M ammonium acetate in water-formic acid (420:350:100:50:0.5) containing 5 percent phosphoric acid (volume:volume).

The neutral lipids, free fatty acids, and neutral phospholipids were dried under nitrogen and then weighed. The acidic phospholipids were evaporated under nitrogen for 10 minutes until the hexane layer was completely removed. Water and chloroform (1 mL each) were added to the remaining acidic phospholipid fraction. After vortexing vigorously for one minute, the vial was left to separate. Separation was complete after approximately 15 minutes. The chloroform layer was collected from the bottom of the vial with a Pasteur pipette and saved. This process of chloroform addition, vortexing, and separation was repeated twice more, with the collected extract layers added to the first. This resulted in approximately 3 mL of combined chloroform extract total containing the acidic phospholipids. About 500 mg of anhydrous sodium sulfate

was added for 1 hour to dry the combined chloroform phase. After drying, the chloroform extract was transferred to a pre-weighted glass test tube and dried under a stream of nitrogen.

The masses of the four lipid classes were recorded by measuring the weight change of the test tubes into which each class was eluted. The masses of the neutral lipids, free fatty acids, neutral phospholipids, and acidic phospholipids are listed in Table 5 and shown in Figure 7. The kidney, temporal lobe, and fat data are averaged from a sample size of ten; the brainstem, frontal lobe, and skull are averaged from a sample size of five; and the cochlea are averaged from a sample size of two. The Total Lipids category listed in the table is the accumulation of all four classes.

Amounts of total lipids and individual lipid classes measured herein confirmed values for adipose, kidney, and whole brain reported by Ruark *et al.* (2014). The highest total lipid measurement was detected in renal fat pads; 93 percent of this fat source consists of neutral lipids. Kidney and brain regions consist of a higher percentage of neutral phospholipids as compared to other lipid classes.

Individual brain regions displayed differences in total lipid content. The highest lipid content was detected in the brainstem when compared to frontal and temporal lobes. Distinct regional lipid composition differences in the rat brain have been found previously. Chavko *et al.* (1993) reported twice as much total lipid in the brainstem as compared to frontal and temporal lobes; our data concur with this conclusion.

The total lipid content of skull or cochlea has not been reported previously. Cochlea from Fisher 344 and Sprague Dawley rats showed similar lipid amounts with a percent standard error between 4.8 and 12.2 percent, as defined by standard deviation*100/average. Both tissues showed very low amounts of total lipids when compared to adipose, kidney and brain. Skull and cochlea had similar amounts of neutral lipids and neutral phospholipids while acidic phospholipids were three times higher in cochlea. These distinct differences in lipid profiles of skull and cochlea are in contrast with the very similar water and protein content profiles for these tissues as measured in Sections 4.3.1 and 4.3.2 above.

Table 5. Tissue Lipid Content

Tissue (n)	Neutral Lipids	Free Fatty Acids	Neutral Phospholipids	Acidic Phospholipids	Total Lipids
Kidney (10)	10.9 (± 1.9)	4.4 (± 1.7)	26.7 (± 6.4)	8.0 (± 3.2)	50.0 (± 8.8)
Brainstem (5)	23.1 (± 6.1)	7.2 (± 2.1)	61.6 (± 6.9)	18.6 (± 4.3)	110.5 (± 4.0)
Temporal Lobe (10)	12.9$^{\#,\%,\wedge}$ (± 5.2)	5.4 (± 1.6)	21.8$^{\#,\%,\&}$ (± 4.1)	11.9$^{\$,\%}$ (± 3.2)	52.0$^{\#,\%,\&}$ (± 2.2)
Frontal Lobe (5)	8.3$^{\#}$ (± 1.2)	6.3 (± 1.2)	23.5$^{\#,\%,\&}$ (± 2.7)	13.6$^{\%,@}$ (± 1.8)	51.7$^{\#,\%,\&}$ (± 2.0)
Renal Fat Pad (10)	780.1^{a} (± 116.4)	15.6 (± 7.6)	34.7 (± 12.6)	9.2 (± 5.1)	839.5 (± 119.0)
Skull (5)	2.4$^{\#}$ (± 0.3)	1.1 (± 0.4)	3.1$^{\#}$ (± 0.5)	1.3$^{\#}$ (± 0.7)	7.8$^{\#}$ (±0.5)
Cochlea (2)	3.0$^{\#}$ (± 0.4)	1.6 (± 0.1)	4.5$^{\#}$ (± 0.3)	4.4$^{\#}$ (± 0.3)	13.6$^{\#}$ (± 0.5)

Note: The average (± standard deviation) content of each lipid fraction for selected tissues is reported in µg lipids/mg tissue. ^{a}Oily residue. $^{\#}p<0.0001$ vs. brainstem, $^{\$}p<0.01$ vs. brainstem, $^{\%}p<0.0001$ vs. skull, $\wedge p<0.01$ vs. cochlea, $^{@}p<0.05$ vs. cochlea, $^{\&}p<0.001$ vs. cochlea.

4.3.4 Predicted Partition Coefficients. Tissue:blood PCs were predicted using the tissue contents (protein, water and lipid) measured above and the algorithm published by Ruark *et al.* (2014). The algorithm calculation was implemented in R version 3.1.3 (R Core Team, 2015). For neutrally charged compounds such as those studied in this report, the algorithm accepts an octanol:water PC (K_{ow}), and a fraction of compound unbound in the plasma (f_{ub}). The f_{ub} was assumed to be small, due to the high likelihood of significant binding of these nonpolar chemicals to albumin. The sensitivity of the model to this parameter was examined, and found to be low. This unexpected lack of sensitivity to f_{ub} is due to the fact that we are predicting tissue:blood, rather than tissue:plasma partitions, and the red blood cell:plasma PC is used to make the conversion, softening the impact of plasma protein binding. The K_{ow} used and references are shown in Table 6. The value for xylene is an average of the ortho- and meta-isomers.

Table 6. Compound-Specific Parameters for PC Estimation

Chemical	K_{ow}	Source
Decane	6.69	Montgomery (2007)
Nonane	4.46	Joshi *et al.* (2010)
Ethylbenzene	3.13	Wasik *et al.* (1981)
Xylene	3.2	Wasik *et al.* (1981)
Toluene	2.69	Montgomery (2007)

Tissue:blood PC values from the published literature were collected for comparison with our measured PCs as well as our predicted values. These data are shown in Table 7. The literature values for decane in kidney are from Merrill *et al.* (2008), those for decane in other tissues are from Perleberg *et al.* (2004), and those for the other chemicals are from Table A-2 of Sterner *et al.* (2004). The literature values for xylene are averages of ortho-, meta-, and para- isomers. The literature brain PC values are not region-specific, but are included for comparison to brain-region data as an approximate match.

Several plots were constructed to facilitate a visual comparison of the data. Figure 7 shows a comparison of the observed (i.e., measured) versus predicted PCs. If the predictions and observations matched perfectly, the symbols would fall on the solid line in the figure. It is apparent that there are some points with poor agreement. The relative error was calculated and is shown in Figure 8 to get a clearer picture of the discrepancies. It appears that there are a couple of clusters that fall further from the line. The outlying points were found to be the predictions for fat (all chemicals), and decane and nonane (all tissues).

Figures 9 and 10 are the same as Figure 7 and 8, respectively, except that the fat, decane, and nonane data have been removed. Better agreement is found between the predicted and observed PC values.

Table 7. Tissue:Blood PC Predictions Compared to Measured and Literature Values

Chemical	Tissue	Measured	Predicted	Literature	Source
Decane	brain frontal	2.1	10	4.8	Perleberg *et al.* (2004)
	brain stem	1.9	21	4.8	Perleberg *et al.* (2004)
	brain temporal	1.4	10	4.8	Perleberg *et al.* (2004)
	cochlea	-0.14	7.6	NA	NA
	fat	260	160	330	Perleberg *et al.* (2004)
	kidney	1.3	9.6	3.0	Merrill *et al.* (2008)
	skull	1.9	5.4	NA	NA
Ethylbenzene	brain frontal	1.4	1.3	0.74	Sterner *et al.* (2004)
	brain stem	2.1	2.8	0.74	Sterner *et al.* (2004)
	brain temporal	1.6	1.3	0.74	Sterner *et al.* (2004)
	cochlea	0.4	1.0	NA	NA
	fat	67	21	33	Sterner *et al.* (2004)
	kidney	3.4	1.3	0.65	Sterner *et al.* (2004)
	skull	0.4	0.73	NA	NA
Nonane	brain frontal	1.6	7.7	5.0	Sterner *et al.* (2004)
	brain stem	2.8	16	5.0	Sterner *et al.* (2004)
	brain temporal	2.5	7.7	5.0	Sterner *et al.* (2004)
	cochlea	-0.32	5.8	NA	NA
	fat	140	120	240	Sterner *et al.* (2004)
	kidney	2.5	7.4	NA	NA
	skull	1.0	4.2	NA	NA
Toluene	brain frontal	1.5	0.53	4.2	Sterner *et al.* (2004)
	brain stem	2.2	1.1	4.2	Sterner *et al.* (2004)
	brain temporal	1.6	0.54	4.2	Sterner *et al.* (2004)
	cochlea	0.80	0.41	NA	NA
	fat	56	8.4	55	Sterner *et al.* (2004)
	kidney	2.9	0.51	4.7	Sterner *et al.* (2004)
	skull	0.47	0.30	NA	NA
Xylene	brain frontal	1.5	1.5	1.4	Sterner *et al.* (2004)
	brain stem	2.5	3.2	1.4	Sterner *et al.* (2004)
	brain temporal	1.7	1.5	1.4	Sterner *et al.* (2004)
	cochlea	0.34	1.1	NA	NA
	fat	75	24	51	Sterner *et al.* (2004)
	kidney	3.1	1.5	1.2	Sterner *et al.* (2004)
	skull	0.38	0.83	NA	NA

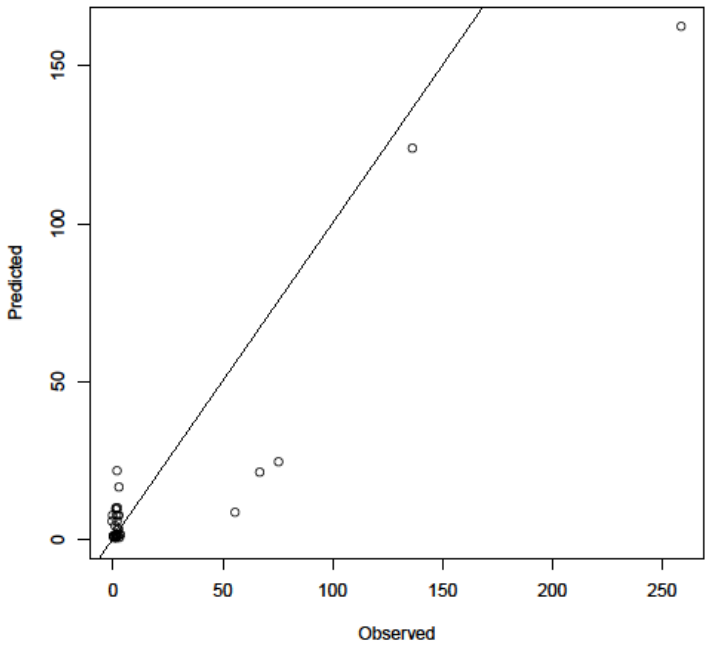

Figure 7. All Observed (Measured) vs. Predicted Tissue:Blood PCs. Solid line represents perfect correspondence.

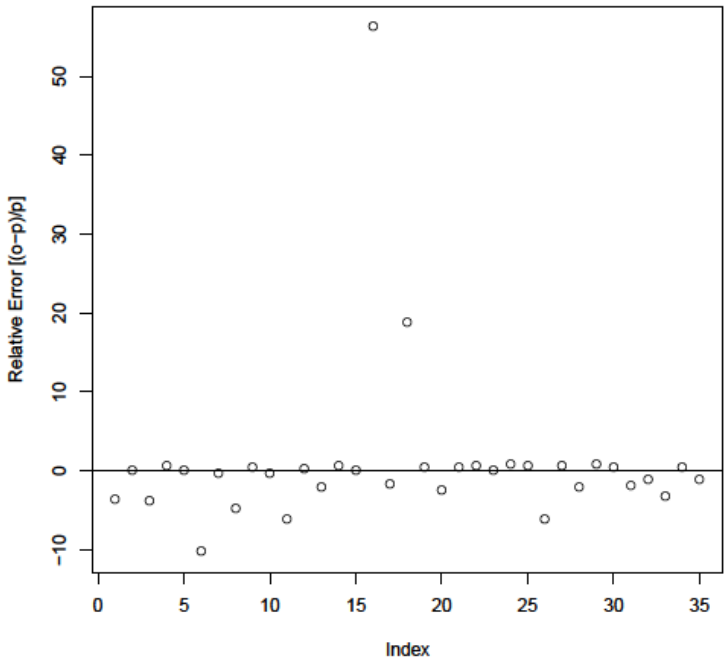

Figure 8. Relative Difference Between All Observed (Measured) and Predicted PCs. Horizontal line represents perfect correspondence.

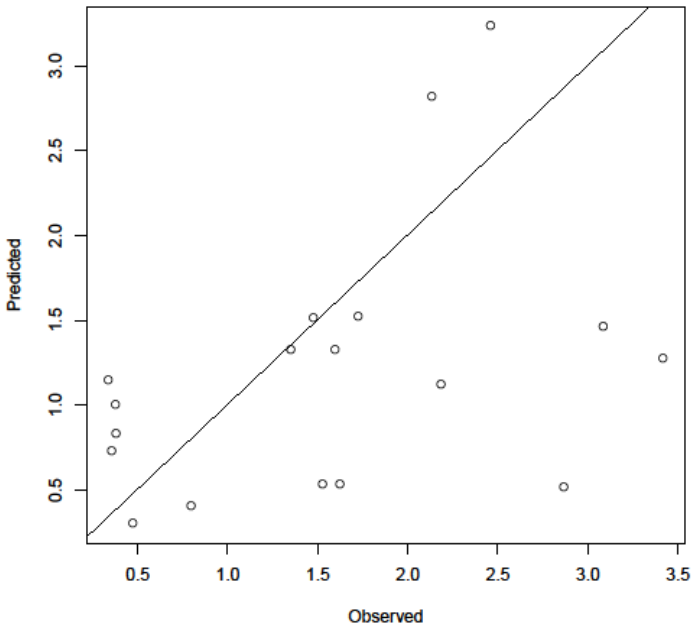

Figure 9. Observed (Measured) vs. Predicted PCs Excluding Fat, Nonane, and Decane. Solid line represents perfect correspondence.

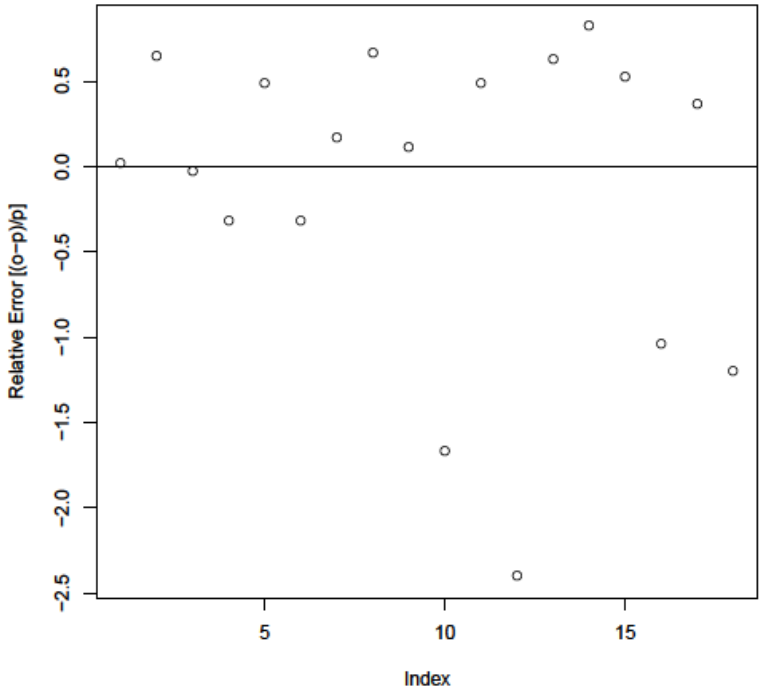

Figure 10. Relative Difference Between All Observed (Measured) and Predicted PCs Excluding Fat, Nonane, and Decane. Horizontal line represents perfect correspondence.

Figure 11 shows a comparison of measured (Section 4.2.2) PC values with those obtained from the literature (Table 7). Overall, the measurements and literature values follow a consistent trend, though the measurement of the fat:blood PC for nonane and decane (i.e., the two right-most circles) are somewhat lower than the values found in the literature. Measurement of the fat:air PC is quite variable, so the deviation is not unexpected.

The standard deviations of the cochlea PC measurements were high relative to the central estimates, and the mean and median were negative for some compounds. This result is most likely due to the very small size of the cochlea, and the fact that the cochlea is mostly bone with relatively little parenchymal tissue.

As discussed in Section 4.2.3, the cochlea PC measurement standard deviations were high and some mean and median values were negative, resulting in low confidence in the measured cochlea PCs. An alternative to measuring whole cochlea PCs, namely measuring epithelial cells derived from rat cochlea, was attempted. Cochlear epithelial cells (HEI-OC1) were cultured *in vitro*, spun down at 500 x g, and resuspended in PBS twice to form a cell pellet for analysis. Theoretically, based on the cochlea being largely bone with a smaller amount of cochlear epithelial cells, the PC should fall in between that of the skull (bone) and the pellet. Measured PCs for bone, cochlea and cell pellets were graphed to examine the trend of the PCs across these tissues (Figure 12). For three of the five chemicals, the expected trend is not observed, further reducing confidence in the measured cochlea PCs.

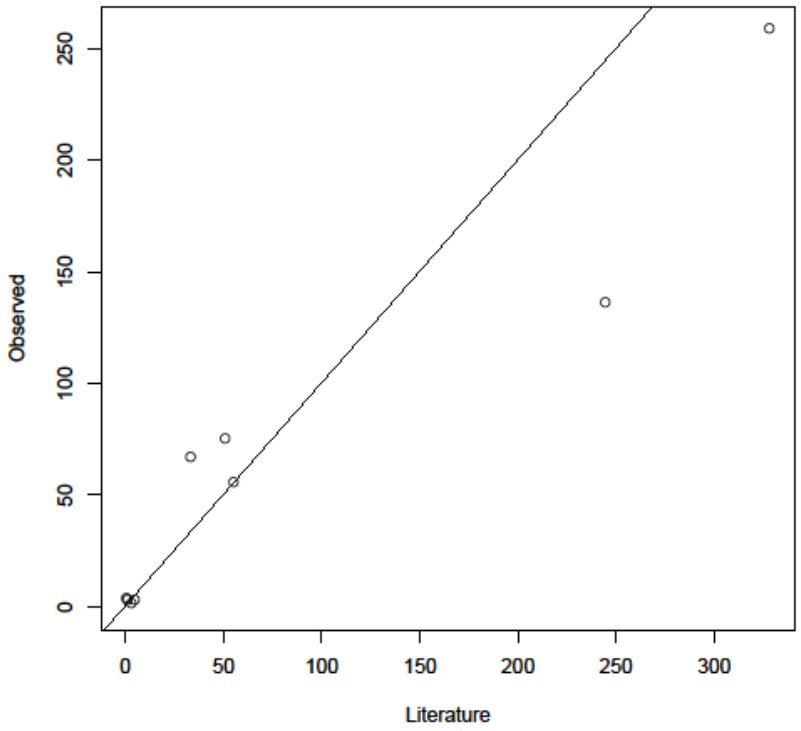

Figure 11. All Observed vs. Literature Reported Tissue:Blood PCs. Solid line represents perfect correspondence.

Due to the difficulties in obtaining measured cochlea PCs (discussed in Section 4.2.2) and the lack of literature PCs for this tissue, cochlea PCs were estimated for use in the PBPK model using a combination of measured and predicted values. Noting that the predicted values are consistently slightly higher than that of skull, the cochlea PC was estimated by scaling the skull PC measurement by the ratio of the cochlea to skull PC predictions (see Section 4.4 below). In this way, the skull PC measurement that is believed to be more accurate is utilized and scaled by using the QSPR PC prediction model.

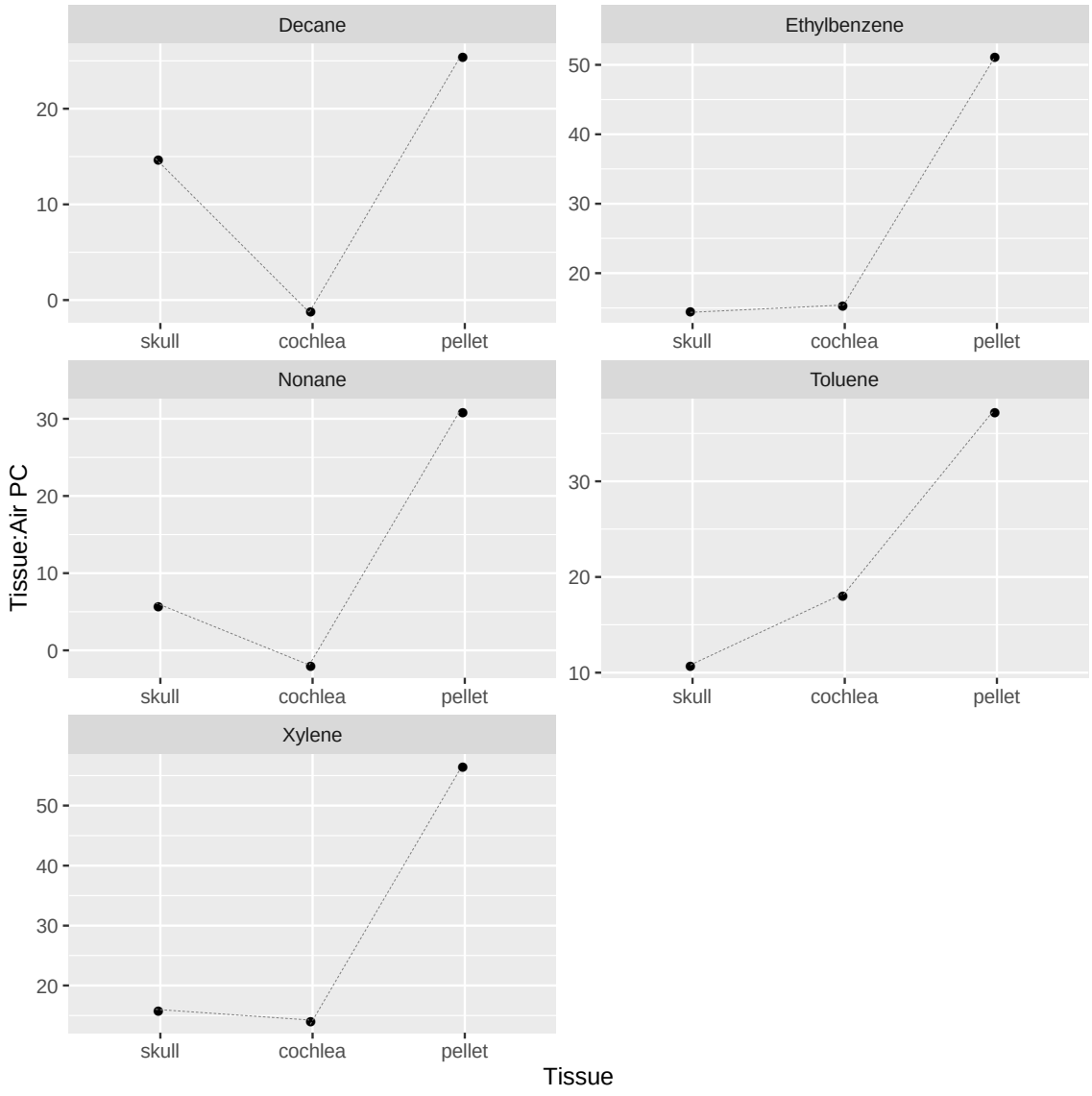

Figure 12. Comparison of PCs for Skull, Cochlea, and Cochlear Epithelial Cell Pellet. The symbols in the figure represent the tissue:air PC, and they should increase from skull to cochlea to pellet for each chemical.

4.4 Physiologically-Based Pharmacokinetic Modeling of Mixtures using Array Coding

Traditionally mixtures models are simply coded as parallel individual models with lines of code for each individual chemical in the mixture, for each and every tissue in each model (Figure 13). Interactions between the chemicals in the mixture are coded within the pertinent tissue; for example, competitive metabolism is coded in the liver. Increasing the number of chemicals in the model increases the lines of code required. This practice results in very long models and many opportunities to incorporate errors into the code.

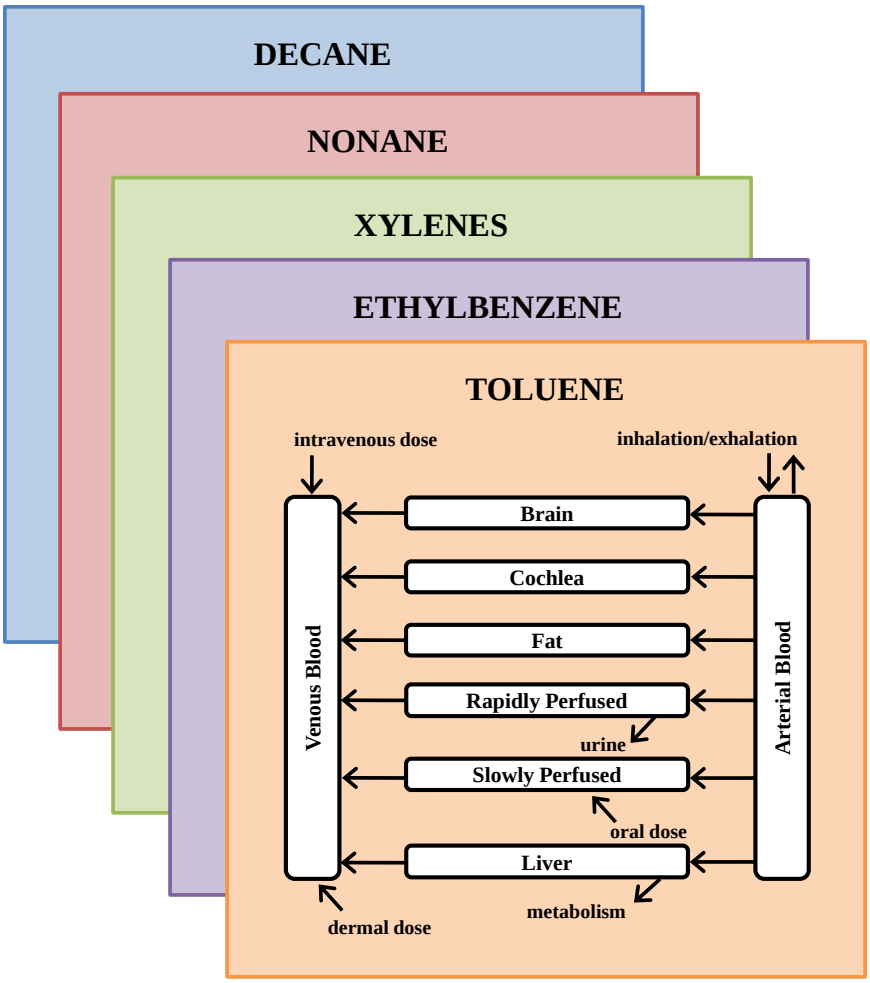

Figure 13. Schematic of Traditional Parallel Style Mixtures PBPK Models. Interactions between the chemicals in the mixture are coded within the pertinent tissue and are not shown in the schematic.

An existing published model for a volatile organic chemical (Clewell *et al.*, 2001) was adapted to an array version in order to streamline the modification process for the mixtures PBPK model being developed in this project. The array model has the same structure (tissues) for all chemicals in the mixture. Each tissue is coded only once, regardless of the number of

components in the mixture. Physiological parameters that would not change based on the chemical are still defined as scalar values, but chemical-specific parameters and physico-chemical properties, which cause each chemical in the model to behave differently, are defined as arrays. Examples of these properties include molecular weights, tissue:blood partition coefficients, and metabolic constants.

The prototype array model was coded to simulate the kinetics of up to five chemicals simultaneously in five tissues or tissue groups: brain, fat, liver, rapidly perfused tissues, and slowly perfused tissues. Once the array model was validated against the original non-array version, a cochlea compartment was added and the brain compartment was split into three parallel tissues, brainstem, temporal lobe, and the remaining brain tissue (Figure 14).

Rat physiological parameters were based on the published version from which the array model was originally adapted (Clewell *et al.*, 2001). The array model was parameterized based largely on physicochemical parameters from published models for toluene, ethylbenzene, and xylene (Haddad *et al.*, 1999), nonane (Robinson and Merrill, 2008), and decane (Merrill *et al.*, 2008) (Table 8). Some parameters required fitting using various inhalation data sources; fitting was necessitated by minor differences in coding from published models.

Cochlea blood flow is well characterized in the literature (Hillerdal, 1987; Hillerdal *et al.*, 1987; Larsen *et al.*, 1984) and averaged for use in modeling by Robinson *et al.* (2013). The proportion of blood in cochlea tissue was calculated from guinea pig data in Morizono *et al.* (1968). The volume of paired cochlea tissue was measured in this study (Section 4.2). The partition coefficients were also derived using results from this study (Sections 4.3 and 4.4).

Brain region volumes were determined both from literature (Delp *et al.*, 1991) and from temporal lobes excised for this study. Blood flow to the brain regions were calculated using Gjedde *et al.* (1980). The proportion of blood in brain tissue was found in Brown *et al.* (1997) and was assumed to be the same between regions. Partition coefficients for the brain regions for different chemicals were found in previously published PBPK models and then scaled using the differing partition coefficients measured in this study (Table 8).

The prototype model best described chemicals which readily partition into tissues from the blood and therefore their movement into a tissue is described by the partition coefficient and the flow of blood into the tissue (i.e., flow limited). For some chemicals, specifically nonane and decane, additional time is required for the chemical to cross membranes into the tissue; this movement is described as diffusion limited. As two of the key hydrocarbons being evaluated in this model are diffusion limited, each tissue in the array model was adapted to accommodate diffusion limited movement between the tissues and the blood entering the tissues. The array model code, written for acslX (Aegis Technologies Group, Orlando FL), is found in Appendix A; the M files required for its execution are found in Appendix B.

Pharmacokinetic studies for each key component were used to parameterize and validate the model structure. Once reasonable fits were obtained for individual components (Appendix C), the model was utilized to predict target tissue concentrations following a select JP-8 exposure. Guthrie *et al.* (2014) exposed Long-Evans rats (males, mean starting body weight 105 g) to 1000

mg/m^3 JP-8, 6 hours per day, 5 days a week, for 4 weeks, without noise. This important exposure resulted in central auditory system deficits but not peripheral hearing changes.

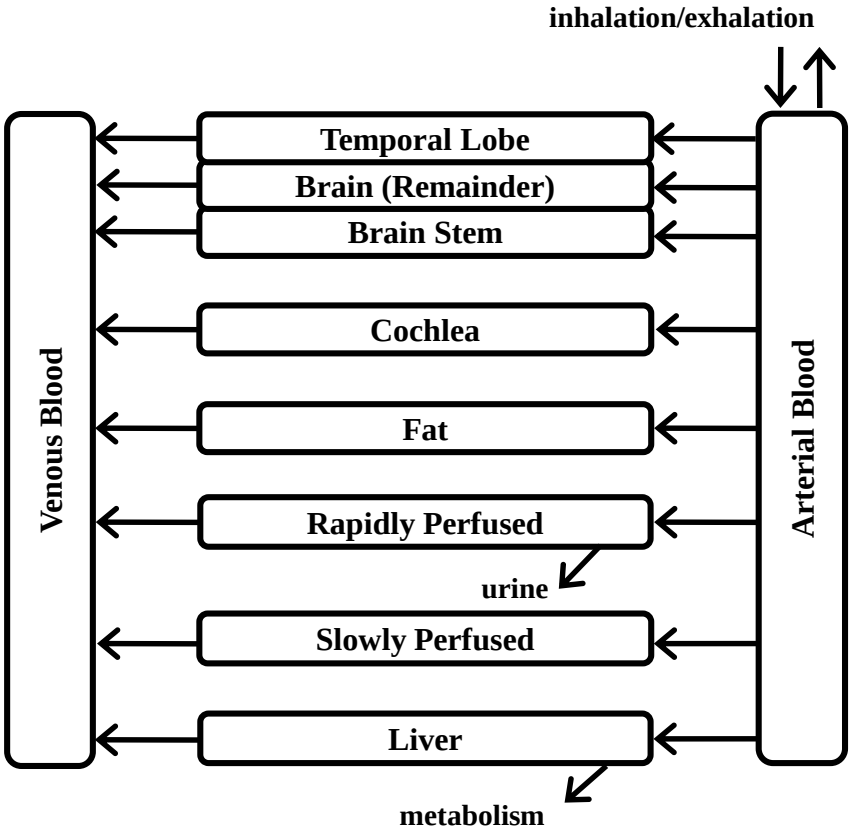

A.

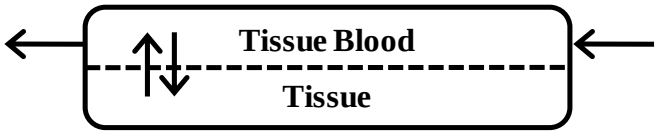

B.

Figure 14. Physiologically-Based Pharmacokinetic Model Schematic. (A) General model schematic. (B) Each tissue represented above is divided into the tissue itself and the tissue blood. This convention allows the model to simulate diffusion limited chemicals.

Table 8. Array PBPK Physico-Chemical Parameters for Key Hydrocarbons

Parameter	Constant Name	Toluene	Ethyl benzene	Xylene	Nonane	Decane
Blood:Air PC	PC	18.0[a]	42.7[a]	46.0[a]	5.2[b]	5.0[c]
Tissue:Blood Partition Coefficients (Unitless)						
Brain Remainder	PBrn	2.0[d]	1.22*	1.38*	5.0[b]	10.0**
Brain Stem	PStm	(1.81/1.26)PBrn[e]	1.93*	2.29*	(2.9/1.7)PBrn[e]	(1.56/1.75)PBrn[e]
Temporal Lobe	PTL	(1.34/1.26)PBrn[e]	1.44*	1.61*	(2.6/1.7)PBrn[e]	(1.16/1.75)PBrn[e]
Cochlea	PCoc	0.54[f]	0.44[f]	0.47[f]	1.45[f]	2.15[f]
Fat	PFat	56.7[a]	36.4[a]	40.4[a]	282.0[b]	328.0[c]
Liver	PLiv	4.64[a]	1.96[a]	1.98[a]	8.0**	3.0**
Rapidly Perfused Tissue	PRap	4.64[a]	1.41[a]	1.98[a]	2.0[b]	3.0[c]
Slowly Perfused Tissue	PSlw	1.54[a]	0.61[a]	0.91[a]	4.0[b]	0.85[c]
Inhalation, Metabolic & Clearance Parameters						
Maximum Rate of Reaction	Vmax	3.44[a]	6.39**	6.49[a]	0.1**	0.005**
Affinity Constant	Km	0.13[a]	1.04**	0.45[a]	0.1**	0.1**
Urinary Clearance	ClUrC	0.004**	0.04**	0.004**	0.04**	0.004**
Upper Respiratory Tract Scrubbing	Scrub	0	0	0	0.4**	0.7[c]
Permeability:Area Affinity Constants						
Brain Remainder	PABrn	1000[g]	1000[g]	1000[g]	0.5[b]	0.005**
Brain Stem	PAStm	1000[g]	1000[g]	1000[g]	0.5[h]	0.005[h]
Temporal Lobe	PATL	1000[g]	1000[g]	1000[g]	0.5[h]	0.005[h]
Cochlea	PACoc	1000[g]	1000[g]	1000[g]	1.0[i]	1.0[j]
Fat	PAFat	1000[g]	1000[g]	1000[g]	0.5**	0.07**
Liver	PALiv	1000[g]	1000[g]	1000[g]	0.07[b]	0.15[c]
Rapidly Perfused Tissues	PARap	1000[g]	1000[g]	1000[g]	1.0[b]	0.005**
Slowly Perfused Tissues	PASlw	1000[g]	1000[g]	1000[g]	0.5[b]	0.14**

Notes: *Measured; **Fit to data; [a]Haddad *et al.* (1999); [b]Robinson & Merrill (2008); [c]Merrill *et al.*(2008); [d]Unpublished in-house model; [e]Scaled using measured PC ratio between regions & fit value; [f]Scaled from measured skull PC using predicted cochlea:skull ratio; [g]No diffusion limitation; [h]Same as PABrn; [i]Same as PARap; [j]PARap in Merrill *et al.* (2008)

In order to simulate this exposure, the relative contribution of the key components to the JP-8 fuel utilized in the study had to be calculated. The study used a Jet A blend composed for research purposes; this blend, known as POSF 4658, is composed of equal parts Jet A fuels from five different manufacturers. POSF log book numbers are provided by the Air Force Research Laboratory Fuels and Energy Branch (AFRL/RQTF) located at WPAFB OH, formerly known as the Air Force Wright Aeronautical Laboratories (AFWAL/POSF). Tandem gas chromatography analysis by the 2006 Shafer *et al.* method indicates that POSF 4658 contains 0.16 percent toluene, 0.12 percent ethylbenzene, 0.66 percent xylenes, 1.14 percent nonane, and 2.55 percent decane; percent values are by weight.

All toxicity tests using POSF 4658 are performed with the commercial Jet A fuel blend following the addition of a standard additive package required for Air Force JP-8 fuel; the additive package comprises less than 0.15 percent by weight. As this is a small percentage, the presence of the additive package in the fuel was not figured into the estimation of the key component concentrations for the purpose of simulation.

4.4.1 PBPK Model Results and Discussion. Target tissue estimations following a single day under the Guthrie *et al.* (2014) 1000 mg/m^3 JP-8 inhalation exposure scenario are shown in Figures 15 through 19. Although JP-8 contains a higher concentration of nonane than xylenes, a higher peak venous blood concentration of xylenes is expected (Figure 15). Merrill *et al.* (2008) incorporated upper respiratory tract scrubbing into their decane model to account for the relative decrease in uptake compared to the inhaled concentration. This scrubbing factor was utilized in the array model and, for nonane, a smaller scrubbing factor was fit to simulate published data (Table 8). In the Guthrie exposure scenario prediction (Figure 15), scrubbing reduces the nonane uptake and a higher xylenes concentration prediction is observed.

Due to nonane and decane having relatively high partition coefficients compared to the aromatic compounds, these alkanes are predicted to have the highest concentrations in target tissues, despite the scrubbing that occurs during inhalation (Figures 16 through 19). Central auditory deficits were observed at this exposure concentration by Guthrie *et al.* (2014); peripheral (cochlear) effects are not. Central auditory effects are associated with alkanes such as nonane and decane (Lund *et al.*, 1996; SCOEL, 2007) while cochlear effects are generally attributed to aromatics such as toluene, ethylbenzene and specific xylenes (Johnson and Morata, 2010). Figure 16 indicates that relatively small concentrations of aromatics are predicted to be found in the cochlea in this inhalation scenario (less than 0.005 mg/L for toluene and ethylbenzene). In contrast, Figures 17 and 18 show that relatively high concentrations of the alkanes are predicted to partition to the brain stem and temporal lobe during exposure (more than 0.3 mg/L decane in the brain stem); these brain tissues are expected to be the active sites for central auditory disruption.

These estimations also are useful for planning a pharmacokinetic study designed to measure key components in these tissues after a similar daily exposure. Figure 16 indicates the very low predicted level of detection required to successfully measure key component concentrations in the cochlea.

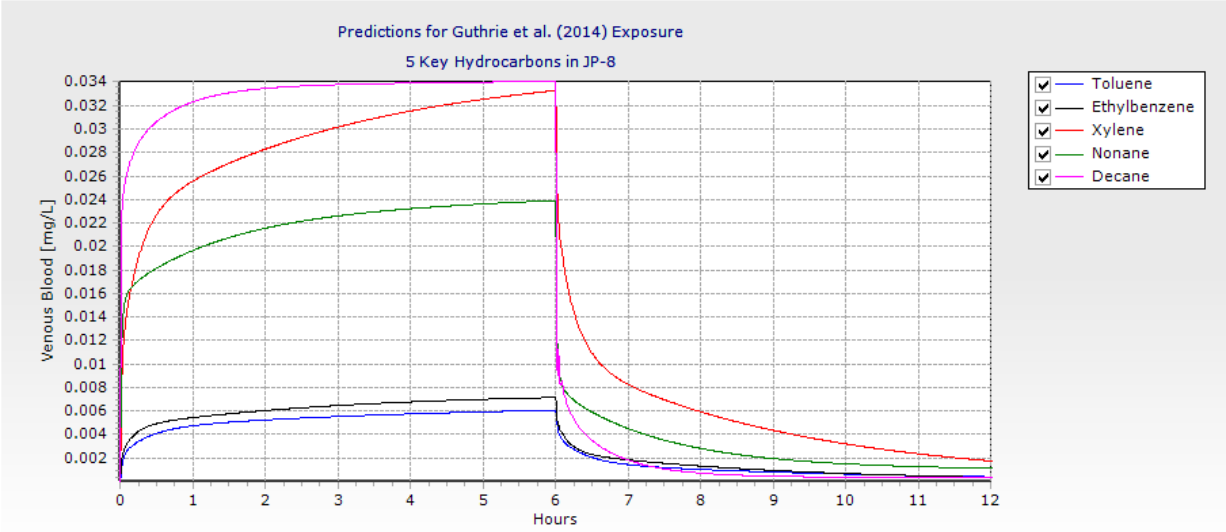

Figure 15. Venous Blood Key Component Concentration Predictions for 1000 mg/m^3 JP-8 Exposure from Guthrie *et al.* (2014) Exposure Profile

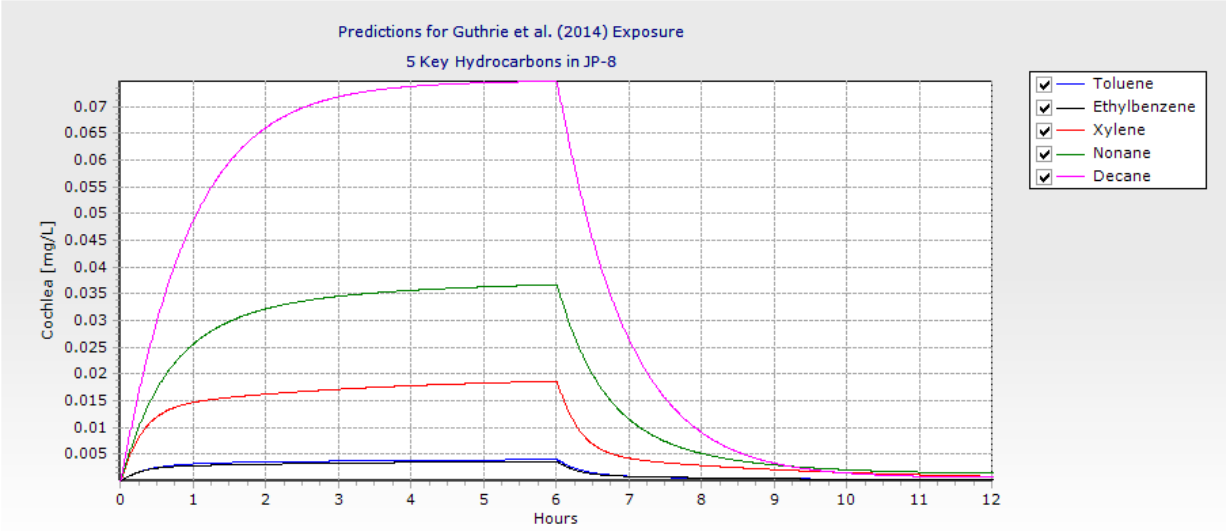

Figure 16. Cochlea Key Component Concentration Predictions for 1000 mg/m^3 JP-8 Exposure from Guthrie *et al.* (2014) Exposure Profile

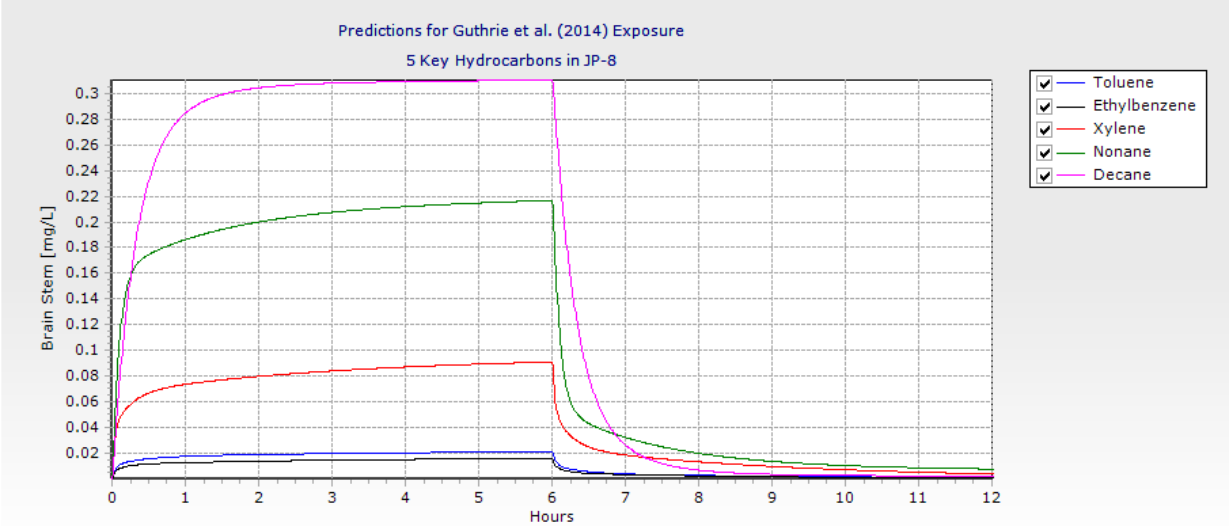

Figure 17. Brain Stem Key Component Concentration Predictions for 1000 mg/m^3 JP-8 Exposure from Guthrie *et al.* (2014) Exposure Profile

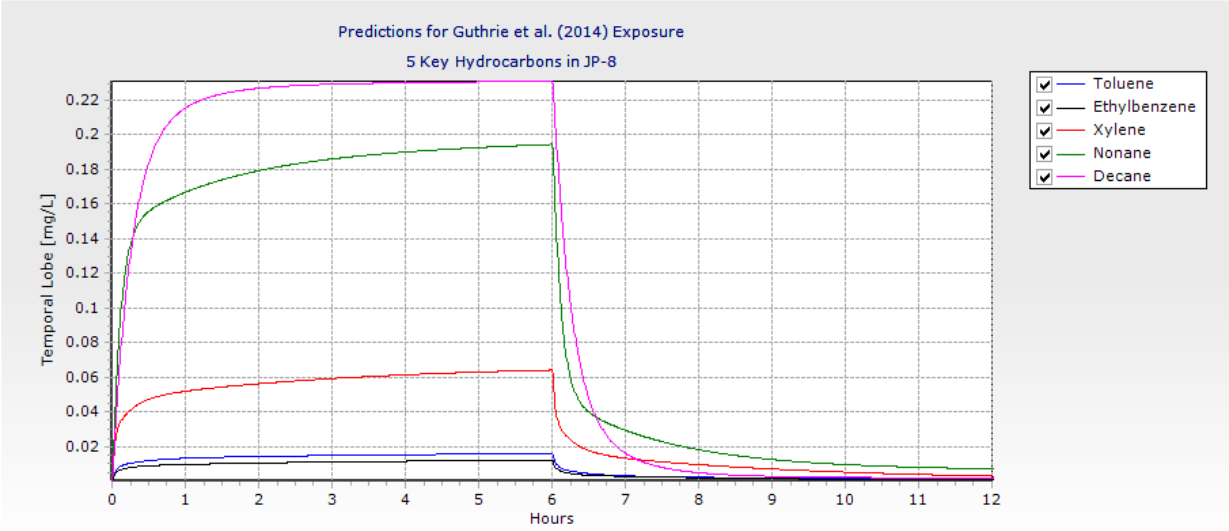

Figure 18. Temporal Lobe Key Component Concentration Predictions for 1000 mg/m^3 JP-8 Exposure from Guthrie *et al.* (2014) Exposure Profile

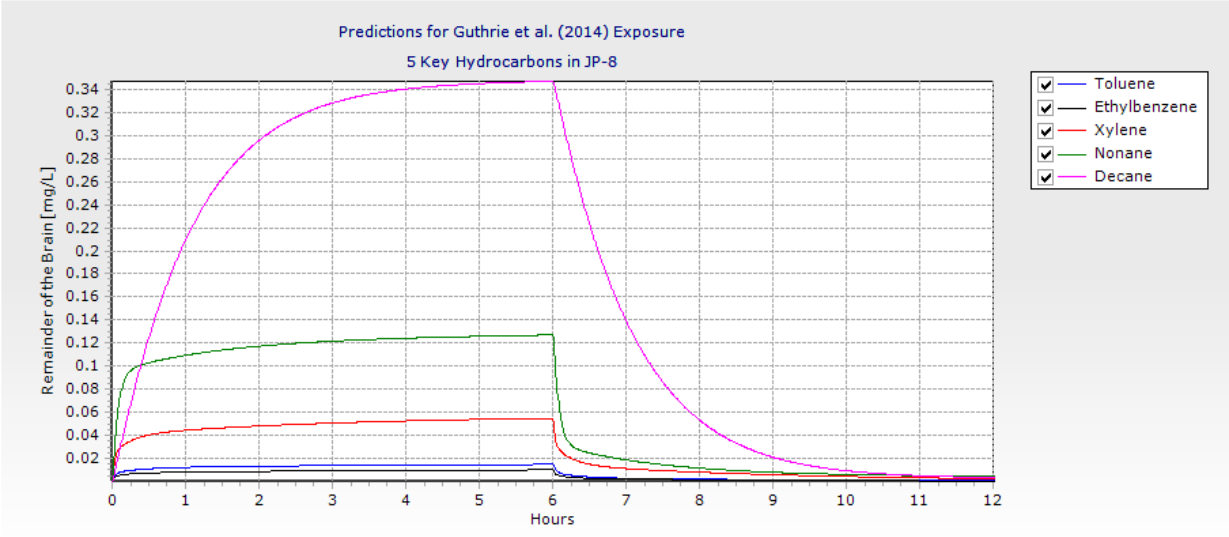

Figure 19. Remainder of Brain Key Component Concentration Predictions for 1000 mg/m^3 JP-8 Exposure from Guthrie *et al.* (2014) Exposure Profile

5.0 PHARMACODYNAMIC MODELING OF JET FUEL EFFECTS ON CENTRAL AUDITORY PATHWAY ENCODING OF AUDITORY STIMULI

Initially, the working hypothesis was that free radical (FR) generation and oxidative stress combine to form the primary mechanism through which ototoxicants disrupt hearing and through which they potentiate the effects of noise on hearing loss. This concept led to a pharmacodynamic model for FR mediated cochlear damage. This model was first outlined in Robinson *et al.* (2013) and further developed in Robinson *et al.* (2015). The model provided a method to combine dosimetric predictions of JP-8 at the target site (via a PBPK model), together with its effect, and the effect of noise, on the generation of free radicals in the cochlea, and their impact on inducing cellular damage and hearing loss. The model assumed that the inactivation of cellular targets, leading to hearing loss, was determined by the area under the FR concentration-time curve for the target (cochlea). The model included lipid peroxidation, the generation of lipid peroxides, such as polyunsaturated fatty acid radicals (PUFAR) and peroxy polyunsaturated fatty acid radicals (PPUFAR), and the model was linked to biomarkers including the oxidative stress marker malondialdehyde and glutathione depletion to facilitate future testing of the FR hypothesis. Finally, loss of functionality (hearing loss) and hair cell death were described as outputs of the model.

The oxidative stress model for jet fuel exacerbation of noise-induced hearing loss is fully described in Robinson *et al.* (2015) and will not be discussed further here, since following analysis of the CAPD shown in the Guthrie *et al.* (2014) data, it became apparent that the effect of jet fuel on central auditory pathway (CAP) encoding of auditory stimuli is a more sensitive endpoint for hearing loss. Literature research resulted in the hypothesis that binding of toluene and other jet fuel components to gamma-aminobutyric acid (GABA) receptors (allosteric modulation) likely leads to increased initial activity and the adaptive response so that binding over time may lead to down regulation of the GABA receptor, thereby diminishing $GABA_A$

currents (see Figure 20) (Bale *et al.*, 2005a; Krasowski and Harrison, 2000). Voltage-dependent Ca^{++} channels (VDCCs) regulate neurotransmitter release in the central synaptic network. Toluene also can mimic the effects of VDCC blockers (Maguin *et al.*, 2009). In this context, a simple neuronal circuit model was developed in order to provide a basis for simulating evoked response waveforms (Figure 20), and a model framework for describing synaptic neurotransmitter kinetics was proposed. Model codes for the pharmacodynamic models are found in Appendix D.

5.1 Justification for Modeling Central Auditory Pathway

Recent evidence suggests that auditory processing dysfunctions are early manifestations of JP-8 induced ototoxicity. Chronic exposure to jet fuel component toluene can impair the functioning of the central nervous system, sharing many effects with nervous system depressant compounds such as ethanol, barbiturates and anesthetics (Maguin *et al.*, 2009). Anesthetics and related compounds were thought to perturb the fluidity of the plasma membrane (LeBel and Schatz, 1989). Several kinds of ion channels expressed in neurons are thought to be affected. For instance, NMDA (Cruz *et al.*, 1998), $GABA_A$ (Krasowski and Harrison, 2000), glycine (Beckstead *et al.*, 2000), ATP (Woodward *et al.*, 2004), serotonin (Lopreato *et al.*, 2003), and nicotinic acetylcholine (Bale *et al.*, 2002, 2005b) receptors are sensitive to toluene. In addition, toluene alters the function of different voltage-dependent ion channels (Cruz *et al.*, 2003) including VDCCs (Tillar *et al.*, 2002). Significant differences are seen between groups of normal-hearing solvent mixtures-exposed humans compared to normal-hearing humans without solvent mixtures exposure, in a battery of central auditory functioning tests which include: pure-tone audiometry, dichotic digits, pitch pattern sequence, filtered speech, random gap detection, masking level difference, and hearing-in-noise tests (Fuente *et al.*, 2011).

Gene expression analysis of JP-8 exposed rats revealed a modulation of several genes, including GABA transporter 3 (GAT-3) (Lin *et al.*, 2001). Components of JP-8 such as toluene have been shown to be $GABA_A$ allosteric modulators. Hester *et al.* (2011) have shown that toluene exposure was associated with induction or repression of genes in pathways associated with synaptic plasticity, including long-term depression, GABA receptor signaling and mitochondrial function. Toluene exposures have also been shown to depress the auditory nervous system in rats by interfering with muscle contractions which help to dampen the effects of loud noises (Maguin *et al.*, 2009). Acute exposures to volatile aromatics such as those found in jet fuel enhance inhibitory $GABA_A$, while prolonged exposures leads to diminished $GABA_A$ currents (Bale *et al.*, 2005a). Changes in the plasticity of the auditory central nervous system can result in tinnitus, an epileptic-like auditory phenomenon (Shulman *et al.*, 2002). Both $GABA_A$ and $GABA_B$ receptor level changes, as well as glutamic acid decarboxylate (GAD-37), have been implicated in CAPDs (Kou *et al.*, 2013). Gene expression analysis of JP-8 exposed rats compared to the control group revealed a modulation of several related genes, including GAT-3 (Lin *et al.*, 2001). Jet fuel exposure alone may increase susceptibility to noise-induced hearing loss and tinnitus.

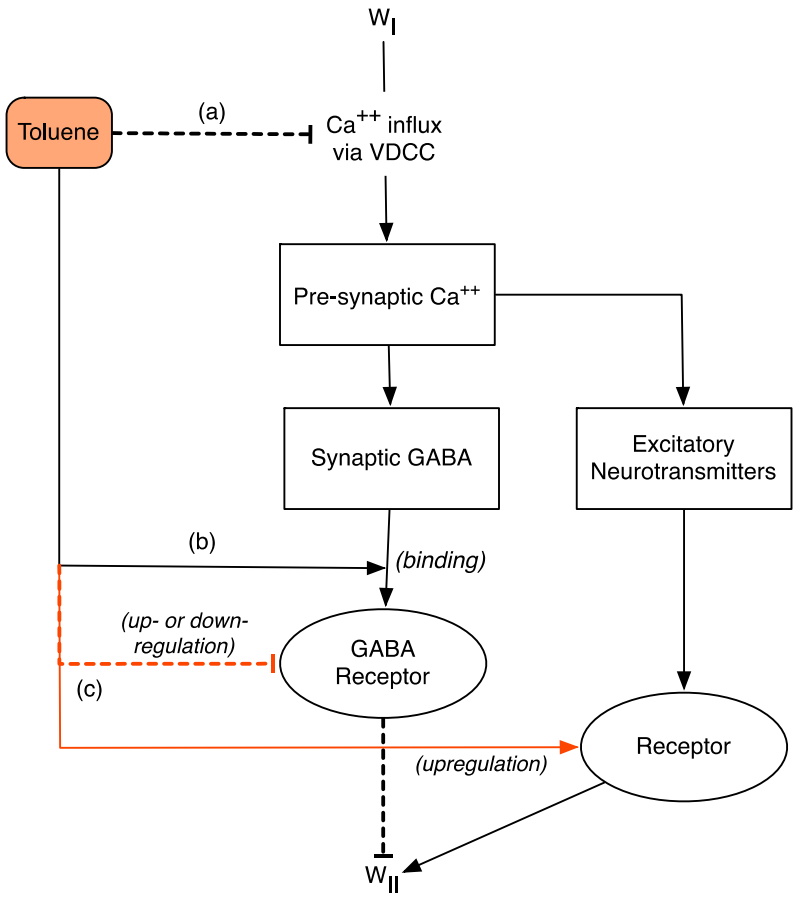

Figure 20. Schematic Showing Potential Impact Sites of Toluene on Transmission of Wave Function W. Potential sites include (a) via voltage dependent calcium channels (VDCC); (b) via binding to and (allosteric) modulation of $GABA_A$ receptors; and (c) via longer term alterations in post-synaptic receptor.

Our recent *in vivo* studies on Long-Evans rats (Guthrie *et al.*, 2014) showed that exposure to subtoxic levels of JP-8 (1000 mg/m^3) did not induce peripheral hearing loss. However, there was impaired brainstem encoding of stimulus intensity at four weeks after the exposure. Furthermore, this impairment in stimulus encoding was exacerbated by low level (non-damaging) noise (8 kHz octave band at 85 dBA sound pressure level) exposure. The results revealed that subototoxic exposures to noise and JP-8 resulted in normal peripheral auditory function concomitant with central auditory processing deficits. Thus it appears that transmission deficits in the auditory pathway may play a critical, and early, role in hearing loss in addition to oxidative stress-induced peripheral hair cell impairment and loss.

Altered growth functions of the brainstem components of the auditory brainstem response are also characteristic of aging (Boettcher *et al.*, 1993; Popelar *et al.*, 2006; Zhou *et al.*, 2006). Potential mechanisms for such a process may include altered membrane fluidity (characteristic of solvent/anesthetic exposure) leading to potential impairments of vesicular transport and/or fusion at the synapses within the auditory brainstem. In humans, CAPD may be a first sign of subtle

brain alteration (Bamiou *et al.*, 2000). Further, abnormal stimulus-response function in the central auditory nervous system has been associated with non-hearing disorders such as migraines and depression (Ambrosini *et al.*, 2003; Gallinat *et al.*, 2000). Oxidative stress may also play a role in CAPD (Henderson *et al.*, 2006). In addition, postulated mechanisms for tinnitus show an interesting connection between loss of peripheral cells and compensatory mechanisms in the remaining auditory pathway (Schaette and Kempter, 2012).

The ABR is a non-invasive biomarker, particularly well-suited for quantifying deficits in auditory information processing of complex noise. These effects were exacerbated when coupled with noise (8 kHz octave band at 85 dBA sound pressure level (SPL)) (Guthrie *et al.*, 2014). In addition, several solvents such as toluene and xylene, which are also JP-8 components, have been shown to induce both CNS toxicity and mid-frequency auditory impairments. In house *in vitro* studies with HEI-OC1 cells (immortalized mouse cochlear epithelial cells) indicate marginal cytotoxicity. Given the minimal effects of JP-8 on peripheral auditory systems, both *in vivo* and *in vitro*, central auditory processing dysfunctions may be an early manifestation of JP-8 induced toxicity.

Based on these data and a review of current literature, the preliminary hypothesis is that chronic JP-8 exposure alters the distribution of excitatory and inhibitory neurotransmission-related proteins, which likely play a key role in hearing loss and, potentially, the development of tinnitus. To test the hypothesis, a cellular network model was built to focus on disruption of receptors $GABA_A\alpha1$ and NMDA (containing NR2A subunit) along the auditory pathway, linking potential mechanisms with the ABR. Model parameters for each neuron type include: receptor densities at the synapse, neurotransmitter kinetic parameters (release/synthesis, removal/degradation) at the synapse and receptor binding kinetics (affinities, maximum capacities). The preliminary model describes qualitatively the ABR data (changes in the auditory evoked potential waveform as a result of fuel exposure, Guthrie *et al.* (2014)), in terms of hypothetical alterations in receptor densities.

Although this is a preliminary model at this stage, mechanism-based pharmacodynamic (PD) models such as the one described here can be used to provide a quantitative basis for extrapolation of CAPD responses over different doses (fuel and/or noise). When linked to the PBPK model described in Section 4 above, the resulting PBPK/PD models would ultimately allow extrapolation of CAPD effects in animals to predict potential quantitative hearing loss effects in humans. As specific causative mechanisms are further uncovered, this work could be expanded to include new approaches to protection and possible future therapeutic intervention.

5.2 Simple Neuronal Circuit Model

In order to link the delivered dose of jet fuel components described above with a potential mechanism for fuel-induced alterations in auditory processing, and in particular for observed deficits in measured evoked response encoding of stimulus intensity, we assume that fuel exposure may alter synaptic transmission through alterations in synaptic receptor densities. To explore this mechanism, a mathematical model of a simple neuronal circuit in the dorsal cochlear nucleus was developed based on Kou *et al.* (2013) (Figure 21). The model includes the

following attributes: frequency coding of signal intensity, saturation of receptors at high signal intensities, and longer term alterations in signal processing mediated by changes in receptor densities at the synapse.

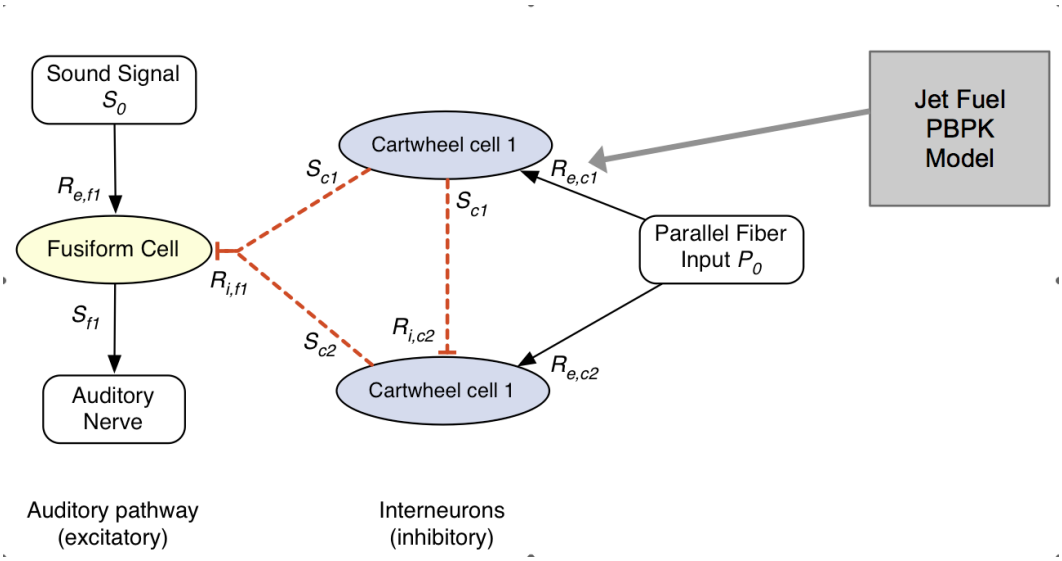

Figure 21. Schematic of a Simple Neuron Circuit in the Dorsal Cochlear Nucleus of the CAP. The model is based on a neuron circuit described in Kou *et al.* (2013). S_{f1}, S_{c1} and S_{c2}, represent signal intensities transmitted by the fusiform cell, and each of the cartwheel cells. R represents receptor densities; subscripts f and c refer to the fusiform and cartwheel cells; and subscripts i and e refer to inhibitory and excitatory connections, respectively. PBPK predicted dosimetry of jet fuel components (not shown) are linked to the circuit model via modulation of receptor densities (R_i and R_e).

The signal intensities S_{f1}, S_{c1} and S_{c2}, transmitted by the fusiform cell, and each of the cartwheel cells, respectively, are given by:

$$S_{f1} = \frac{R_{e,f1} \cdot S_0}{S_0 + K_{e,f1}} - \frac{R_{i,f1} \cdot (S_{c1} + S_{c2})}{S_{c1} + S_{c2} + K_{e,f1}}$$

Equation 2

$$S_{c1} = \frac{R_{e,c1} \cdot P_0}{P_0 + K_{e,c1}}$$

Equation 3

$$S_{c2} = \frac{R_{e,c2} \cdot P_0}{P_0 + K_{e,c2}} - \frac{R_{i,c2} \cdot S_{c1}}{S_{c1} + K_{i,c2}}$$

Equation 4

…where subscripts *i* and *e* refer to inhibitory and excitatory connections; *K* represents signal intensities that half the maximum response; and P_0 represents parallel fiber (inhibitory) input.

5.3 Evoked Response Waveform Simulation

The ABR allows for simultaneous evaluation of the peripheral cochlear nerve and the ascending auditory brainstem pathway. Guthrie *et al.* (2014) measured impairment in brainstem response in rats to changes in sound stimulus level. The green line in Figure 22 shows the effect of prior long-term fuel exposure on WII waveform, compared with control (black thick line). The upper dotted curve shows preliminary model simulations using the simple neuron circuit model described above. The lower dotted curve shows the effect of reducing the inhibitory receptor density $R_{i,c2}$ by a factor of 10 from the upper curve, leading to a decrease in the evoked response that roughly corresponds to the impact of fuel exposure.

5.4 Model of Synaptic Neurotransmitter Kinetics

In the simple neuron circuit model proposed here, neurotransmitter levels in the synaptic cleft link the firing rate of the pre-synaptic neuron (related to the sound intensity), with the activation of receptors on the post-synaptic membrane (via receptor), and the transmission of the signal. The blocking effect of jet fuel components such as toluene on VDCCs will directly impact the release of neurotransmitters, and can be incorporated into the model at this point.

The model of synaptic neurotransmitter kinetics works on the following assumptions: A) presynaptic axonal firing rate (frequency *f*) is proportional to input sound intensity; B) each pre-synaptic action potential causes the release of a standard unit of neurotransmitter (NT); and C) neurotransmitters are removed from the synaptic cleft with a first-order rate constant *k*, which represent the "refractory period" of the signal (turnover of NT). Altering pre-synaptic firing rates (*f*) then would affect NT concentrations in the synaptic cleft (Figure 23). After a sufficiently long period of time, NT levels in the synaptic cleft would reach a plateau value, as shown by the dotted line in Figure 23.

The pre-synaptic neuron input signal intensity can now be linked with neurotransmitter levels at its axonal output. Using receptor occupancy modeling, this neurotransmitter level will then determine the response of the post-synaptic neuron, and (ultimately) signal transmission along the CAP.

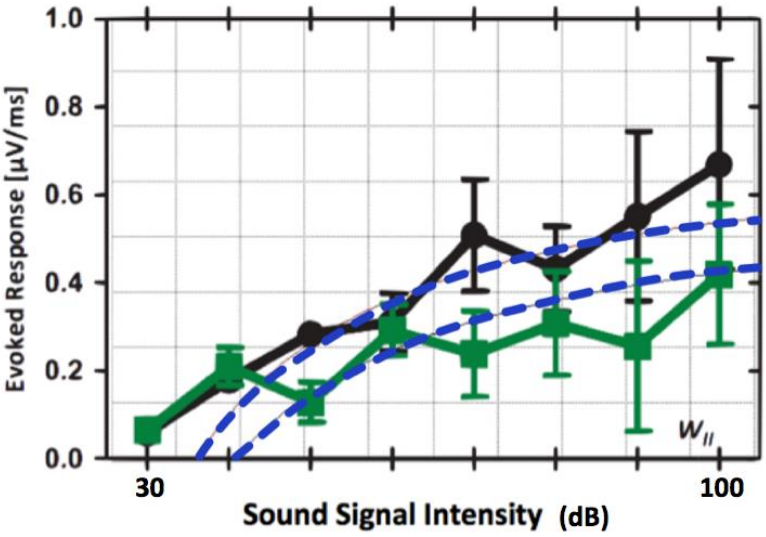

Figure 22. Evoked Response Encoding of Stimulus Intensity. See text for explanation.

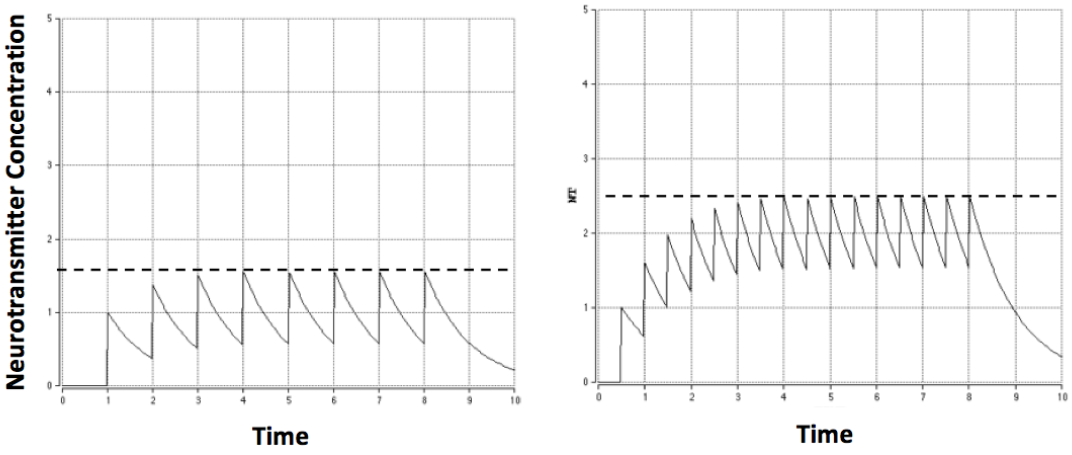

Figure 23. Simulations of Neurotransmitter Concentrations in Synaptic Cleft of Unit Volume for Two Different Pre-Synaptic Firing Rates. Firing rates for these simulations are f = 1 (left) and f = 2 (right).

6.0 CONCLUSIONS AND FUTURE WORK

6.1 PBPK Model Parameter Measurement

Overall, obtaining reasonable partition coefficients for the PBPK model was more challenging than predicted. The inherent properties (size, bony nature) of cochlea made it difficult to get measured PCs. Due to the unavailability of previously measured PCs for cochlea, it is difficult

to determine if the predicted values were appropriate or not. Cochlea and other boney structures are heterogeneous tissues with compositions consisting largely of hydroxyapatite (a mineral phase) (Boskey, 2013). The algorithms in Ruark *et al.* (2014) do not account for this composition. As the cochleae are a very small tissue in the body, the overall PBPK model is not very sensitive to the cochlea PC for an individual chemical; however, the predicted tissue concentration for the cochleae will be greatly affected. Therefore, the predicted concentration could be an order of magnitude higher or lower than predicted, making lower detection limits in the cochlea tissue even more important in order to quantify the hydrocarbon level present.

The equation from Ruark *et al.* (2014) appeared to be inadequate to predict fat partition coefficients for any of these very lipophilic compounds. Further, the equation did not agree well with measurements of nonane and decane partition coefficients in any tissues. These two aliphatic hydrocarbons have different chemical properties than toluene, ethylbenzene and xylene, and are not at all related to the chemicals (drugs) in the database from which the equation was developed. A reinvestigation of the Ruark equations to accommodate highly lipophilic compounds and better predict fat concentrations is recommended.

A theoretical approach to predicting partition coefficients in different brain regions, based on regional white matter to gray matter ratios, is presented in Appendix E. Although insufficient data on regional brain compositions were found to progress the theory beyond a preliminary concept, it should be noted that this capability is not restricted to hearing loss simulation, but could be beneficial to any project that involves determining regional brain delivery of a chemical (and for which such data is limited).

6.2 PBPK Model Improvements

Since central auditory pathway dysfunction has been found as an early indicator of JP-8 hearing loss in rats (Guthrie *et al.*, 2014), the PBPK model was expanded to contain not only a cochlea compartment, but also a brainstem and temporal lobe (central auditory pathway regions) plus a brain remainder compartment. In order to streamline the addition of these tissues, the model was first re-written into array format, allowing the addition of only one set of code per tissue, instead of five sets of code corresponding to each key hydrocarbon per tissue added. Addition of tissues into a PBPK model requires parameterization, including tissue weights (fraction of body weight), partition coefficients, and blood flows (fraction of cardiac output). Data reported herein and literature values were both utilized to parameterize the PBPK model.

The parameterized model was then utilized to estimate concentrations of the key hydrocarbons in cochlea, brain stem, temporal lobe, and the remaining brain tissue for the 1000 mg/m^3 JP-8 exposure scenario detailed by Guthrie *et al.* (2014). These predictions indicate the anticipated levels of detection needed to measure the key hydrocarbons in these tissues in a pharmacokinetic experiment using this exposure scenario. The PBPK model in its current state requires validation with tissue concentrations from such an experiment. Following validation, predicted concentrations of hydrocarbons in target brain regions can be linked to waveforms in the neural network model to estimate the magnitude of effect.

6.3 Pharmacodynamic Models

The multistage model described in Section 5 above needs to be parameterized in a future project using experimental data. In such an experiment, brain slices collected from JP-8 exposed rats could be used for quantification of changes in the inhibitory signaling system (e.g., $GABA_A$ receptor subtypes, GABA transaminase, GAT-3) within specific auditory nuclei along the central auditory pathway, using immunohistochemistry and other techniques.

Predictions from our model, suitably parameterized and validated, can be compared with human exposure/effect studies currently being conducted in Japan. Our laboratory has initiated an international agreement with the Japanese Air Self Defense Force Aeromedical Laboratory for the "Comparison of Operational Jet Fuel and Noise Exposures."

7.0 REFERENCES

Ambrosini, A., Rossi, P., De Pasqua, V., Pierelli, F., and Schoenen, J. 2003. Lack of habituation causes high intensity dependence of auditory evoked cortical potentials in migraine. Brain. 126: 2009-2015.

Bale, A., Meacham, A., Benignus, V., Bushnell, P., and Shafer, T. 2005b. Volatile organic compounds inhibit human and rat neuronal nicotinic acetylcholine receptors expressed in *Xenopus* oocytes. Toxicol.Appl.Pharmacol. 205: 77-88.

Bale, A., Smothers, C.T., and Woodward, J.J. 2002. Inhibition of neuronal nicotinic acetylcholine receptors by the abused solvent, toluene. Br.J.Pharmacol. 137: 375-383.

Bale, A.S., Tu, Y., Carpenter-Hyland, E.P., Chandler, L.J., and Woodward, J.J. 2005a. Alterations in glutamatergic and GABAergic ion channel activity in hippocampal neurons following exposure to the abused inhalant toluene. Neuroscience. 130: 197-20.

Bamiou, D. E., Liasis, A., Boyd, S., Cohen, M., and Raglan, E. 2000. Central auditory processing disorder as the presenting manifestation of subtle brain pathology. Audiology. 39: 168-172.

Beckstead, M.J., Weiner, J.L., Eger, E.I., Gong, D., and Mihic, S. 2000. Glycine and gamma-aminobutyric acid receptor function is enhanced by inhaled drugs of abuse. Mol.Pharmacol. 57: 1199-1205.

Bernabei, M., Bocchinfuso, G., Carrozzo, P., and De Angelis, C. 2000. Determination of phenolic antioxidants in aviation jet fuel. J.Chromatogr.A. 871:235-41.

Bligh, E.G. and Dyer, W.J. 1959. A rapid method of total lipid extraction and purification. Can.J.Biochem.Physiol. 37: 911-917.

Boettcher, F.A., Mills, J.H., and Norton, B.L. 1993. Age-related changes in auditory evoked potentials of gerbils. I. Response amplitudes. Hear.Res. 71: 137-145.

Bonnefont-Rousselot, D., Rouscilles, A., Bizard, C., Delattre, J., Jore, D., and Gardès-Albert, M. 2001. Antioxidant effect of ethanol toward *in vitro* peroxidation of human low-density lipoproteins initiated by oxygen free radicals. Radiat.Res. 155: 279-287.

Boskey, A.L. 2013. Bone composition: relationship to bone fragility and antiosteoporotic drug effects. BoneKEy Rep. 2:447.

Boulares, A.H., Contreras, F.J., Espinoza, L.A., and Smulson, M.E. 2002. Roles of oxidative stress and glutathione depletion in JP-8 jet fuel- induced apoptosis in rat lung epithelial cells. Toxicol.Appl.Pharmacol. 180: 92-99.

Brown, R.P., Delp, M.D., Lindstedt, S.L., Rhomberg, L.R., and Beliles, R.P. 1997. Physiological parameter values for physiologically based pharmacokinetic models. Toxicol.Ind.Health 13: 407-484.

Campo, P., Lataye, R., Loquet, G., and Bonnet, P. 2001. Styrene-induced hearing loss: a membrane insult. Hear.Res. 154: 170-180.

Chavko, M., Nemoto, E.M., and Melick, J.A. 1993. Regional lipid composition in the rat brain. Molec.Chem.Neuropathol. 18: 123-131.

Clewell, H.J., III, Gentry, P.R., Gearhart, J.M., Covington, T.R., Banton, M.I., and Andersen, M.E. 2001. Development of a physiologically based pharmacokinetic model of isopropanol and its metabolite acetone. Toxicol.Sci. 63: 160-172.

Cruz, S.L., Balster, R.L., Orta-Salazar, G., Gathereau, M.Y., Millan- Perez, P.L., and Salinas-Stefanon, E.M. 2003. Inhibition of cardiac sodium currents by toluene exposure. Br. J. Pharmacol. 140: 653–660.

Cruz, S.L., Mirshahi, T., Thomas, B., Balster, R.L., and Woodward, J.J. 1998. Effects of the abused solvent toluene on recombinant N-methyl-D- aspartate and non-N-methyl-D-aspartate receptors expressed in Xenopus oocytes. J.Pharmacol.Exp.Ther. 286: 334-340.

Delp, M.D., Manning, R.O., Bruckner, J.V. and Armstrong, R.B. 1991. Distribution of cardiac output during diurnal changes of activity in rats. Am.J.Physiol. 261(5 Pt 2): H1487-H1493.

Fechter, L.D. 1999. Mechanisms of ototoxicity by chemical contaminants: Prospects for intervention. Noise.Health 1: 10-27.

Fechter, L.D. 2005. Oxidative stress: a potential basis for potentiation of noise-induced hearing loss. Environ.Toxicol.Pharmacol. 19: 543-546.

Fechter, L.D., Fisher, J.W., Chapman, G.D., Mokashi, V.P., Ortiz, P.A., Reboulet, J.E., Stubbs, J.E., Lear, A.M., McInturf, S.M., Prues, S.L., Gearhart, C.A., Fulton, S., and Mattie, D.R. 2012. Subchronic JP-8 jet fuel exposure enhances vulnerability to noise-induced hearing loss in rats. J.Toxicol.Environ.Health.A 75: 299-317.

Fechter, L.D., Gearhart, C., Fulton, S., Campbell, J., Fisher, J., Na, K., Cocker, D., Nelson-Miller, A., Moon, P., and Pouyatos, B. 2007. JP-8 jet fuel can promote auditory impairment resulting from subsequent noise exposure in rats. Toxicol.Sci. 98: 510-525.

Fechter, L.D., Gearhart, C.A., and Fulton, S. 2010. Ototoxic potential of JP-8 and a Fischer-Tropsch synthetic jet fuel following subacute inhalation exposure in rats. Toxicol.Sci. 116: 239-248.

Fuente, A., McPherson, B., and Hickson, L. 2011. Central auditory dysfunction associated with exposure to a mixture of solvents. Int.J.Audiol. 50: 857-65.

Gallinat, J., Bottlender, R., Juckel, G., Munke-Puchner, A., Stotz, G., Kuss, H. J., Mavrogiorgou, P., and Hegerl, U. 2000. The loudness dependency of the auditory evoked N1/P2-component as a predictor of the acute SSRI response in depression. Psychopharmacology. 148: 404-411.

Gargas, M.L., Burgess, R.J., Voisard, D.E., Cason, G.H., and Andersen, M.E. 1989. Partition coefficients of low-molecular-weight volatile chemicals in various liquids and tissues. Toxicol.Appl.Pharmacol. 98: 87-99.

Gjedde, A., Hansen, A.J., and Siemkowicz, E. 1980. Rapid simultaneous determination of regional blood flow and blood-brain glucose transfer in brain of rat. Acta Physiol.Scand. 108: 321-330.

Guest, M., Boggess, M., Attia, J., D'Este, C., Brown, A., Gibson, R., Tavener, M., Gardner, I., Harrex, W., Horsley, K., and Ross, J. 2010. Hearing impairment in F-111 maintenance workers: The study of health outcomes in aircraft maintenance personnel (SHOAMP) general health and medical study. Am.J.Ind.Med. 53: 1159-1169.

Guthrie, O.W., Xu, H., Wong, B.A., McInturf, S.M., Reboulet, J.E., Ortiz, P.A., and Mattie, D.R. 2014. Exposure to low levels of jet-propulsion fuel impairs brainstem encoding of stimulus intensity. J.Toxicol.Environ.Health.A 77: 261-280.

Haddad, S., Tardif, R., Charest-Tardif, G., and Krishnan, K. 1999. Physiological modeling of the toxicokinetic interactions in a quaternary mixture of aromatic hydrocarbons. Toxicol.Appl.Pharmacol. 161: 249-257.

Henderson, D., Bielefeld, E.C., Harris, K.C., and Hu, B.H. 2006. The role of oxidative stress in noise-induced hearing loss. Ear.Hear. 27: 1-19.

Hester, S.D., Johnstone, A.F.M., Boyes, W.K., Bushnell, P.J., and Shafer, T.J. 2011. Acute toluene exposure alters expression of genes in the central nervous system associated with synaptic structure and function. Neurotoxicol.Teratol. 33: 521–529.

Hillerdal, M. 1987. Cochlear blood flow in the rat. A methodological evaluation of the microsphere method. Hear.Res. 27: 27-35.

Hillerdal, M., Sperber, G.O., and Bill, A. 1987. The microsphere method for measuring low blood flows: theory and computer simulations applied to findings in the rat cochlea. Acta Physiol.Scand. 130: 229-235.

Jaruchinda, P., Thongdeetae, T., Panichkul, S., and Hanchumpol, P. 2005. Prevalence and an analysis of noise--induced hearing loss in army helicopter pilots and aircraft mechanics. J.Med.Assoc.Thai 88 Suppl 3: S232-239.

Johnson, A.C. and Morata, T.C. 2010. The Nordic Expert Group for Criteria Documentation of Health Risks from Chemicals. 142. Occupational Exposure to Chemicals and Hearing Impairment. Gothenburg, Sweden: Arbete och Halsa, University of Gothenburg.

Joshi, G., Tremblay, R.T., Martin, S.A., and Fisher, J.W. 2010. Partition coefficients for nonane and its isomers in the rat. Toxicol.Mechan.Methods. 20: 594-599.

Kalinec, G.M., Webster, P., Lim, D.J., and Kalinec, F. 2003. A cochlear cell line as an *in vitro* system for drug ototoxicity screening. Audiol.Neurootol. 8: 177-189.

Kaufman, L.R., LeMasters, G.K., Olsen, D.M., and Succop, P. 2005. Effects of concurrent noise and jet fuel exposure on hearing loss. J Occup.Environ.Med. 47: 212-218.

Kim, H.Y. and Salem, N. 1990. Separation of lipid classes by solid phase extraction. J.Lipid Res. 31: 2285-9.

Kou, Z.Z., Qu, J., Zhang, D.L., Li, H., and Li, Y.Q. 2013. Noise-induced hearing loss is correlated with alterations in the expression of $GABA_B$ receptors and PKC gamma in the murine cochlear nucleus complex. Front.Neuroanat, 7: 25.

Krasowski, M. and Harrison, N. 2000. The actions of ether, alcohol and alkane general anaesthetics on GABAA and glycine receptors and the effects of TM2 and TM3 mutations. Br.J.Pharmacol. 129: 731-743

Kruger, L., Saporta, S., and Swanson, L.W. 1995. Photographic Atlas of the Rat Brain: The Cell and Fiber Architecture Illustrated in Three Planes with Stereotaxic Coordinates. Cambridge University Press, New York, NY

Larsen, H.C., Angelborg, C., and Slepecky, N. 1984. Determination of the regional cochlear blood flow in the rat cochlea using non-radioactive microspheres and serially sectioned cochleas. Hear.Res. 16: 127-132.
Lataye, R., Campo, P., and Loquet, G. 2000. Combined effects of noise and styrene exposure on hearing function in the rat. Hear.Res. 139: 86-96.
Lawoko-Kerali, G., Milo, M., Davies, D., Halsall, A., Helyer, R., Johnson, C.M., Rivolta, M.N., Tones, M.A., and Holley, M.C. 2004. Ventral otic cell lines as developmental models of auditory epithelial and neural precursors. Dev. Dyn. 231: 801-814.
LeBel, C.P. and Schatz, R.A. 1989. Effect of toluene on rat synaptosomal phospholipid methylation and membrane fluidity Biochem.Pharmacol. 38: 4005-4011.
Lin, B., Ritchie, G.D., Rossi, J.R., and Pancrazio, J.J. 2001. Identification of target genes responsive to JP-8 exposure in the rat. Toxicol.Ind.Health. 17: 262–269.
Liu, Y. and Fechter, L.D. 1997. Toluene disrupts outer hair cell morphometry and intracellular calcium homeostasis in cochlear cells of guinea pigs. Toxicol.Appl.Pharmacol. 142: 270-277.
Liu, Y., Rao, D., and Fechter, L.D. 1997. Correspondence between middle frequency auditory loss *in vivo* and outer hair cell shortening *in vitro*. Hear.Res. 112: 134-140.
Lopreato, G.F., Phelan, R., Borghese, C.M., Beckstead, M.J., and Mihic, S.J. 2003. Inhaled drugs of abuse enhance serotonin-3 receptor function. Drug Alcohol Depend. 70: 11-15.
Lund, S.P., Simonsen, L., Hass, U., Ladefoged, O., Lam, H.R., and Ostergaard, G. 1996. Dearomatized white spirit inhalation exposure causes long-lasting neurophysiological changes in rats. Neurotoxicol.Teratol. 18: 67-76.
Maguin, K., Campo, P., and Parietti-Winkler, C. 2009. Toluene can perturb the neuronal voltage-dependent Ca^{2+} channels involved in the middle-ear reflex. Toxicol.Sci. 107: 473-481.
Mahle, D.A., Gearhart, J.M., Grigsby, C.C., Mattie, D.R., Barton, H.A., Lipscomb, J.C., and Cook, R.S. 2007. Age-dependent partition coefficients for a mixture of volatile organic solvents in Sprague-Dawley rats and humans. J.Toxicol.Environ.Health A 70: 1745-1751.
Merrill, E.A., Gearhart, J.M., Sterner, T.R., and Robinson, P.J. 2008. Improved predictive model for n-decane kinetics across species, as a component of hydrocarbon mixtures. Inhal.Toxicol. 20: 851-863.
Montgomery, J. 2007. Groundwater Chemicals Desk Reference, 4th Edition. CRC Press.
Morizono, T., Johnstone, B.M., and Kaldor, I. 1968. Cochlear blood volume in the guinea pig measured with Cr^{51} labelled red blood cells. Jibi to Rinsho. 14: 82-89.
Perleberg, U.R., Keys, D.A., and Fisher, J.W. 2004. Development of a physiologically based pharmacokinetic model for decane, a constituent of Jet Propellent-8. Inhal.Toxicol. 16: 771-783.
Poirrier, A.L., Pincemail, J., Van Den, A.P., Lefebvre, P.P., and Malgrange, B. 2010. Oxidative stress in the cochlea: an update. Curr.Med.Chem. 17: 3591-3604.
Popelar, J., Groh, D., Pelanova, J., Canlon, B., and Syka, J. 2006. Age-related changes in cochlear and brainstem auditory functions in Fischer 344 rats. Neurobiol.Aging 27: 490-500.
R Core Team. 2015. R: A language and environment for statistical computing. R Foundation for Statistical Computing, Vienna, Austria. URL http://www.R-project.org/.
Rahman I. 2003. Oxidative stress, chromatin remodeling and gene transcription in inflammation and chronic lung diseases. J. Biochem. Mol. Biol. 36: 95-109.

Rao, D. and Fechter, L.D. 2000. Protective effects of phenyl-N-tert-butylnitrone on the potentiation of noise-induced hearing loss by carbon monoxide. Toxicol.Appl.Pharmacol 167: 125-131.

Raynal, M., Kossowski, M., and Job, A. 2006. Hearing in military pilots: one-time audiometry in pilots of fighters, transports, and helicopters. Aviat.Space Environ.Med. 77: 57-61.

Rengachary, S.S. and Ellenbogen, R.G. Principles of Neurosurgery, Elsevier Mosby, 2005

Rivolta, M.N. and Holley, M.C. 2002. Cell lines in inner ear research. J.Neurobiol. 53:306-18.

Robinson, P.J. and Merrill, E.A. 2008. A harmonized physiologically based pharmacokinetic model for nonane as a component of jet fuel. Wright-Patterson AFB, OH: Air Force Research Laboratory, Applied Biotechnology Branch. AFRL-RH-WP-TR-2008-0067, ADA502610.

Robinson, P.J., Merrill, E.A., Hoffmann, A., Sterner, T.R., Meade, M.L., and Mattie, D.R. 2015. *In vitro* studies and preliminary mathematical model for jet fuel and noise induced auditory impairment. Wright-Patterson AFB, OH: Air Force Research Laboratory, Applied Biotechnology Branch. AFRL-RH-WP-TR-2015-0084.

Robinson, P.J., Sterner, T.R., Merrill, E.A., Gearhart, J.M., and Mattie, D.R. 2013. Preliminary Mathematical Model for Jet Fuel Exacerbated Noise-Induced Hearing Loss Wright-Patterson AFB, OH: Air Force Research Laboratory, 711th Human Performance Wing, Human Effectiveness Directorate, Bioeffects Division, Molecular Bioeffects Branch. AFRL-RH-WP-TR-2013-0044, ADA582106.

Ruark, C.D., Hack, C.E., Robinson, P.J., Mahle, D.A., and Gearhart, J.M. 2014. Predicting passive and active tissue:plasma partition coefficients: Interindividual and interspecies variability. J.Pharm.Sci. 103: 2189-2198.

Sanmartín-Suárez C, Soto-Otero R, Sánchez-Sellero I, Méndez-Álvarez E. 2011. Antioxidant properties of dimethyl sulfoxide and its viability as a solvent in the evaluation of neuroprotective antioxidants. J.Pharmacol.Toxicol.Methods. 63: 209-15.

Schaette, R. and Kempter, R. 2012. Computational models of neurophysiological correlates of tinnitus. Front.Syst.Neurosci. 6: 34.

Schmitt, W. 2008. General approach for the calculation of tissue to plasma partition coefficients. Toxicol.InVitro 22: 457-467.

SCOEL. 2007. Recommendation of the Scientific Committee on Occupational Exposure Limits for "White Spirit". Bilbao, Spain: Scientific Committee on Occupational Exposure Limits, European Commission. SCOEL/SUM/87.

Shafer, L.M., Striebich, R.C., Gomach, J. and Edwards, T. 2006. Chemical class composition of commercial jet fuels and other specialty kerosene fuels: 14th AIAA/AHI Space Planes and Hypersonic Systems and Technologies Conference, American Institute of Aeronautics and Astronautics. AIAA 2006-7972.

Shulman, A., Strashun, A.M., and Goldstein, B.A. 2002. $GABA_A$ - benzodiazepine-chloride receptor-targeted therapy for tinnitus control: Preliminary report. Int.Tinnitus J. 8: 30-36.

Smedje, G., Lunden, M., Gartner, L., Lundgren, H., and Lindgren, T. 2011. Hearing status among aircraft maintenance personnel in a commercial airline company. 13: 364-370.

Sterner, T.R., Robinson, P.J., Mattie, D.R., Burton, G.A. 2004. Analysis of algorithms for predicting blood: air and tissue partition coefficients from solvent partition coefficients for use in complex mixture physiologically based pharmacokinetic/pharmacodynamics modeling. AFRL Technical Report No. AFRL-HE-WP-TR-2004-0032.

Stucker, J.P., Schank, J.F., Dombey-Moore, B. 1994. Assessment of DoD fuel standardization policies. Santa Monica CA: RAND National Defense Research Institute.
Tillar, R., Shafer, T., and Woodward, J. 2002. Toluene inhibits voltage- sensitive Ca2þ channels expressed in pheochromocytoma cells. Neurochem. Int. 41: 391-397.
Wasik, S.P., Tewari, Y.B., Miller, M.M., and Martire, D.E. 1981. Octanol/Water Partition Coefficients and Aqueous Solubilities of Organic Compounds. National Bureau of Standards Report No. NBSIR-81-2406.
Woodward, J. J., Nowak, M., and Davies, D. L. 2004. Effects of the abused solvent toluene on recombinant P2X receptors expressed in HEK293 cells. Brain Res.Mol.Brain Res. 125: 86–95.
Work, F. 2011. Development of multi-fuel, power dense engines for maritime combat craft, J.Marine Eng.Technol. 10: 37-46.
Zhou, X., Jen, P.H., Seburn, K.L., Frankel, W.N., and Zheng, Q.Y. 2006. Auditory brainstem responses in 10 inbred strains of mice. Brain.Res. 1091: 16-20.

APPENDIX A. ARRAY PHARMACOKINETIC MODEL CODE

Note that acslX allows for longer lines than Microsoft Word, in which this appendix is formatted. Use of this code in acslX will require careful vetting to ensure that lines are begun in a format acceptable in acslX and to ensure that code is not arbitrarily split between lines.

```
PROGRAM: JFHL_5HC.CSL
!   NOTE: CINT is only 2x TSQInf - may have to decrease CINT for SQ somulations

! Model currently set up to run for 5 chemicals
! Will run for fewer chemicals without modifications as long as parameters are set
accordingly
! Can change the model to run for more or less by only changing the "5" in the line
"PARAMETER (NChem=5)"


! ******************  SET INIT.M TO LOAD AT RUN TIME  *****************


INITIAL
  INTEGER NChem
  PARAMETER (NChem=5)

  DIMENSION MW(NChem), PB(NChem), PLq(NChem), PMuc(NChem), PBrn(NChem), PStm(NChem),
PTL(NChem)
  DIMENSION PCoc(NChem), PFat(NChem), PLiv(NChem), PRap(NChem), PSlw(NChem),
PSQ(NChem)
  DIMENSION PABrn(NChem), PAStm(NChem), PATL(NChem), PACoc(NChem), PAFat(NChem),
PALiv(NChem), PARap(NChem), PASlw(NChem), PASQ(NChem)
  DIMENSION VMaxC(NChem), KM(NChem), KFC(NChem), ClUrC(NChem), kUrtC(NChem),
Scrub(NChem)
  DIMENSION kAD(NChem), kAS(NChem), kTD(NChem), kTSD(NChem)
  DIMENSION Conc(NChem), IVDose(NChem), PDose(NChem), PDrink(NChem), SQDose(NChem)
  DIMENSION VMax(NChem), KF(NChem), ClUr(NChem), kUrt(NChem)
  DIMENSION IAArt(NChem), IABrn(NChem), IABrnBld(NChem), IAStm(NChem),
IAStmBld(NChem), IATL(NChem), IATLBld(NChem)
  DIMENSION IACoC(NChem), IACocBld(NChem), IAFat(NChem), IAFatBld(NChem),
IALiv(NChem), IALivBld(NChem)
  DIMENSION IARap(NChem), IARapBld(NChem), IASlw(NChem), IASlwBld(NChem), IASQ(NChem),
IASQBld(NChem)
  DIMENSION AI0(NChem), Drink(NChem), IVR(NChem), SQR(NChem), TotDose(NChem)
  DIMENSION IAExh(NChem), IAMuc(NChem), IAO(NChem), IAExc(NChem), IADu(NChem),
IASt(NChem), IAMet1(NChem), IAMet2(NChem)
  DIMENSION IAUrn(NChem), IAUCCArt(NChem), IAUCCBrn(NChem), IATotInh(NChem),
IATotIV(NChem), IATotDrink(NChem), IATotSQ(NChem)
  DIMENSION DAUCCArt(NChem), DAUCCBrn(NChem), PAUCCArt(NChem), PAUCCBrn(NChem)
  DIMENSION CAlv(NChem), CAlvPPM(NChem), CP(NChem), CEnd(NChem), CEndPPM(NChem),
PerEnd(NChem), CMix(NChem), CMixPPM(NChem), PerMix(NChem)
  DIMENSION RACh(NChem), RAMuc(NChem), RAArt(NChem), RAExh(NChem), RABrn(NChem),
RABrnBld(NChem), RAStm(NChem), RAStmBld(NChem)
  DIMENSION RATL(NChem), RATLBld(NChem), RACoc(NChem), RACocBld(NChem), RAFat(NChem),
RAFatBld(NChem)
  DIMENSION RAO(NChem), RAExc(NChem), RADu(NChem), RASt(NChem)
  DIMENSION RALiv(NChem), RALivBld(NChem), RAMet1(NChem), RAMet2(NChem), RARap(NChem),
RARapBld(NChem)
  DIMENSION RASlw(NChem), RASlwBld(NChem), RASQ(NChem), RASQBld(NChem), RAUrn(NChem),
RATotInh(NChem)
  DIMENSION CInh(NChem), CMuc(NChem), CArt(NChem), CBrn(NChem), CBrnBld(NChem),
CBrnDif(NChem)
```

```
  DIMENSION CStm(NChem), CStmBld(NChem), CStmDif(NChem), CTL(NChem), CTLBld(NChem),
CTLDif(NChem)
  DIMENSION CCoc(NChem), CCocBld(NChem), CCocDif(NChem), CFat(NChem), CFatDif(NChem),
CFatBld(NChem)
  DIMENSION CLiv(NChem), CLivBld(NChem), CLivDif(NChem), CRap(NChem), CRapBld(NChem),
CRapDif(NChem)
  DIMENSION CSFC(NChem), CSlw(NChem), CSlwBld(NChem), CSlwDif(NChem), CSQ(NChem),
CSQBld(NChem), CSQDif(NChem)
  DIMENSION CVen(NChem)
  DIMENSION ACh(NChem), AMuc(NChem), AArt(NChem), AUCCArt(NChem), AExh(NChem),
ABrn(NChem), ABrnBld(NChem), AUCCBrn(NChem)
  DIMENSION AStm(NChem), AStmBld(NChem), ATL(NChem), ATLBld(NChem), ACoc(NChem),
ACocBld(NChem)
  DIMENSION AFat(NChem), AFatBld(NChem), AO(NChem), AExc(NChem), ADu(NChem),
ASt(NChem)
  DIMENSION ALiv(NChem), ALivBld(NChem), AMet1(NChem), AMet2(NChem), ARap(NChem),
ARapBld(NChem)
  DIMENSION ASlw(NChem), ASlwBld(NChem), ASQ(NChem), ASQBld(NChem), AUrn(NChem)
  DIMENSION ATotInh(NChem), ATotIV(NChem), ATotDrink(NChem), ATotSQ(NChem)
  DIMENSION CBrnTotBld(NChem), CBrnTot(NChem), TDose(NChem), AmtBody(NChem),
MassBal(NChem)

  INTEGER i, j1, j2, j3, j4, j5, j6, j7, i1, i2, i3, i4, i5, i6, i7, i8, i9, i10, i11,
i12, i13, i14, i15, i16, i17, i18
  LOGICAL  CC                          ! To control whether closed or open chamber


! Total Pulmonary Ventilation Rate (L/hr for 1 kg animal)
  CONSTANT     QPC = 24.75             ! Total pulmonary ventilation (L/hr - 1 kg)

! Blood Flows (fraction of cardiac output)
  CONSTANT   QCC   = 14.6              ! Cardiac output (L/hr - 1 kg animal)
  CONSTANT   QBrnC = 0.013             ! Brain Remainder (0.02 - QStmC - QTLC)
    CONSTANT QStmC = 0.004             ! Brain Stem
    CONSTANT QTLC  = 0.003             ! Temporal Lobe
  CONSTANT   QCocC = 0.00004           ! Cochlea pair
  CONSTANT   QFatC = 0.07              ! Fat
  CONSTANT   QLivC = 0.183             ! Liver
  CONSTANT   QRapC = 0.557             ! Rapidly perfused
  CONSTANT   QSlwC = 0.16996           ! Slowly perfused (includes skin and
subcutaneous compartment)

  CONSTANT   QSQg  = 0.012             ! Flow to subcutaneous compartment per g
(L/(hr*g), based on rat muscle
                                       !  (slowly perfused), from Sterner et al. 2013

! Tissue Volumes (fraction of body weight)
  CONSTANT   BW    = 0.22              ! Body weight (kg)
  CONSTANT   VAlvC = 0.007             ! Alveolar blood
  CONSTANT   VBrnC = 0.004             ! Brain Remainder (0.006 - VStmC - VTLC)
    CONSTANT VStmC = 0.001             ! Brain Stem
    CONSTANT VTLC  = 0.001             ! Brain Temporal Lobe
  CONSTANT   VFatC = 0.10              ! Fat
  CONSTANT   VLivC = 0.034             ! Liver
  CONSTANT   VMucC = 0.0001            ! Mucous
  CONSTANT   VRapC = 0.044             ! Rapidly perfused
  CONSTANT   VSlwC = 0.65              ! Slowly perfused (includes skin, cochlea, SQ)
  CONSTANT   DS    = 0.15              ! Dead space volume (fraction)

  CONSTANT   VolSQ = 0.282             ! mL ~= g; Max value for this protocol = 0.282
mL = 0.282 g
                                       ! Parameter max value should be no larger than
25 mL/kg BW for a rat,
```

```
                                    !   per AALAS Learning Library, 2005

!Tissue Volumes (fraction of tissue volume)
  CONSTANT   VBrnBldC = 0.03            ! Brain Remainder
    CONSTANT VStmBldC = 0.03            ! Brain Stem
    CONSTANT VTLBldC  = 0.03            ! Brain Temporal Lobe
  CONSTANT   VCocBldC = 0.0183          ! Cochlea
  CONSTANT   VFatBldC = 0.0154          ! Fat
  CONSTANT   VLivBldC = 0.034           ! Liver
  CONSTANT   VRapBldC = 0.2075          ! Rapidly Perfused Tissues
  CONSTANT   VSlwBldC = 0.0333          ! Slowly Perfused Tissues
  CONSTANT   VSQBldC  = 0.0167          ! Equals 1/2 VSlwBldC
                                        ! Only half the compartment will have blood
flow, the other half is injection

! Molecular Weights (mg/mmole)
  CONSTANT      MW = NChem*1.0

! Tissue/Blood Partition Coefficients
  CONSTANT    PB   = NChem*1.0          ! Blood/air
  CONSTANT    PLq  = NChem*1.0          ! Saline/air
  CONSTANT    PMuc = NChem*1.0          ! Mucous/air
  CONSTANT    PBrn = NChem*1.0          ! Brain Remainder
    CONSTANT  PStm = NChem*1.0          ! Brain Stem
    CONSTANT  PTL  = NChem*1.0          ! Brain Temporal Lobe
  CONSTANT    PCoc = NChem*1.0          ! Cochlea
  CONSTANT    PFat = NChem*1.0          ! Fat
  CONSTANT    PLiv = NChem*1.0          ! Liver
  CONSTANT    PRap = NChem*1.0          ! Rapidly perfused tissue
  CONSTANT    PSlw = NChem*1.0          ! Slowly perfused tissue
  CONSTANT    PSQ  = NChem*1.0          ! Subcutaneous compartment

! Tissue Permeability Coefficients
  CONSTANT   PABrn = NChem*1000.0       ! Brain remainder diffusion limitation
    CONSTANT PAStm = NChem*1000.0       ! Brain stem diffusion limitation
    CONSTANT PATL  = NChem*1000.0       ! Brain temporal lobe diffusion limitation
  CONSTANT   PACoc = NChem*1000.0       ! Cochlea diffusion limitation
  CONSTANT   PAFat = NChem*1000.0       ! Fat diffusion limitation
  CONSTANT   PALiv = NChem*1000.0       ! Liver diffusion limitation
  CONSTANT   PARap = NChem*1000.0       ! Rapidly perfused tissues diffusion limitation
  CONSTANT   PASlw = NChem*1000.0       ! Slowly perfused tissues diffusion limitation
  CONSTANT   PASQ  = NChem*1000.0       ! Subcutaneous compartment diffusion limitation

! Metabolism Parameters
  CONSTANT   VMaxC = NChem*0.0          ! Maximum reaction rate (mg/hr)
  CONSTANT   KM    = NChem*1.0          ! Michaelis-Menten (mg/L)
  CONSTANT   KFC   = NChem*0.0          ! First order rate constant (/hr)

! Uptake and Clearance Parameters
  CONSTANT   ClUrC = NChem*0.0          ! Urinary clearance (L/hr)
  CONSTANT   kUrtC = NChem*0.0          ! URT uptake into mucus (L/hr)
  CONSTANT   Scrub = NChem*0.0          ! Fraction of inhaled dose scrubbed (not
absorbed into blood or mucus)
  CONSTANT   kAD   = NChem*0.0          ! Absorption from duodenum (/hr)
  CONSTANT   kAS   = NChem*0.0          ! Absorption from stomach (/hr)
  CONSTANT   kTD   = NChem*0.0          ! Excretion (/hr)
  CONSTANT   kTSD  = NChem*0.0          ! Transfer - stomach to duodenum (/hr)

! Dosing Parameters
  CONSTANT  Conc      = NChem*0.0         ! Inhaled concentration (ppm)
  CONSTANT  IVDose    = NChem*0.0         ! IV dose (mg/kg)
  CONSTANT  PDose     = NChem*0.0         ! Oral dose (mg/kg)
  CONSTANT  PDrink    = NChem*0.0         ! Drinking water dose (mg/kg/day)
```

```
  CONSTANT  SQDose    = NChem*0.0         ! Subcutaneous dose (mg/kg)
  CONSTANT  TChng     = 0.0               ! Length of inhalation exposure (hrs)
  CONSTANT  DaysWk    = 1.0               ! Number of exposure days per week
  CONSTANT  TMax      = 24.0              ! Maximum time for exposures
  CONSTANT  TInf      = 0.20              ! Length of IV injection (hrs)
  CONSTANT  TSQInf    = 0.02              ! Length of SQ injection (hrs)
  CONSTANT  Rats      = 1.0               ! Number of animals in experiment

! Chamber Parameter
  CONSTANT    CC   = .FALSE.           ! Default to open chamber
  CONSTANT    VChC = 9.1               ! Volume of closed chamber
  CONSTANT    kLCC = 0.0               ! Chamber loss

! Simulation Control Parameters
  CONSTANT   TStop = 24.0
  CINTERVAL  CINT  = 0.01

! Set Chamber Volume and Loss for Open and Closed Chamber Exposures
  IF (.NOT. CC) THEN
      VCh = 1.0e+20                   ! Large chamber = open chamber
      kLC = 0.0
  ELSE
      VCh = VChC - (Rats * BW)        ! Calculate net chamber volume
      kLC = kLCC
  ENDIF

! Scaled Pulmonary Ventilation Rate (L/hr)
        QCN  = QCC * (BW**0.75)
        QP   = QPC * (BW**0.75)
        QAlv = 0.67 * QP


! Scaled Blood Flows (L/hr) and Tissue Volumes (L)
       QSQC = QSQg * VolSQ     ! [L/(hr*g) * g] = L/(hr)
                               ! Compartment is assumed to affect tissue equal to the
size of injection,
                               ! with appropriate flow for that size; See Sterner et
al., 2013
       QBrn = QBrnC * QCN
         QStm = QStmC * QCN
         QTL  = QTLC * QCN
       QCoc = QCocC * QCN       ! cochlea pair
       QFat = QFatC * QCN
       QLiv = QLivC * QCN
       QRap = QRapC * QCN
       QSQ  = QSQC  * QCN


       VSQC = ((VolSQ*2.0)/1000.0)/BW          ! fraction BW
                                               ! Volume of subcutaneous tissue
compartment is 2x the size of the injection
                                               ! (equal tissue affected balooned to
twice its size by the injection)
       VAlv  = VAlvC * BW
       VMuc  = VMucC * BW
       VBrn  = (VBrnC * (1 - VBrnBldC) ) * BW
         VStm  = (VStmC * (1 - VStmBldC) ) * BW
         VTL   = (VTLC * (1 - VTLBldC) ) * BW
       VCocM = 0.00007 *(BW**0.2348)           ! Data based calculation of cochlea
pair mass (kg)
         VCoc  = VCocM * (1 - VCocBldC)
       VFat  = (VFatC * (1 - VFatBldC) ) * BW
       VLiv  = (VLivC * (1 - VLivBldC) ) * BW
```

```
        VRap  = (VRapC * (1 - VRapBldC) ) * BW
        VSQ   = (VSQC  * (1 - VSQBldC)  ) * BW

     VBrnBld = VBrnBldC * (VBrnC * BW)
       VStmBld = VStmBldC * (VStmC * BW)
       VTLBld  = VTLBldC * (VTLC * BW)
     VCocBld = VCocBldC * VCocM
     VFatBld = VFatBldC * (VFatC * BW)
     VLivBld = VLivBldC * (VLivC * BW)
     VRapBld = VRapBldC * (VRapC * BW)
     VSlwBld = VSlwBldC * (VSlwC * BW)
     VSQBld  = VSQBldC  * (VSQC  * BW)

        QSlw = (QSlwC * QCN) - QSQ
        QC   = QBrn + QStm + QTL + QCoc + QFat + QLiv + QRap + QSlw + QSQ
        QTot = QCN - QC

        VSlw    = ((VSlwC * (1 - VSlwBldC) ) * BW) - VCoc - VCocBld - VSQ - VSQBld
        VTotTis = VBrn + VStm + VTL + VCoc + VFat + VLiv + VRap + VSlw + VSQ
        VTotBld = VBrnBld + VStmBld + VTLBld + VCocBld + VFatBld + VLivBld + VRapBld +
VSlwBld + VSQBld
        VTot    = (VTotTis + VTotBld)/BW


DO 1030 i=1, NChem
! Scaled Metabolism Parameters
     VMax(i) = VMaxC(i) * (BW**0.75)
     KF(i) = KFC(i) / (BW**0.25)

! Scaled Clearance Rates
     ClUr(i) = ClUrC(i) * (BW**0.75)
     kUrt(i) = (min(kUrtC(i), QPC)) * (BW**0.75)

! Initial Amounts (mg)
  IAArt(i) = 0.0
  IABrn(i) = 0.0
    IAStm(i) = 0.0
    IATL(i) = 0.0
  IABrnBld(i) = 0.0
    IAStmBld(i) = 0.0
    IATLBld(i) = 0.0
  IACoc(i) = 0.0
    IACocBld(i) = 0.0
  IAFat(i) = 0.0
    IAFatBld(i) = 0.0
  IALiv(i) = 0.0
    IALivBld(i) = 0.0
  IARap(i) = 0.0
    IARapBld(i) = 0.0
  IASlw(i) = 0.0
    IASlwBld(i) = 0.0
  IASQ(i) = 0.0
    IASQBld(i) = 0.0

! Scaled and Initial Doses
     AI0(i) = (Conc(i) * VCh * MW(i)) / 24450.0                    ! Initial amount
in chamber
     Drink(i) = (PDrink(i) * BW) / 24.0                            ! Drinking water
dose (mg/hr)
     IVR(i) = 0.0                                                  ! IV dose
     SQR(i) = 0.0                                                  ! SQ Dose
     TotDose(i) = 0.0                                              ! Facilitate mass
balance check
```

```
! Initialize Initial Values for Integrating State Variables
     IAExh(i) = 0.0
     IAMuc(i) = 0.0
     IAO(i) = 0.0
     IAExc(i) = 0.0
     IADu(i) = 0.0
       IASt(i) = 0.0
     IAMet1(i) = 0.0
       IAMet2(i) = 0.0
     IAUrn(i) = 0.0
     IAUCCArt(i) = 0.0
       IAUCCBrn(i) = 0.0
     IATotInh(i) = 0.0
     IATotIV(i) = 0.0
     IATotDrink(i) = 0.0
     IATotSQ(i) = 0.0

! Initialize Starting Values
     DAUCCArt(i) = 0.0
       DAUCCBrn(i) = 0.0
     PAUCCArt(i) = 0.0
       PAUCCBrn(i) = 0.0
     PerEnd(i) = 0.0
     PerMix(i) = 0.0
1030: CONTINUE


! Initialize Starting Values
      CIZone = 1.0
     CSFZone = 0.0
      DayExp = 1.0

END               ! End of Initial


DYNAMIC
  ALGORITHM  IALG = 2                                                  ! Gear stiff
method


DISCRETE DoseOn    ! Start dosing
  INTERVAL DoseInt = 24.0                                              ! Interval to
repeat dosing
  SCHEDULE DoseOffIV .AT. T + TInf
  SCHEDULE DoseOffIhl .AT. T + TChng
  SCHEDULE DoseOffSQ .AT. T + TSQInf

  IF (((T .LT. TMax) .AND. (DayExp .LE. DaysWk)) .OR. CC) THEN
    CIZone = 1.0
  ENDIF

  DayExp = DayExp + 1.0

 IF (DayExp .GT. 7.0) THEN
    DayExp = 0.5
  ENDIF

DO 1040 j1=1, NChem
   IF (T .LE. TInf) THEN
     IVR(j1) = (IVDose(j1) * BW) / TInf              ! Rate of intravenous dosing
(mg/hr)
     TotDose(j1) = TotDose(j1) + (PDose(j1) * BW)
```

```
   ENDIF
1040: CONTINUE

DO 1045 j6=1, NChem
   IF (T. LE. TSQInf) THEN
     SQR(j6) = (SQDose(j6) * BW) / TSQInf            ! Rate of SQ dosing (mg/hr)
   ENDIF
1045: CONTINUE

END


DISCRETE DoseOffIV
DO 1050 j2=1, NChem
     IVR(j2) = 0.0
1050: CONTINUE
END


DISCRETE DoseOffIhl
  IF (.NOT. CC) THEN
    CIZone = 0.0
  ENDIF
END


DISCRETE DoseOffSQ
  DO 1055 j7=1, NChem
       SQR(j7) = 0.0
  1055: CONTINUE
END


DISCRETE Calc      ! Calculate daily average AUC (D) using previous value (P)
! Note that this is calculated for the Brain Remainder and not the whole brain
  INTERVAL CalcInt = 24.0

DO 1060 j3=1, NChem
     DAUCCArt(j3) = (AUCCArt(j3) - PAUCCArt(j3)) / (CalcInt / 24.0)
     DAUCCBrn(j3) = (AUCCBrn(j3) - PAUCCBrn(j3)) / (CalcInt / 24.0)

     IF (T .GT. 0.0) THEN
         PAUCCArt(j3) = AUCCArt(j3)
         PAUCCBrn(j3) = AUCCBrn(j3)
     ENDIF
1060: CONTINUE
END      ! End of Calc


!-------------------- Calculate Parameters Used for Plotting -------------------------
-----------------------------------------
       Hours = T
     Minutes = T * 60.0
        Days = T / 24.0

DO 2010 i1=1, NChem
! Concentration in Alveolar Air (mg/L and ppm)
     CAlv(i1) = CArt(i1) / PB(i1)
     CAlvPPM(i1) = (CArt(i1) / PB(i1)) * (24450.0 / MW(i1))

! Concentration in Inhaled Air (ppm)
     CP(i1) = (CInh(i1) * 24450.0) / MW(i1)
```

```
! Concentration in End-Exhaled Air (mg/L, ppm and percent)
     CEnd(i1) = RAExh(i1) / QAlv
     CEndPPM(i1) = CEnd(i1) * (24450.0 / MW(i1))

     IF (Conc(i1) .GT. 0.0) THEN
       PerEnd(i1) = (CEnd(i1) / ((Conc(i1) * MW(i1)) / 24450.0)) * 100.0
     ENDIF

! Concentration in Mixed Exhaled Air (mg/L, ppm and percent)
     CMix(i1) = ((1.0 - DS) * CEnd(i1)) + (DS * CInh(i1))
     CMixPPM(i1) = CMix(i1) * (24450.0 / MW(i1))

     IF (Conc(i1) .GT. 0.0) THEN
       PerMix(i1) = (CMix(i1) / ((Conc(i1) * MW(i1)) / 24450.0)) * 100.0
     ENDIF
2010: CONTINUE

     CArtTot = 0.0
     AExhAll = 0.0

DO 2020 i2=1, NChem
! Total Concentration in Arterial Blood (mg/L)
      CArtTot = CArtTot + CArt(i2)

! Total Amount Exhaled (mg)
      AExhAll = AExhAll + AExh(i2)
2020: CONTINUE


DERIVATIVE
!-------------------------------------------------------------------------------------------
-----------------------------------------
! Amount in Inhaled Air (mg)
         ACh = INTVC(RACh, AI0)

! Concentration in Inhaled Air (mg/L) and Rate of Change in Chamber Concentration
(mg/hr)
  PROCEDURAL (CInh, RACh = QAlv, VCh, kLC, kUrt, CIZone, CMuc, CArt)
DO 3030 i3=1, NChem
       CInh(i3) = ( (ACh(i3) / VCh) * (1-Scrub(i3)) ) * CIZone
       RACh(i3) = (Rats * ((-QAlv * CInh(i3)) + (QAlv * (CArt(i3) / PB(i3))) +
(kUrt(i3) * ((CMuc(i3) / PMuc(i3)) - (CArt(i3) / PB(i3))))))&
              & - (kLC * ACh(i3))
3030: CONTINUE
  END

! Amount in Mucous (mg)
        AMuc = INTVC(RAMuc, IAMuc)

! Amount in Arterial Blood (mg)
        AArt = INTVC(RAArt, IAArt)
     AUCCArt = INTVC(CArt, IAUCCArt)

! Amount in Exhaled Air (mg)
        AExh = INTVC(RAExh, IAExh)

  PROCEDURAL (CMuc, CArt = VAlv, VMuc)
    DO 3040 i4=1, NChem
       CMuc(i4) = AMuc(i4) / VMuc                                    ! Concentration
of in mucous (mg/L)
       CArt(i4) = AArt(i4) / VAlv                                    ! Concentration
of in arterial blood (mg/L)
3040: CONTINUE
```

```
  END
!-----------------------------------------------------------------------------------------
-----------------------------------------


!-----------------------------------------------------------------------------------------
-----------------------------------------
  PROCEDURAL (CVen, RAMuc, RAArt, RAExh = QBrn, CBrnBld, QStm, CStmBld, QTL, CTLBld,
QCoc, CCocBld, QFat, CFatBld, QLiv, CLivBld, &
            & QRap, CRapBld, QSlw, CSlwBld, QSQ, CSQBld, IVR, QC, kUrt, CInh, CMuc,
PMuc, CArt, PB, QAlv, CVen, RAUrn, QAlv)
DO 3050 i5=1, NChem
! Concentration in Mixed Venous Blood (mg/L)
       CVen(i5) = (QBrn*CBrnBld(i5) + QStm *CStmBld(i5) + QTL*CTLBld(i5) +
QCoc*CCocBld(i5) + QFat*CFatBld(i5) + QLiv*CLivBld(i5) &
             & + QRap*CRapBld(i5) + QSlw*CSlwBld(i5) + QSQ*CSQBld(i5) + IVR(i5)) / QC

! Rate of Change in Mucus (mg/hr)
       RAMuc(i5) = (kUrt(i5) * (CInh(i5) - (CMuc(i5) / PMuc(i5)))) - (kUrt(i5) *
((CMuc(i5) / PMuc(i5)) - (CArt(i5) / PB(i5))))

! Rate of Change in Arterial Blood (mg/hr)
       RAArt(i5) = (QAlv * CInh(i5)) - (kUrt(i5) * (CInh(i5) - (CMuc(i5) / PMuc(i5))))
- (QAlv * (CArt(i5) / PB(i5))) &
              & + (QC * (CVen(i5) - CArt(i5))) - RAUrn(i5)

! Rate of Change in Exhaled Air (mg/hr)
       RAExh(i5) = (QAlv * (CArt(i5) / PB(i5))) + (kUrt(i5) * ((CMuc(i5) / PMuc(i5)) -
(CArt(i5) / PB(i5))))
3050: CONTINUE
  END
!-----------------------------------------------------------------------------------------
-----------------------------------------


!-----------------------------------------------------------------------------------------
-----------------------------------------
! Brain Remainder Blood and Brain Remainder Tissue

     ABrnBld = INTVC(RABrnBld, IABrnBld)                                ! Amount in
brain remainder blood (mg)
        ABrn = INTVC(RABrn, IABrn)                                      ! Amount in
brain remainder tissue (mg)
     AUCCBrn = INTVC(CBrn, IAUCCBrn)                                    ! Area under the
curve for the concentration in brain remainder tissue (hr*mg/L)

  PROCEDURAL (CBrnBld, CBrn, CBrnDif, RABrnBld, RABrn = ABrnBld, VBrnBld, ABrn, VBrn,
PBrn, QBrn, CArt, PABrn)
DO 3060 i6=1, NChem
       CBrnBld(i6) = ABrnBld(i6) / VBrnBld                              ! Concentration
in brain remainder blood (mg/L)
          CBrn(i6) = ABrn(i6) / VBrn                                    ! Concentration
in brain remainder tissue (mg/L)
       CBrnDif(i6) = CBrn(i6) / PBrn(i6)                                ! Concentration
available for diffusion (mg/L)
      RABrnBld(i6) = (QBrn *(CArt(i6) - CBrnBld(i6)))+(PABrn(i6) * (CBrnDif(i6) -
CBrnBld(i6)))
                                                                       ! Rate of change
in brain remainder blood (mg/hr)
         RABrn(i6) = PABrn(i6) * (CBrnBld(i6) - CBrnDif(i6))           ! Rate of change
in brain remainder tissue (mg/hr)

3060: CONTINUE
```

```
  END
!-------------------------------------------------------------------------------------------
-----------------------------------------

!-------------------------------------------------------------------------------------------
-----------------------------------------
! Brain Stem and Brain Stem Tissue

     AStmBld = INTVC(RAStmBld, IAStmBld)                                  ! Amount in
brain stem blood (mg)
        AStm = INTVC(RAStm, IAStm)                                        ! Amount in
brain stem tissue (mg)

  PROCEDURAL (CStmBld, CStm, CStmDif, RAStmBld, RAStm = AStmBld, VStmBld, AStm, VStm,
PStm, QStm, CArt, PAStm)
DO 3062 i16=1, NChem
       CStmBld(i16) = AStmBld(i16) / VStmBld                               !
Concentration in brain stem blood (mg/L)
          CStm(i16) = AStm(i16) / VStm                                     !
Concentration in brain stem tissue (mg/L)
       CStmDif(i16) = CStm(i16) / PStm(i16)                                !
Concentration available for diffusion (mg/L)
      RAStmBld(i16) = (QStm *(CArt(i16) - CStmBld(i16)))+(PAStm(i16) * (CStmDif(i16) -
CStmBld(i16)))
                                                                          ! Rate of
change in brain stem blood (mg/hr)
         RAStm(i16) = PAStm(i16) * (CStmBld(i16) - CStmDif(i16))          ! Rate of
change in brain stem tissue (mg/hr)

3062: CONTINUE
  END
!-------------------------------------------------------------------------------------------
-----------------------------------------


!-------------------------------------------------------------------------------------------
-----------------------------------------
! Brain Temporal Lobe and Brain Temporal Lobe Tissue

     ATLBld = INTVC(RATLBld, IATLBld)                                   ! Amount in brain
temporal lobe blood (mg)
        ATL = INTVC(RATL, IATL)                                         ! Amount in brain
temporal lobe tissue (mg)

  PROCEDURAL (CTLBld, CTL, CTLDif, RATLBld, RATL = ATLBld, VTLBld, ATL, VTL, PTL, QTL,
CArt, PATL)
DO 3064 i17=1, NChem
       CTLBld(i17) = ATLBld(i17) / VTLBld                                 ! Concentration
in brain temporal lobe blood (mg/L)
          CTL(i17) = ATL(i17) / VTL                                       ! Concentration
in brain temporal lobe tissue (mg/L)
       CTLDif(i17) = CTL(i17) / PTL(i17)                                  ! Concentration
available for diffusion (mg/L)
      RATLBld(i17) = (QTL *(CArt(i17) - CTLBld(i17)))+(PATL(i17) * (CTLDif(i17) -
CTLBld(i17)))
                                                                         ! Rate of change
in brain temporal lobe blood (mg/hr)
         RATL(i17) = PATL(i17) * (CTLBld(i17) - CTLDif(i17))             ! Rate of change
in brain tissue (mg/hr)

3064: CONTINUE
  END
```

```
!-------------------------------------------------------------------------------------------
-----------------------------------------


!-------------------------------------------------------------------------------------------
-----------------------------------------
! Cochlea Tissue Blood and Cochlea Tissue

     ACocBld = INTVC(RACocBld, IACocBld)                                  ! Amount in
cochlea blood (mg)
        ACoc = INTVC(RACoc, IACoc)                                        ! Amount in
cochlea tissue (mg)

  PROCEDURAL (CCoCBld, CCoC, CCoCDif, RACoCBld, RACoC = ACocBld, VCoCBld, ACoC, VCoC,
PCoC, QCoC, CArt, PACoC)
DO 3070 i15=1, NChem
       CCocBld(i15) = ACocBld(i15) / VCocBld                              ! Concentration
in cochlea blood (mg/L)
          CCoc(i15) = ACoc(i15) / VCoc                                    ! Concentration
in cochlea (mg/L)
       CCocDif(i15) = CCoc(i15) / PCoc(i15)                               ! Concentration
available for diffusion (mg/L)
      RACocBld(i15) = (QCoc *(CArt(i15) - CCocBld(i15)))+(PACoc(i15) * (CCocDif(i15) -
CCocBld(i15)))
                                                                         ! Rate of change
in cochlea blood (mg/hr)
         RACoc(i15) = PACoc(i15) * (CCocBld(i15) - CCocDif(i15))         ! Rate of change
in cochlea (mg/hr)
3070: CONTINUE
  END
!-------------------------------------------------------------------------------------------
-----------------------------------------


!-------------------------------------------------------------------------------------------
-----------------------------------------
! Fat Blood and Fat Tissue
     AFatBld = INTVC(RAFatBld, IAFatBld)
                                                    ! Amount in fat blood (mg)
        AFat = INTVC(RAFat, IAFat)                                        ! AMount in fat
tissue (mg)

  PROCEDURAL (CFatBld, CFat, CFatDif, RAFatBld, RAFat = AFatBld, VFatBld, AFat, VFat,
PFat, QFat, CArt, PAFat)
DO 3075 i7=1, NChem
      CFatBld(i7) = AFatBld(i7) / VFatBld                                ! Concentration
in fat blood (mg/L)
         CFat(i7) = AFat(i7) / VFat                                      ! Concentration
in fat tissue (mg/L)
      CFatDif(i7) = CFat(i7) / PFat(i7)                                  ! Concentration
available for diffusion (mg/L)
     RAFatBld(i7) = (QFat *(CArt(i7) - CFatBld(i7)))+(PAFat(i7) * (CFatDif(i7) -
CFatBld(i7)))
                                                                         ! Rate of change
in fat blood (mg/hr)
        RAFat(i7) = PAFat(i7) * (CFatBld(i7) - CFatDif(i7))              ! Rate of change
in fat tissue (mg/hr)
3075: CONTINUE
  END
!-------------------------------------------------------------------------------------------
-----------------------------------------
```

```
!-------------------------------------------------------------------------------------------
-----------------------------------------
! Digestive Tract
!  Amount Absorbed (mg)
          AO = INTVC(RAO, IAO)

!  Amount Excreted (mg)
        AExc = INTVC(RAExc, IAExc)

!  Amount Duodenum (mg)
         ADu = INTVC(RADu, IADu)

!  Amount Leaving the Stomach (mg)
!  (ASt changed to (INTVC(RASt, IASt)) and is replaced in other equations with
(TotDose(i) - ASt(i)) since ASt
!   could not be defined as (TotDose - INTVC(RASt, 0.0)))
         ASt = INTVC(RASt, IASt)

! Rate of Change in Amount Absorbed, Amount Excreted, Amount in Duodenum and Amount
Leaving Stomach (mg/hr)
  PROCEDURAL (RAO, RAExc, RADu, RASt = TotDose)
DO 3080 i8=1, NChem
       RAO(i8) = (kAS(i8) * (TotDose(i8) - ASt(i8))) + (kAD(i8) * ADu(i8))
       RAExc(i8) = kTD(i8) * ADu(i8)
       RADu(i8) = (kTSD(i8) * (TotDose(i8) - ASt(i8))) - (kAD(i8) * ADu(i8)) -
(kTD(i8) * ADu(i8))
       RASt(i8) = (kAS(i8) * (TotDose(i8) - ASt(i8))) + (kTSD(i8) * (TotDose(i8) -
ASt(i8)))
3080: CONTINUE
  END
!-------------------------------------------------------------------------------------------
-----------------------------------------


!-------------------------------------------------------------------------------------------
-----------------------------------------
! Liver Blood and Liver Tissue
     ALivBld = INTVC(RALivBld, IALivBld)                              ! Amount in liver
blood (mg)
        ALiv = INTVC(RALiv, IALiv)                                    ! Amount in
liver tissue (mg)

       AMet1 = INTVC(RAMet1, IAMet1)                                  ! Amount
metabolized, saturable (mg)
       AMet2 = INTVC(RAMet2, IAMet2)                                  ! Amount
metabolized, first order (mg)

  PROCEDURAL (CLivBld, CLiv, CLivDif, RALivBld, RAMet1, RAMet2, RALiv = ALivBld,
VLivBld, ALiv, VLiv, PLiv, QLiv, CArt, PALiv, VMax, KF, RAO, Drink)
DO 3090 i9=1, NChem
       CLivBld(i9) = ALivBld(i9) / VLivBld                            !
Concentration in liver blood (mg/L)
          CLiv(i9) = ALiv(i9) / VLiv                                  !
Concentration in liver tissue (mg/L)
       CLivDif(i9) = CLiv(i9) / PLiv(i9)                              !
Concentration available for diffusion (mg/L)
      RALivBld(i9) = (QLiv *(CArt(i9) - CLivBld(i9)))+(PALiv(i9) * (CLivDif(i9) -
CLivBld(i9)))
                                                                     ! Rate of
change in liver blood (mg/hr)
        RAMet1(i9) = (VMax(i9) * CLivDif(i9)) / (KM(i9) + CLivDif(i9))  ! Saturable
rate of metabolism in liver (mg/hr)
```

```
        RAMet2(i9) = KF(i9) * CLivDif(i9) * VLiv                              ! First-
order rate of metabolism in liver (mg/hr)
         RALiv(i9) = (PALiv(i9) * (CLivBld(i9) - CLivDif(i9))) - RAMet1(i9) -
RAMet2(i9) + RAO(i9) + Drink(i9)
                                                                              ! Rate of
change in liver tissue (mg/hr)
3090: CONTINUE
  END
!-------------------------------------------------------------------------------------
-----------------------------------------


!-------------------------------------------------------------------------------------
-----------------------------------------
! Rapidly Perfused Tissue Blood and Rapidly Perfused Tissue

     ARapBld = INTVC(RARapBld, IARapBld)                                  ! Amount in
rapidly perfused tissue blood (mg)
        ARap = INTVC(RARap, IARap)                                        ! Amount in
rapidly perfused tissue (mg)

  PROCEDURAL (CRapBld, CRap, CRapDif, RARapBld, RARap = ARapBld, VRapBld, ARap, VRap,
PRap, QRap, CArt, PARap)
DO 3100 i10=1, NChem
       CRapBld(i10) = ARapBld(i10) / VRapBld                              ! Concentration
in rapidly perfused tissue blood (mg/L)
          CRap(i10) = ARap(i10) / VRap                                    ! Concentration
in rapidly perfused tissue (mg/L)
       CRapDif(i10) = CRap(i10) / PRap(i10)                               ! Concentration
available for diffusion (mg/L)
      RARapBld(i10) = (QRap *(CArt(i10) - CRapBld(i10)))+(PARap(i10) * (CRapDif(i10) -
CRapBld(i10)))
                                                                          ! Rate of change
in rapidly perfused tissue blood (mg/hr)
         RARap(i10) = PARap(i10) * (CRapBld(i10) - CRapDif(i10))          ! Rate of change
in rapidly perfused tissue (mg/hr)
3100: CONTINUE
  END
!-------------------------------------------------------------------------------------
-----------------------------------------


!-------------------------------------------------------------------------------------
-----------------------------------------
! Slowly Perfused Tissue Blood and Slowly Perfused Tissue

     ASlwBld = INTVC(RASlwBld, IASlwBld)                                  ! Amount in
slowly perfused tissue blood (mg)
        ASlw = INTVC(RASlw, IASlw)                                        ! Amount in
slowly perfused tissue (mg)

  PROCEDURAL (CSlwBld, CSlw, CSlwDif, RASlwBld, RASlw = ASlwBld, VSlwBld, ASlw, VSlw,
PSlw, QSlw, CArt, PASlw)
DO 3120 i12=1, NChem
       CSlwBld(i12) = ASlwBld(i12) / VSlwBld                              ! Concentration
in slowly perfused tissue blood (mg/L)
          CSlw(i12) = ASlw(i12) / VSlw                                    ! Concentration
in slowly perfused tissue (mg/L)
       CSlwDif(i12) = CSlw(i12) / PSlw(i12)                               ! Concentration
available for diffusion (mg/L)
      RASlwBld(i12) = (QSlw *(CArt(i12) - CSlwBld(i12)))+(PASlw(i12) * (CSlwDif(i12) -
CSlwBld(i12)))
```

```
                                                                        ! Rate of change
in slowly perfused tissue blood (mg/hr)
         RASlw(i12) = PASlw(i12) * (CSlwBld(i12) - CSlwDif(i12))      ! Rate of change
in slowly perfused tissue (mg/hr)
3120: CONTINUE
  END
!-------------------------------------------------------------------------------------
-----------------------------------------


!-------------------------------------------------------------------------------------
-----------------------------------------
! Subcutaneous Compartment Blood and Subcutaneous Compartment Tissue

     ASQBld = INTVC(RASQBld, IASQBld)                                ! Amount in blood
(mg)
        ASQ = INTVC(RASQ, IASQ)                                      ! Amount in tissue
(mg)

  PROCEDURAL (CSQBld, CSQ, CSQDif, RASQBld, RASQ = ASQBld, VSQBld, ASQ, VSQ, PSQ, QSQ,
CArt, PASQ)
DO 3025 i18=1, NChem
       CSQBld(i18) = ASQBld(i18) / VSQBld                            ! Concentration in
blood (mg/L)
          CSQ(i18) = ASQ(i18) / VSQ                                  ! Concentration in
tissue (mg/L)
       CSQDif(i18) = CSQ(i18) / PSQ(i18)                             ! Concentration
available for diffusion (mg/L)
      RASQBld(i18) = (QSQ *(CArt(i18) - CSQBld(i18)))+(PASQ(i18) * (CSQDif(i18) -
CSQBld(i18)))
                                                                     ! Rate of change in
blood (mg/hr)
         RASQ(i18) = PASQ(i18) * (CSQBld(i18) - CSQDif(i18)) + SQR(i18)
                                                                     ! Rate of change in
tissue (mg/hr)
3025: CONTINUE
  END
!-------------------------------------------------------------------------------------
-----------------------------------------


!-------------------------------------------------------------------------------------
-----------------------------------------
! Amount in Urine (mg)
        AUrn = INTVC(RAUrn, IAUrn)

! Rate of Excretion (mg/hr)
  PROCEDURAL (RAUrn = ClUr, CArt)
DO 3130 i13=1, NChem
       RAUrn(i13) = ClUr(i13) * CArt(i13)
3130: CONTINUE
  END
!-------------------------------------------------------------------------------------
-----------------------------------------


!----------------- CHECK MASS BALANCE ------------------------------------------------
-----------------------------------------
! Total Amount Inhaled (mg)
     ATotInh = INTVC(RATotInh, IATotInh)

! Total Amount Injected (mg)
      ATotIV = INTVC(IVR, IATotIV)
```

```
! Total Amount Drunk (mg)
   ATotDrink = INTVC(Drink, IATotDrink)

! Total Amount SQ (mg)
      ATotSQ = INTVC (SQR, IATotSQ)


! Calculating Total Brain Concentration (mg/kg), Total Dose (mg), Total Amount in Body
(mg) and Mass Balance (mg)
  PROCEDURAL (CBrnTotBld, CBrnTot, TDose, AmtBody, MassBal, RATotInh = ABrnBld,
AStmBld, ATLBld, VBrnBld, VStmBld, VTLBld, ABrn, AStm, ATL, VBrn, VStm, VTL,&
             & QAlv, CInh, ATotInh, ATotIV, TotDose, ATotDrink, ATotSQ, AMuc, AArt,
ACoc, ACocBld, AFat, AFatBld, ALiv, ALivBld, ARap, ARapBld, ASlw, ASlwBld, &
             & ASQ, ASQBld, AExh, AUrn, AMet1, AMet2, AExc, ADu, ASt)
DO 3140 i14=1, NChem
       CBrnTotBld(i14) = (ABrnBld(i14) + AStmBld(i14) + ATLBld(i14))/(VBrnBld +
VStmBld + VTLBld)
       CBrnTot(i14) = (ABrn(i14) + AStm(i14) + ATL(i14))/(VBrn + VStm + VTL)

       RATotInh(i14) = QAlv * CInh(i14)
       TDose(i14) = ATotInh(i14) + ATotIV(i14) + TotDose(i14) + ATotDrink(i14) +
ATotSQ(i14)
       AmtBody(i14) = AMuc(i14) + AArt(i14) + ABrn(i14) + ABrnBld(i14) &
                  & + AStm(i14) + AStmBld(i14) + ATL(i14) + ATLBld(i14) &
                  & + ACoc(i14) + ACocBld(i14) + AFat(i14) + AFatBld(i14) + ALiv(i14)
+ ALivBld(i14) &
                  & + ARap(i14) + ARapBld(i14) + ASlw(i14) + ASlwBld(i14) + ASQ(i14) +
ASQBld(i14) &
                  & + AExh(i14) + AUrn(i14) + AMet1(i14) + AMet2(i14) + AExc(i14) +
ADu(i14) + ASt(i14)

       IF (i14 .GT. 1) THEN
           MassBal(i14) = TDose(i14) - AmtBody(i14)
       ELSE
           MassBal(i14) = TDose(i14) - AmtBody(i14)
       ENDIF
3140: CONTINUE
  END


TERMT(T.GT.TStop, 'Simulation Finished')

END                ! End of Derivative
END                ! End of Dynamic
END                ! End of Program
```

APPENDIX B. SELECT M FILES FOR PHARMACOKINETIC ARRAY MODEL

The following m files are to be used with the csl file in Appendix A. They contain all necessary files to execute the simulations in Section 4.4.1 and Appendix C.

Note that acslX allows for longer lines than Microsoft Word, in which this appendix is formatted. Use of this code in acslX will require careful vetting to ensure that lines are begun in a format acceptable in acslX and to ensure that code is not arbitrarily split between lines.

SET M FILE TO LOAD AT RUN TIME

Init.m

```
prepare T HOURS MINUTES DAYS CP CMUC CALV CALVPPM CART AUCCART AEXH CEND CENDPPM
PEREND PERMIX
prepare CBRN CBRNBLD AUCCBRN CCOC CCOCBLD CFAT CFATBLD CLIV CLIVBLD AMET1 AMET2
prepare CRAP CRAPBLD CSLW CSLWBLD CBRNTOT CBRNTOTBLD CSTM CSTMBLD CTL CTLBLD CSQ
CSQBLD
prepare CVEN AURN TDOSE AMTBODY MASSBAL

HVDPRN=0;
WESITG=0;
WEDITG=0;
```

DOSE RESET M FILE

ResetDoses.m

```
  CONC(1)=0.0; IVDOSE(1)=0.0; PDOSE(1)=0.0; PDRINK(1)=0.0; SQDOSE(1)=0.0;
  CONC(2)=0.0; IVDOSE(2)=0.0; PDOSE(2)=0.0; PDRINK(2)=0.0; SQDOSE(2)=0.0;
  CONC(3)=0.0; IVDOSE(3)=0.0; PDOSE(3)=0.0; PDRINK(3)=0.0; SQDOSE(3)=0.0;
  CONC(4)=0.0; IVDOSE(4)=0.0; PDOSE(4)=0.0; PDRINK(4)=0.0; SQDOSE(4)=0.0;
  CONC(5)=0.0; IVDOSE(5)=0.0; PDOSE(5)=0.0; PDRINK(5)=0.0; SQDOSE(5)=0.0;

  TCHNG=0.0; DAYSWK=1.0; TMAX=24.0; DOSEINT=1000.0;
  TINF=0.2; TSQINF = 0.02; VOLSQ = 0.282;
  RATS=1.0;

  CC=0; VCHC=9.1; KLCC=0.0;

  CINT=0.01
```

SPECIES AND CHEMICAL SPECIFIC M FILES

Rattus.m

```
% Generic rat parameters

% All cochlea parameters are for paired cochlea.

% Values from REF1, unless otherwise stated
  BW=0.3;          %REF1 = 0.22, REF8&9 = 0.3
  QCC=14.6;
  QPC=24.75;

  QBRNC=0.013;    %Remainder only; Adds up to 0.02
    QSTMC=0.004;
    QTLC=0.003;   %Calculated using brain volumes & REF2
  QCOCC=0.00004;  %REF3
  QFATC=0.07;
  QLIVC=0.183;
  QRAPC=0.557;
  QSLWC=0.16996;
  QSQG=0.012;     %Flow to subcutaneous compartment per g (L/(hr*g), based on rat
muscle
                  %  (slowly perfused) (REF4)

  VBRNC=0.004;    %Remainder only; 0.006 - VSTMC - VTLC; 0.006 from REF5 Table 3
    VSTMC=0.001;  %REF5 Table 3
    VTLC=0.001;   %in-house research
  VALVC=0.007;
  VFATC=0.10;
  VLIVC=0.034;
  VMUCC=0.0001;
  VRAPC=0.044;
  VSLWC=0.65;

  VOLSQ=0.282;     % mL ~= g; Max value for this protocol = 0.282 mL = 0.282 g
                   % Parameter max value should be no larger than 25 mL/kg BW for a
rat (REF6)

  % Blood content values for most tissues from REF5
  VBRNBLDC=0.03;   %REF4
    VSTMBLDC=0.03; %Assumed same across the brain
    VTLBLDC=0.03;
  VCOCBLDC=0.0183; %Calculated from data in REF7
  VFATBLDC=0.0154;
  VLIVBLDC=0.034;
  VRAPBLDC=0.2075;
  VSLWBLDC=0.0333;


  % REF1
  % Clewell HJ, III, Gentry PR, Gearhart JM, Covington TR, Banton MI, Andersen ME:
  %   Development of a physiologically based pharmacokinetic model of isopropanol
  %   and its metabolite acetone. Toxicol Sci 2001, 63(2):160-172.

  % REF2
  % Gjedde et al 1980 Rapid simultan determinat of regional blood flow_blood-brain
glucose transfer in brain of rats

  % REF3
```

```
  % Robinson et al. 2013 TR

  % REF4
  % Sterner et al. 2014 TMB-4 model

  % REF5
  % Delp et al. 1991

  % REF6
  % AALAS Learning Library, 2005

  % REF7
  % Morizono et al 1968 Cochlear blood vol in Gpig measured w Cr51 label RBC (Hearing
Loss reference file)

  % REF8
  % Merrill et al 2008 Improved predictive model 4 decane kinetics across species.pdf

  % REF9
  % Robinson and Merrill 2008 Harmonized PBPK mdl 4 nonane as component of jet
fuel.pdf
```

DecaneRat.m

```
  % Sets decane parameters for rat (chemical 5)

  MW(5)=142.3;

  DS=0.15;         %Per REF2: acetone = 0.25, isopropanol = 0.15, typical lipophilics
= 0.3, csl default=0.15

  PB(5)=5.0;       %Current study=7.9, REF1=5.0
    PLQ(5)=0.0041;    %Saline:air REF3=0.0041
    PMUC(5)=0.0041;   %Set same as water:air REF4
% Measured brain PCs indicated less partitioning into stem and temporal lobe than
expected
%   based on fat content and nonane measured PCs
  PBRN(5)=10.0;     %Current study frontal lobe = 1.75, REF1= 4.8, Fit to Perleberg
data
    PSTM(5)=(1.56/1.75)*PBRN(5);   %Current study = 1.56, Scaled (PBRN*(measured
PSTM/measured frontal lobe))
    PTL(5)=(1.16/1.75)*PBRN(5);    %Current study = 1.16, Scaled (PBRN*(measured
PTL/measured frontal lobe))
  PCOC(5)=2.15;    %Current study: scaled from measured skull PC using cochlea:skull
prediction ratio
  PFAT(5)=328.0;    %REF1 =328., Current results = 211.71
  PLIV(5)=3.0;     %Fitting to Perleberg data
  PRAP(5)=3.0;     %REF1=3.0
  PSLW(5)=0.85;    %REF1=0.85
  PSQ(5)=PFAT(5)*2;

  VMAXC(5)=0.005;    %REF1=0.4
  KM(5)=0.1;       %REF1=1.5
  KFC(5)=0.0;      %Not expecting first order metabolism for this compound

  CLURC(5)=0.004;  %Urinary clearnace, L/hr, REF2 = 0.004, NonanaRat.m=0.4
  KURTC(5)=0.0;    %URT uptake, L/hr, absorption into mucus, 0 = no scrubbing
                   %QPC = 24.75
  SCRUB(5)=0.7;    %Fraction of concentration in air that is scrubbed out (not
absorbed), 0=no scrubbing
```

```
  %oral dosing parameters from REF1
  KAD(5)=0.5;
  KAS(5)=2.0;
  KTD(5)=0.25;
  KTSD(5)=3.0;

  % If PA = 1000.0 = flow limited
  PABRN(5)=0.005;    %REF1=0.009
    PASTM(5)=0.005;
    PATL(5)=0.005;
  PACOC(5)=1.0;    %Same as PARAP in REF1
  PAFAT(5)=0.07;    %REF1=0.7
  PALIV(5)=0.15;   %REF1=0.15
  PARAP(5)=0.005;    %REF1= 1.0
  PASLW(5)=0.14;    %REF1 did not use, NonaneRat.m=0.5
  PASQ(5)=0.02;    %Fit to toluene data


  % REF1
  % Merrill et al 2008 Improved predictive model 4 decane kinetics across species.pdf

  % REF2
  % Clewell HJ, III, Gentry PR, Gearhart JM, Covington TR, Banton MI, Andersen ME:
  %   Development of a physiologically based pharmacokinetic model of isopropanol
  %   and its metabolite acetone. Toxicol Sci 2001, 63(2):160-172.

  %REF3
  % Sterner et al 2004 AFRL-HE-WP-TR-2004-0032 Analysis of algorithms predicting
blood-air_tissue-blood PCs fr solvent PCs.pdf

  %REF4
  % Schlosser PM, Asgharian BA, Medinsky M. 2010 Chapter 1.04 Inhalation Exposure and
Absorption of Toxicants.
  %   In: McQueen CA (ed).  Comprehensive Toxicology. Volume 14.  Elsevier e-book
```

EthylbenzeneRat.m

```
  % Sets ethylbenzene parameters for rat (chemical 2)

  MW(2)=106.17;     %Wikipedia

  DS=0.15;          %Per REF2: acetone = 0.25, isopropanol = 0.15, typical lipophilics
= 0.3, csl default=0.15

  PB(2)=42.7;       %REF1=42.7, In house study=41.1
    PLQ(2)=1.69;    %Saline:air REF2=1.69
    PMUC(2)=1.69;   %Set same as water:air REF3
  PBRN(2)=1.22;     %In house study frontal lobe = 1.22, REF2 whole brain=0.80
    PSTM(2)=1.93;   %Current study = 1.93
    PTL(2)=1.44;    %Current study = 1.44
  PCOC(2)=0.44;     %Current study: scaled from measured skull PC using cochlea:skull
prediction ratio
  PFAT(2)=36.4;     %REF1 =1556./42.7=36.4, In-house study=59.62
  PLIV(2)=1.96;     %REF1=83.8/42.7=1.96, Current study: kidney = 3.02
  PRAP(2)=1.41;     %REF1=60.3/42.7=1.41
  PSLW(2)=0.61;     %REF1=26.0/42.7=0.61
  PSQ(2)=PFAT(2)*2;

  VMAXC(2)=6.39;    %REF1=3.44
  KM(2)=1.04;       %REF1=0.13
  KFC(2)=0.0;       %Not expecting first order metabolism for this compound
```

```
  CLURC(2)=0.04;   %Urinary clearnace, L/hr
  KURTC(2)=0.0;     %URT uptake, L/hr, uptake into mucus, 0.0 = no scrubbing
                    %QPC = 24.75
  SCRUB(2)=0.0;     %Fraction of concentration in air that is scrubbed out (not
absorbed), 0=no scrubbing

  %oral dosing parameters from REF1
  KAD(2)=0.5;
  KAS(2)=2.0;
  KTD(2)=0.25;
  KTSD(2)=3.0;

  % If PA = 1000.0 = flow limited
  PABRN(2)=1000.0;
    PASTM(2)=1000.0;
    PATL(2)=1000.0;
  PACOC(2)=1000.0;
  PAFAT(2)=1000.0;
  PALIV(2)=1000.0;
  PARAP(2)=1000.0;
  PASLW(2)=1000.0;
  PASQ(2)=0.02;   %Fit to toluene data


  % REF1
  %Haddad et al 1999 Physiological modeling of the toxicokinetic interactions in a
quaternary mixture
  %  of aromatic hydrocarbons.  Toxicol Appl Physiol. 161:249-57.

  %REF2
  % Sterner et al 2004 AFRL-HE-WP-TR-2004-0032 Analysis of algorithms predicting
blood-air_tissue-blood PCs fr solvent PCs.pdf

  %REF3
  % Schlosser PM, Asgharian BA, Medinsky M. 2010 Chapter 1.04 Inhalation Exposure and
Absorption of Toxicants.
  %   In: McQueen CA (ed).  Comprehensive Toxicology. Volume 14.  Elsevier e-book
```

NonaneRat.m

```
  % Sets nonane parameters for rat (chemical 4)
  % *******Significant difference between values from different sources

  MW(4)=128.0;

  DS=0.15;         %Per REF1: acetone = 0.25, isopropanol = 0.15, typical lipophilics
= 0.3, csl default=0.15

  PB(4)=5.2;       %Current study=5.9, REF5=5.2
    PLQ(4)=0.004;  %REF6 decane saline:air PC=0.0041 (Log Kow values are similar so
assumed saline:air PCs are similar)
    PMUC(4)=0.004; %Set same as water:air REF7
  PBRN(4)=5.0;     %Current study frontal lobe = 1.70, REF5 = 5.0
    PSTM(4)=(2.9/1.7)*PBRN(4);   %Current study = 2.9, Scaled (PBRN*(measured
PSTM/measured frontal lobe))
    PTL(4)=(2.6/1.7)*PBRN(4);    %Current study = 2.6, Scaled (PBRN*(measured
PTL/measured frontal lobe))
  PCOC(4)=1.45;    %Current study: scaled from measured skull PC using cochlea:skull
prediction ratio
  PFAT(4)=282.0;   %REF5 = 282.0, Current results = 145.01, average[145,282]=214
```

```
  PLIV(4)=8.0;    %Fitting to data; REF5 found protein binding to be a factor; wonder
if this could concentrate more in liver than PC alone allows; REF5 used decane value
  PRAP(4)=2.0;     %REF5-2.0, Current study: kidney = 2.59
  PSLW(4)=4.0;      %REF2: muscle = 4.0, , REF5 = 4.0
  PSQ(4)=PFAT(4)*2;

  VMAXC(4)=0.1;   %REF5=0.0
  KM(4)=0.1;       %REF5=1.5
  KFC(4)=0.0;      %Not expecting first order metabolism for this compound

  CLURC(4)=0.4;    %Urinary clearnace, L/hr, REF1 = 0.004
  KURTC(4)=0.0;    %URT uptake, L/hr, deposition in mucus, model uses minimum value of
QPC or this, 0 = no scrubbing
                   %QPC = 24.75 default rat
  SCRUB(4)=0.4;    %Fraction of concentration in air that is scrubbed out (not
absorbed), 0=no scrubbing

  %oral dosing parameters from REF1
  KAD(4)=0.5;
  KAS(4)=2.0;
  KTD(4)=0.25;
  KTSD(4)=3.0;

  % If PA = 1000.0 = flow limited
  PABRN(4)=0.5;    %REF5=0.5
    PASTM(4)=0.5;
    PATL(4)=0.5;
  PACOC(4)=1.0;    %Same as PARAP
  PAFAT(4)=0.5;    %REF5=0.8
  PALIV(4)=0.07;   %REF5=0.07
  PARAP(4)=1.0;    %REF5= 1.0
  PASLW(4)=0.5;    %REF5=0.5
  PASQ(4)=0.02;   %Fit to toluene data


  % REF1
  % Clewell HJ, III, Gentry PR, Gearhart JM, Covington TR, Banton MI, Andersen ME:
  %   Development of a physiologically based pharmacokinetic model of isopropanol
  %   and its metabolite acetone. Toxicol Sci 2001, 63(2):160-172.

  % REF2
  % Robinson, P.J. and Merrill, E.A. 2008. A harmonized physiologically based
pharmacokinetic model
  %   for nonane as a component of jet fuel. Wright-Patterson AFB, OH: Air Force
Research Laboratory,
  %   Applied Biotechnology Branch. AFRL-RH-WP-TR-2008-0067, ADA502610.

  % REF3
  % Sterner et al 2006 Analysis of algorithms...

  %REF4
  % Joshi et al. 2010 PCs 4 nonane_isomers in rat.pdf

  %REF5
  % Robinson and Merrill 2008 Harmonized PBPK mdl 4 nonane as component of jet
fuel.pdf

  %REF6
  % Sterner et al 2004 AFRL-HE-WP-TR-2004-0032 Analysis of algorithms predicting
blood-air_tissue-blood PCs fr solvent PCs.pdf

  %REF7
```

```
  % Schlosser PM, Asgharian BA, Medinsky M. 2010 Chapter 1.04 Inhalation Exposure and
Absorption of Toxicants.
  %   In: McQueen CA (ed).  Comprehensive Toxicology. Volume 14.  Elsevier e-book
```

TolueneRat.m

```
  % Sets toluene parameters for rat (chemical 1)

  MW(1)=92.14;      %Wikipedia

  DS=0.15;          %Per REF2: acetone = 0.25, isopropanol = 0.15, typical lipophilics
= 0.3, csl default=0.15

  PB(1)=18.0;       %REF1=REF4=18.0, current study=22.8
    PLQ(1)=1.99;    %Saline:air REF2=1.99
    PMUC(1)=1.99;   %Set same as water:air REF3
  PBRN(1)=2.0;      %Current study frontal lobe = 1.26, REF2= 4.22, REF4=2.0
    PSTM(1)=2.87;   %Current study = 1.81, Scaled PBRN*(1.81/1.26)
    PTL(1)=2.13;    %Current study = 1.34, Scaled PBRN*(1.34/1.26)
  PCOC(1)=0.54;     %Current study: scaled from measured skull PC using cochlea:skull
prediction ratio
  PFAT(1)=56.7;     %REF1 =1021./18.=56.7, Current study: 46.82, REF4=56.7
  PLIV(1)=4.64;     %REF1=83.6/18.=4.64, REF4=4.64
  PRAP(1)=4.64;     %Current study: kidney = 2.37, REF1=83.6/18.=4.64, REF4=4.64

  PSLW(1)=1.54;     %REF1=27.7/18.=1.54, REF4=1.54
  PSQ(1)=PFAT(1)*2;

  VMAXC(1)=3.44;    %REF1=3.44, REF4=4.81 except 3.44 for Haddad data
  KM(1)=0.13;       %REF1=0.13, REF4=0.55 except 0.13 for Haddad data
  KFC(1)=0.0;       %Not expecting first order metabolism for this compound

  CLURC(1)=0.004;     %Urinary clearnace, L/hr, REF4=0
  KURTC(1)=0.0;     %URT uptake, L/hr, uptake into mucus, 0.0 = no scrubbing, REF4=0
  SCRUB(1)=0.0;     %Fraction of concentration in air that is scrubbed out (not
absorbed), 0=no scrubbing

  %oral dosing parameters from REF1
  KAD(1)=0.5;
  KAS(1)=2.0;
  KTD(1)=0.25;
  KTSD(1)=3.0;

  % If PA = 1000.0 = flow limited
  PABRN(1)=1000.0;
    PASTM(1)=1000.0;
    PATL(1)=1000.0;
  PACOC(1)=1000.0;
  PAFAT(1)=1000.0;
  PALIV(1)=1000.0;
  PARAP(1)=1000.0;
  PASLW(1)=1000.0;
  PASQ(1)=0.02;   %Fit to toluene data


  % REF1
  %Haddad et al 1999 Physiological modeling of the toxicokinetic interactions in a
quaternary mixture
  %  of aromatic hydrocarbons.  Toxicol Appl Physiol. 161:249-57.

  %REF2
```

```
  % Sterner et al 2004 AFRL-HE-WP-TR-2004-0032 Analysis of algorithms predicting
blood-air_tissue-blood PCs fr solvent PCs.pdf

  %REF3
  % Schlosser PM, Asgharian BA, Medinsky M. 2010 Chapter 1.04 Inhalation Exposure and
Absorption of Toxicants.
  %   In: McQueen CA (ed).  Comprehensive Toxicology. Volume 14.  Elsevier e-book

  %REF4
  % Hack Toluene model, rat_toluene.m
```

XyleneRat.m

```
  % Sets xylene parameters for rat (chemical 3)

  MW(3)=106.17;     %Wikipedia

  DS=0.15;          %Per REF2: acetone = 0.25, isopropanol = 0.15, typical lipophilics
= 0.3, csl default=0.15

  PB(3)=46.0;       %REF1=46.0; In house study=42.3
    PLQ(3)=2.03;    %Saline:air REF2 m=1.79, o=2.64, p=1.67, average=2.03
    PMUC(3)=2.03;   %Set same as water:air REF3
  PBRN(3)=1.38;     %In house study frontal lobe = 1.38, REF2 whole brain m=1.2,
o=1.7, p=1.2
    PSTM(3)=2.29;   %Current study = 2.29
    PTL(3)=1.61;    %Current study = 1.61
  PCOC(3)=0.47;     %Current study: scaled from measured skull PC using cochlea:skull
prediction ratio
  PFAT(3)=40.4;     %REF1 =1859./46.=40.4, In-house study=70.09
  PLIV(3)=1.98;     %REF1=90.9/46.=1.98, Current study: kidney = 2.84
  PRAP(3)=1.98;     %REF1=90.9/46.=1.98
  PSLW(3)=0.91;     %REF1=41.9/46.=0.91
  PSQ(3)=PFAT(3)*2;

  VMAXC(3)=6.49;    %REF1=6.49
  KM(3)=0.45;       %REF1=0.45
  KFC(3)=0.0;       %Not expecting first order metabolism for this compound

  CLURC(3)=0.004;   %Urinary clearnace, L/hr
  KURTC(3)=0.0;     %URT uptake, L/hr, uptake into mucus, 0.0 = no scrubbing
                    %QPC = 24.75
  SCRUB(3)=0.0;     %Fraction of concentration in air that is scrubbed out (not
absorbed), 0=no scrubbing

  %oral dosing parameters from REF1
  KAD(3)=0.5;
  KAS(3)=2.0;
  KTD(3)=0.25;
  KTSD(3)=3.0;

  % If PA = 1000.0 = flow limited
  PABRN(3)=1000.0;
    PASTM(3)=1000.0;
    PATL(3)=1000.0;
  PACOC(3)=1000.0;
  PAFAT(3)=1000.0;
  PALIV(3)=1000.0;
  PARAP(3)=1000.0;
  PASLW(3)=1000.0;
  PASQ(3)=0.02;   %Fit to toluene data
```

```
  % REF1
  %Haddad et al 1999 Physiological modeling of the toxicokinetic interactions in a
quaternary mixture
  %  of aromatic hydrocarbons.  Toxicol Appl Physiol. 161:249-57.

  %REF2
  % Sterner et al 2004 AFRL-HE-WP-TR-2004-0032 Analysis of algorithms predicting
blood-air_tissue-blood
  %   PCs fr solvent PCs.pdf

  %REF3
  % Schlosser PM, Asgharian BA, Medinsky M. 2010 Chapter 1.04 Inhalation Exposure and
Absorption of Toxicants.
  %   In: McQueen CA (ed).  Comprehensive Toxicology. Volume 14.  Elsevier e-book
```

M FILE FOR SIMULATIONS IN SECTION 4.4.1

Predict_Guthrie14.m

```
%Simulates 5 key hydrocarbons for Guthrie et al. 2014 exposure to predict rat target
tissue concentrations

%Guthrie, O.W., Xu, H., Wong, B.A., McInturf, S.M., Reboulet, J.E., Ortiz, P.A. and
Mattie, D.R. 2014.
%     Exposure to low levels of jet-propulsion fuel impairs brainstem encoding of
stimulus intensity.
%     J Toxicol Environ Health A 77(5): 261-280.

resetdoses
rattus
toluenerat
ethylbenzenerat
xylenerat
nonanerat
decanerat

BW=0.105; %average starting BW in Guthrie et al. 2014

%Calculates concentration of each component in POSF 4658, converted from 1000 mg/m3 to
ppm, assuming STP
%Weight percent values from tandem gas chromatography analysis by the 2006 Shafer et
al. method
%POSF 4658 contains 0.16 percent toluene, 0.12 percent ethylbenzene,
%     0.66 percent xylenes, 1.14 percent nonane, and 2.55 percent decane

CONC(1)=((0.0016*1000)*24.45)/MW(1);
CONC(2)=((0.0012*1000)*24.45)/MW(2);
CONC(3)=((0.0066*1000)*24.45)/MW(3);
CONC(4)=((0.0114*1000)*24.45)/MW(4);
CONC(5)=((0.0255*1000)*24.45)/MW(5);

TCHNG=6.0; %Simulates 1 day of 4 week study
TSTOP=12.0;
start @nocallback

plotcven = plot (0, _t, _cven(:,1), '-b', _t, _cven(:,2),'-k');
    plot (plotcven, 1, _t, _cven(:,3),'-r', _t, _cven(:,4),'-g');
```

```
    plot (plotcven, 1, _t, _cven(:,5),'-m');
plotccoc = plot (0, _t, _ccoc(:,1), '-b', _t, _ccoc(:,2),'-k');
    plot (plotccoc, 1, _t, _ccoc(:,3),'-r', _t, _ccoc(:,4),'-g');
    plot (plotccoc, 1, _t, _ccoc(:,5),'-m');
plotcbrn = plot (0, _t, _cbrn(:,1), '-b', _t, _cbrn(:,2),'-k');
    plot (plotcbrn, 1, _t, _cbrn(:,3),'-r', _t, _cbrn(:,4),'-g');
    plot (plotcbrn, 1, _t, _cbrn(:,5),'-m');
plotcstm = plot (0, _t, _cstm(:,1), '-b', _t, _cstm(:,2),'-k');
    plot (plotcstm, 1, _t, _cstm(:,3),'-r', _t, _cstm(:,4),'-g');
    plot (plotcstm, 1, _t, _cstm(:,5),'-m');
plotctl = plot (0, _t, _ctl(:,1), '-b', _t, _ctl(:,2),'-k');
    plot (plotctl, 1, _t, _ctl(:,3),'-r', _t, _ctl(:,4),'-g');
    plot (plotctl, 1, _t, _ctl(:,5),'-m');


set @preference=BackslashEscapeS

    pltscript(plotcven, "Chart.Header.Text = \"Predictions for Guthrie et al. (2014)
Exposure\";")
    pltscript(plotcven, "Chart.SubHeader.Text = \"5 Key Hydrocarbons in JP-8\";")
    pltscript(plotcven, "Chart.SubHeader.Visible=true;")
    pltscript(plotcven, "Chart.Axes.Left.Title.Text=\"Venous Blood [mg/L]\";")
    pltscript(plotcven, "Chart.Axes.Bottom.Title.Text=\"Hours\";")
    pltscript(plotcven, "Chart.Series[0].Title=\"Toluene\";")
    pltscript(plotcven, "Chart.Series[1].Title=\"Ethylbenzene\";")
    pltscript(plotcven, "Chart.Series[2].Title=\"Xylene\";")
    pltscript(plotcven, "Chart.Series[3].Title=\"Nonane\";")
    pltscript(plotcven, "Chart.Series[4].Title=\"Decane\";")

    pltscript(plotccoc, "Chart.Header.Text = \"Predictions for Guthrie et al. (2014)
Exposure\";")
    pltscript(plotccoc, "Chart.SubHeader.Text = \"5 Key Hydrocarbons in JP-8\";")
    pltscript(plotccoc, "Chart.SubHeader.Visible=true;")
    pltscript(plotccoc, "Chart.Axes.Left.Title.Text=\"Cochlea [mg/L]\";")
    pltscript(plotccoc, "Chart.Axes.Bottom.Title.Text=\"Hours\";")
    pltscript(plotccoc, "Chart.Series[0].Title=\"Toluene\";")
    pltscript(plotccoc, "Chart.Series[1].Title=\"Ethylbenzene\";")
    pltscript(plotccoc, "Chart.Series[2].Title=\"Xylene\";")
    pltscript(plotccoc, "Chart.Series[3].Title=\"Nonane\";")
    pltscript(plotccoc, "Chart.Series[4].Title=\"Decane\";")

    pltscript(plotcbrn, "Chart.Header.Text = \"Predictions for Guthrie et al. (2014)
Exposure\";")
    pltscript(plotcbrn, "Chart.SubHeader.Text = \"5 Key Hydrocarbons in JP-8\";")
    pltscript(plotcbrn, "Chart.SubHeader.Visible=true;")
    pltscript(plotcbrn, "Chart.Axes.Left.Title.Text=\"Remainder of the Brain
[mg/L]\";")
    pltscript(plotcbrn, "Chart.Axes.Bottom.Title.Text=\"Hours\";")
    pltscript(plotcbrn, "Chart.Series[0].Title=\"Toluene\";")
    pltscript(plotcbrn, "Chart.Series[1].Title=\"Ethylbenzene\";")
    pltscript(plotcbrn, "Chart.Series[2].Title=\"Xylene\";")
    pltscript(plotcbrn, "Chart.Series[3].Title=\"Nonane\";")
    pltscript(plotcbrn, "Chart.Series[4].Title=\"Decane\";")

    pltscript(plotcstm, "Chart.Header.Text = \"Predictions for Guthrie et al. (2014)
Exposure\";")
    pltscript(plotcstm, "Chart.SubHeader.Text = \"5 Key Hydrocarbons in JP-8\";")
    pltscript(plotcstm, "Chart.SubHeader.Visible=true;")
    pltscript(plotcstm, "Chart.Axes.Left.Title.Text=\"Brain Stem [mg/L]\";")
    pltscript(plotcstm, "Chart.Axes.Bottom.Title.Text=\"Hours\";")
    pltscript(plotcstm, "Chart.Series[0].Title=\"Toluene\";")
    pltscript(plotcstm, "Chart.Series[1].Title=\"Ethylbenzene\";")
    pltscript(plotcstm, "Chart.Series[2].Title=\"Xylene\";")
```

```
    pltscript(plotcstm, "Chart.Series[3].Title=\"Nonane\";")
    pltscript(plotcstm, "Chart.Series[4].Title=\"Decane\";")

    pltscript(plotctl, "Chart.Header.Text = \"Predictions for Guthrie et al. (2014)
Exposure\";")
    pltscript(plotctl, "Chart.SubHeader.Text = \"5 Key Hydrocarbons in JP-8\";")
    pltscript(plotctl, "Chart.SubHeader.Visible=true;")
    pltscript(plotctl, "Chart.Axes.Left.Title.Text=\"Temporal Lobe [mg/L]\";")
    pltscript(plotctl, "Chart.Axes.Bottom.Title.Text=\"Hours\";")
    pltscript(plotctl, "Chart.Series[0].Title=\"Toluene\";")
    pltscript(plotctl, "Chart.Series[1].Title=\"Ethylbenzene\";")
    pltscript(plotctl, "Chart.Series[2].Title=\"Xylene\";")
    pltscript(plotctl, "Chart.Series[3].Title=\"Nonane\";")
    pltscript(plotctl, "Chart.Series[4].Title=\"Decane\";")

set @preference=NoBackslashEscapeS
```

M FILES FOR SIMULATIONS IN APPENDIX C

Toluene Study Simulation M Files

C1_Haddad.m

```
%Haddad, S., Tardif, R., Charest-Tardif, G. and Krishnan, K. 1999. Physiological
modeling
%     of the toxicokinetic interactions in a quaternary mixture of aromatic
hydrocarbons.
%     Toxicol.Appl.Pharmacol. 161(3): 249-257.

resetdoses
rattus
toluenerat

%T, CVEN
had50 = [
 4.0    0.472
 4.0    0.546
 4.5    0.210
 4.5    0.281
 4.5    0.354
 5.0    0.093
 5.0    0.136
 5.0    0.182
 5.5    0.083
 5.5    0.133
 5.5    0.108
 6.0    0.045
 6.0    0.059
 6.0     0.072];

%T, CVEN
had100 = [
4.0     0.751
 4.0     1.033
 4.0     1.464
 4.5     0.547
 4.5     0.632
```

```
 4.5     0.798
 5.0     0.281
 5.0     0.345
 5.0     0.435
 5.5     0.199
 5.5     0.290
 5.5     0.230
 6.0     0.112
 6.0     0.133
 6.0     0.173];

%T, CVEN
had200 = [
 4.0     3.205
 4.0     4.042
 4.0     5.099
 4.5     2.334
 4.5     3.120
 4.5     3.714
 5.0     1.559
 5.0     1.856
 5.0     2.274
 5.5     0.826
 5.5     1.352
 5.5     1.072
 6.0     0.602
 6.0     0.716
 6.0     0.804];

% Study specific values as found in Hack tolune model, Haddad.m
BW=0.235;
VMAXC(1)=3.44;
KM(1)=0.13;

CONC(1)=50.0, TCHNG=4.0;
TSTOP=8.0;
start @nocallback

plotcven = plot (0, had50(:,1), had50(:,2), '+b', _t, _cven(:,1), '-b');


CONC(1)=100.0;
start @nocallback

plot (plotcven, 1, had100(:,1), had100(:,2), '+k', _t, _cven(:,1), '-k');

CONC(1)=200.0;
start @nocallback

plot (plotcven, 1, had200(:,1), had200(:,2), '+g', _t, _cven(:,1), '-g');


set @preference=BackslashEscapeS

    pltscript(plotcven, "Chart.Header.Text = \"Haddad et al. (1999) Toluene Inhalation
Study\";")
    pltscript(plotcven, "Chart.SubHeader.Text = \"50, 100, 200 ppm Inhalation for 4
Hours\";")
    pltscript(plotcven, "Chart.SubHeader.Visible=true;")
    pltscript(plotcven, "Chart.Axes.Left.Title.Text=\"Toluene in Venous Blood
[mg/L]\";")
    pltscript(plotcven, "Chart.Axes.Bottom.Title.Text=\"Hours\";")
    pltscript(plotcven, "Chart.Series[0].Title=\"50 ppm\";")
```

```
    pltscript(plotcven, "Chart.Series[1].Title=\"Simulation 50 ppm\";")
    pltscript(plotcven, "Chart.Series[2].Title=\"100 ppm\";")
    pltscript(plotcven, "Chart.Series[3].Title=\"Simulation 100 ppm\";")
    pltscript(plotcven, "Chart.Series[4].Title=\"200 ppm\";")
    pltscript(plotcven, "Chart.Series[5].Title=\"Simulation 200 ppm\";")

set @preference=NoBackslashEscapeS
```

C1_Lam.m

```
%Lam, C.W., Galen, T.J., Boyd, J.F. and Pierson, D.L. 1990. Mechanism of transport and
distribution
%     of organic solvents in blood. Toxicol.Appl.Pharmacol. 104(1): 117-129.

%Male Sprague-Dawley rats, BW about 300 g.
%  2-hour whole-body inhalation of 488 +/- 24 ppm toluene.
%  n = 5 rats, put in 10 minutes apart.
%  30 L closed chamber with 5 rats, but CONC is maintained at 488 ppm, rather than
depleted, so run as open chamber.
%Data from Plasma+RBC column, Table 1, page 121

resetdoses
rattus
toluenerat

%T (hr), CVEN (mg/L)
lam = [
2      10.90
2      15.03
2      14.98
2      15.02
2      15.09];

% Study specific values as found in Hack tolune model, Lam.m
BW=0.3;

CONC(1)=488.0, TCHNG=2.0;
TSTOP=4.0;
start @nocallback

plotcven = plot (0, lam(:,1), lam(:,2), '+b', _t, _cven(:,1), '-b');


set @preference=BackslashEscapeS

    pltscript(plotcven, "Chart.Header.Text = \"Lam et al. (1990) Toluene Inhalation
Study\";")
    pltscript(plotcven, "Chart.SubHeader.Text = \"488 ppm Inhalation for 2 Hours\";")
    pltscript(plotcven, "Chart.SubHeader.Visible=true;")
    pltscript(plotcven, "Chart.Axes.Left.Title.Text=\"Toluene in Venous Blood
[mg/L]\";")
    pltscript(plotcven, "Chart.Axes.Bottom.Title.Text=\"Hours\";")
    pltscript(plotcven, "Chart.Series[0].Title=\"488 ppm\";")
    pltscript(plotcven, "Chart.Series[1].Title=\"Simulation 488 ppm\";")

set @preference=NoBackslashEscapeS
```

C1_Romer.m

```
%Romer, K.G., Federsel, R.J. and Freundt, K.J. 1986. Rise of inhaled toluene, ethyl
benzene,
%     m-xylene, or mesitylene in rat blood after treatment with ethanol. Bull Environ
Contam
%     Toxicol 37(6): 874-876.

%Adult female SPF Sprague-Dawley rats
%  200 - 220 g BW
%Groups of 3 rats exposed in a 20 L glass chamber, air flow 1.25 L/min, for 2 hr.
%  20 L closed chamber with 3 rats, but CONC is maintained at 220 ppm, rather than
depleted, so run as open chamber.
%Aromatic conc varied < 5%, delivered via evaporator.
%  Sham-treated groups given 5 mL/kg physiological saline.
%Exposure conc monitored via GC using 100 uL air samples.
%Blood (0.02 mL) collected from retro-orbital plexus.
%  Blood conc of aromatics determined by GC.

resetdoses
rattus
toluenerat

%T(hr), CVEN(mg/L)
romer = [
2.0   5.23
2.0   5.04
2.0   5.43];

BW=0.210;

CONC(1)=220.0;
TCHNG=2.0;
TSTOP=3.0;
start @nocallback

plotcven = plot (0, romer(:,1), romer(:,2), '+b', _t, _cven(:,1), '-b');


set @preference=BackslashEscapeS

    pltscript(plotcven, "Chart.Header.Text = \"Romer et al. (1986) Toluene Inhalation
Study\";")
    pltscript(plotcven, "Chart.SubHeader.Text = \"220 ppm Inhalation for 2 Hours\";")
    pltscript(plotcven, "Chart.SubHeader.Visible=true;")
    pltscript(plotcven, "Chart.Axes.Left.Title.Text=\"Toluene in Venous Blood
[mg/L]\";")
    pltscript(plotcven, "Chart.Axes.Bottom.Title.Text=\"Hours\";")
    pltscript(plotcven, "Chart.Series[0].Title=\"220 ppm mean value\";")
    pltscript(plotcven, "Chart.Series[1].Title=\"Simulation 220 ppm\";")

set @preference=NoBackslashEscapeS
```

C1_Tardif.m

```
%Tardif, R., Charest-Tardif, G. and Brodeur, J. 1996. Comparison of the influence
%     of binary mixtures versus a ternary mixture of inhaled aromatic hydrocarbons
%     on their blood kinetics in the rat. Arch Toxicol 70(7): 405-413.

%Adult male SD rats
```

```
%  235-245 g

resetdoses
rattus
toluenerat

%T, CVEN from Figure 1, mean followed by +SD then -SD
tar100 = [
4.1    1.14
4.5    0.69
5.0    0.36
5.5    0.23
6.0    0.13
4.1    1.53
4.5    0.82
5.0    0.44
5.5    0.29
6.0    0.19
4.1    0.76
4.5    0.55
5.0    0.27
5.5    0.17
6.0    0.08];

%T, CVEN from Figure 2, mean followed by +SD then -SD
tar200 = [
4.1    4.34
4.5    3.17
5.0    1.96
5.5    1.19
6.0    0.79
4.1    5.29
4.5    3.94
5.0    2.31
5.5    1.42
6.0    0.89
4.1    3.37
4.5    2.47
5.0    1.66
5.5    0.93
6.0    0.64];

BW=0.240;

CONC(1)=100.0;
TCHNG=4.0;
TSTOP=6.0;
start @nocallback

plotcven = plot (0, tar100(:,1), tar100(:,2), '+b', _t, _cven(:,1), '-b');

CONC(1)=200.0;
start @nocallback

plot (plotcven, 1, tar200(:,1), tar200(:,2), '+k', _t, _cven(:,1), '-k');


set @preference=BackslashEscapeS

    pltscript(plotcven, "Chart.Header.Text = \"Tardif et al. (1996) Toluene Inhalation
Study\";")
    pltscript(plotcven, "Chart.SubHeader.Text = \"100, 200 ppm Inhalation for 4
Hours\";")
```

```
    pltscript(plotcven, "Chart.SubHeader.Visible=true;")
    pltscript(plotcven, "Chart.Axes.Left.Title.Text=\"Toluene in Venous Blood
[mg/L]\";")
    pltscript(plotcven, "Chart.Axes.Bottom.Title.Text=\"Hours\";")
    pltscript(plotcven, "Chart.Series[0].Title=\"100 ppm\";")
    pltscript(plotcven, "Chart.Series[1].Title=\"Simulation 100 ppm\";")
    pltscript(plotcven, "Chart.Series[2].Title=\"200 ppm\";")
    pltscript(plotcven, "Chart.Series[3].Title=\"Simulation 200 ppm\";")

set @preference=NoBackslashEscapeS
```

Ethylbenzene Study Simulation M Files

C2_Haddad.m

```
%Haddad, S., Tardif, R., Charest-Tardif, G. and Krishnan, K. 1999. Physiological
modeling
%     of the toxicokinetic interactions in a quaternary mixture of aromatic
hydrocarbons.
%     Toxicol.Appl.Pharmacol. 161(3): 249-257.

resetdoses
rattus
ethylbenzenerat

%T, CVEN (mean, +SD, -SD)
had50 = [
4.1    0.66
4.5    0.46
5.0    0.28
5.5    0.17
6.0    0.13
4.1    0.78
4.5    0.53
5.0    0.32
5.5    0.20
6.0    0.17
4.1    0.59
4.5    0.33
5.0    0.22
5.5    0.15
6.0    0.09];

%T, CVEN
had100 = [
4.1    1.52
4.5    1.02
5.0    0.70
5.5    0.45
6.0    0.31
4.1    1.68
4.5    1.15
5.0    0.89
5.5    0.58
6.0    0.36
4.1    1.36
4.5    0.94
5.0    0.57
5.5    0.38
```

```
6.0    0.28];

%T, CVEN
had200 = [
4.1    5.73
4.5    3.79
5.0    2.70
5.5    1.92
6.0    1.36
4.1    6.57
4.5    4.24
5.0    3.02
5.5    2.21
6.0    1.66
4.1    5.05
4.5    3.42
5.0    2.44
5.5    1.72
6.0    1.12];

BW=0.235;

CONC(2)=50.0, TCHNG=4.0;
TSTOP=8.0;
start @nocallback

plotcven = plot (0, had50(:,1), had50(:,2), '+b', _t, _cven(:,2), '-b');

CONC(2)=100.0;
start @nocallback

plot (plotcven, 1, had100(:,1), had100(:,2), '+k', _t, _cven(:,2), '-k');

CONC(2)=200.0;
start @nocallback

plot (plotcven, 1, had200(:,1), had200(:,2), '+g', _t, _cven(:,2), '-g');


set @preference=BackslashEscapeS

    pltscript(plotcven, "Chart.Header.Text = \"Haddad et al. (1999) Ethylbenzene
Inhalation Study\";")
    pltscript(plotcven, "Chart.SubHeader.Text = \"50, 100, 200 ppm Inhalation for 4
Hours\";")
    pltscript(plotcven, "Chart.SubHeader.Visible=true;")
    pltscript(plotcven, "Chart.Axes.Left.Title.Text=\"Ethylbenzene in Venous Blood
[mg/L]\";")
    pltscript(plotcven, "Chart.Axes.Bottom.Title.Text=\"Hours\";")
    pltscript(plotcven, "Chart.Series[0].Title=\"50 ppm\";")
    pltscript(plotcven, "Chart.Series[1].Title=\"Simulation 50 ppm\";")
    pltscript(plotcven, "Chart.Series[2].Title=\"100 ppm\";")
    pltscript(plotcven, "Chart.Series[3].Title=\"Simulation 100 ppm\";")
    pltscript(plotcven, "Chart.Series[4].Title=\"200 ppm\";")
    pltscript(plotcven, "Chart.Series[5].Title=\"Simulation 200 ppm\";")

set @preference=NoBackslashEscapeS
```

C2_Tardif.m

```
%Tardif, R., Charest-Tardif, G. and Brodeur, J. 1996. Comparison of the influence
%     of binary mixtures versus a ternary mixture of inhaled aromatic hydrocarbons
%     on their blood kinetics in the rat. Arch Toxicol 70(7): 405-413.

%Adult male SD rats
%  235-245 g

resetdoses
rattus
ethylbenzenerat

%T, CVEN from Figure 1, mean followed by +SD then -SD
tar100 = [
4.1    1.92
4.5    1.27
5.0    0.86
5.5    0.53
6.0    0.35
4.1    2.11
4.5    1.42
5.0    1.08
5.5    0.66
6.0    0.41
4.1    1.79
4.5    1.14
5.0    0.63
5.5    0.43
6.0    0.29];

%T, CVEN from Figure 4, mean followed by +SD then -SD
tar200 = [
4.1    7.67
4.5    4.96
5.0    3.47
5.5    2.50
6.0    1.71
4.1    8.22
4.5    5.51
5.0    3.82
5.5    2.78
6.0    2.01
4.1    6.92
4.5    4.42
5.0    3.25
5.5    2.20
6.0    1.39];

BW=0.240;

CONC(2)=100.0;
TCHNG=4.0;
TSTOP=6.0;
start @nocallback

plotcven = plot (0, tar100(:,1), tar100(:,2), '+b', _t, _cven(:,2), '-b');

CONC(2)=200.0;
start @nocallback

plot (plotcven, 1, tar200(:,1), tar200(:,2), '+k', _t, _cven(:,2), '-k');
```

```
set @preference=BackslashEscapeS

    pltscript(plotcven, "Chart.Header.Text = \"Tardif et al. (1996) Ethylbenzene
Inhalation Study\";")
    pltscript(plotcven, "Chart.SubHeader.Text = \"100, 200 ppm Inhalation for 4
Hours\";")
    pltscript(plotcven, "Chart.SubHeader.Visible=true;")
    pltscript(plotcven, "Chart.Axes.Left.Title.Text=\"Ethylbenzene in Venous Blood
[mg/L]\";")
    pltscript(plotcven, "Chart.Axes.Bottom.Title.Text=\"Hours\";")
    pltscript(plotcven, "Chart.Series[0].Title=\"100 ppm\";")
    pltscript(plotcven, "Chart.Series[1].Title=\"Simulation 100 ppm\";")
    pltscript(plotcven, "Chart.Series[2].Title=\"200 ppm\";")
    pltscript(plotcven, "Chart.Series[3].Title=\"Simulation 200 ppm\";")

set @preference=NoBackslashEscapeS
```

Xylene Study Simulation M Files

C3_Haddad.m

```
%Haddad, S., Tardif, R., Charest-Tardif, G. and Krishnan, K. 1999. Physiological
modeling
%     of the toxicokinetic interactions in a quaternary mixture of aromatic
hydrocarbons.
%     Toxicol.Appl.Pharmacol. 161(3): 249-257.

resetdoses
rattus
xylenerat

%T, CVEN (mean, +SD, -SD)
had50 = [
4.1    0.49
4.5    0.32
5.0    0.24
5.5    0.17
6.0    0.12
4.1    0.55
4.5    0.40
5.0    0.29
5.5    0.21
6.0    0.15
4.1    0.43
4.5    0.23
5.0    0.20
5.5    0.14
6.0    0.09];

%T, CVEN
had100 = [
4.1    1.20
4.5    0.86
5.0    0.50
5.5    0.37
6.0    0.24
4.1    1.46
```

```
4.5    1.02
5.0    0.62
5.5    0.45
6.0    0.33
4.1    1.10
4.5    0.73
5.0    0.44
5.5    0.33
6.0    0.17];

%T, CVEN
had200 = [
4.1    6.26
4.5    4.13
5.0    2.83
5.5    1.97
6.0    1.33
4.1    7.60
4.5    5.68
5.0    3.93
5.5    2.83
6.0    1.97
4.1    4.96
4.5    2.80
5.0    1.77
5.5    1.12
6.0    0.71];

BW=0.235;

CONC(3)=50.0, TCHNG=4.0;
TSTOP=8.0;
start @nocallback

plotcven = plot (0, had50(:,1), had50(:,2), '+b', _t, _cven(:,3), '-b');

CONC(3)=100.0;
start @nocallback

plot (plotcven, 1, had100(:,1), had100(:,2), '+k', _t, _cven(:,3), '-k');

CONC(3)=200.0;
start @nocallback

plot (plotcven, 1, had200(:,1), had200(:,2), '+g', _t, _cven(:,3), '-g');


set @preference=BackslashEscapeS

    pltscript(plotcven, "Chart.Header.Text = \"Haddad et al. (1999) m-Xylene
Inhalation Study\";")
    pltscript(plotcven, "Chart.SubHeader.Text = \"50, 100, 200 ppm Inhalation for 4
Hours\";")
    pltscript(plotcven, "Chart.SubHeader.Visible=true;")
    pltscript(plotcven, "Chart.Axes.Left.Title.Text=\"m-Xylene in Venous Blood
[mg/L]\";")
    pltscript(plotcven, "Chart.Axes.Bottom.Title.Text=\"Hours\";")
    pltscript(plotcven, "Chart.Series[0].Title=\"50 ppm\";")
    pltscript(plotcven, "Chart.Series[1].Title=\"Simulation 50 ppm\";")
    pltscript(plotcven, "Chart.Series[2].Title=\"100 ppm\";")
    pltscript(plotcven, "Chart.Series[3].Title=\"Simulation 100 ppm\";")
    pltscript(plotcven, "Chart.Series[4].Title=\"200 ppm\";")
    pltscript(plotcven, "Chart.Series[5].Title=\"Simulation 200 ppm\";")
```

```
set @preference=NoBackslashEscapeS
```

C3_Tardif.m

```
%Tardif, R., Charest-Tardif, G. and Brodeur, J. 1996. Comparison of the influence
%     of binary mixtures versus a ternary mixture of inhaled aromatic hydrocarbons
%     on their blood kinetics in the rat. Arch Toxicol 70(7): 405-413.

%Adult male SD rats
%  235-245 g

resetdoses
rattus
xylenerat

%T, CVEN from Figure 1, mean followed by +SD then -SD
tar100 = [
4.1    1.26
4.5    0.86
5.0    0.51
5.5    0.37
6.0    0.24
4.1    1.44
4.5    1.01
5.0    0.62
5.5    0.43
6.0    0.30
4.1    1.09
4.5    0.71
5.0    0.43
5.5    0.31
6.0    0.15];

%T, CVEN from Figure 3, mean followed by +SD then -SD
tar200 = [
4.1    6.32
4.5    4.26
5.0    2.83
5.5    1.99
6.0    1.37
4.1    7.80
4.5    5.74
5.0    3.95
5.5    2.83
6.0    2.04
4.1    4.89
4.5    2.83
5.0    1.75
5.5    1.12
6.0    0.74];

BW=0.240;

CONC(3)=100.0;
TCHNG=4.0;
TSTOP=6.0;
start @nocallback

plotcven = plot (0, tar100(:,1), tar100(:,2), '+b', _t, _cven(:,3), '-b');
```

```
CONC(3)=200.0;
start @nocallback

plot (plotcven, 1, tar200(:,1), tar200(:,2), '+k', _t, _cven(:,3), '-k');


set @preference=BackslashEscapeS

    pltscript(plotcven, "Chart.Header.Text = \"Tardif et al. (1996) m-Xylene
Inhalation Study\";")
    pltscript(plotcven, "Chart.SubHeader.Text = \"100, 200 ppm Inhalation for 4
Hours\";")
    pltscript(plotcven, "Chart.SubHeader.Visible=true;")
    pltscript(plotcven, "Chart.Axes.Left.Title.Text=\"Xylene in Venous Blood
[mg/L]\";")
    pltscript(plotcven, "Chart.Axes.Bottom.Title.Text=\"Hours\";")
    pltscript(plotcven, "Chart.Series[0].Title=\"100 ppm\";")
    pltscript(plotcven, "Chart.Series[1].Title=\"Simulation 100 ppm\";")
    pltscript(plotcven, "Chart.Series[2].Title=\"200 ppm\";")
    pltscript(plotcven, "Chart.Series[3].Title=\"Simulation 200 ppm\";")

set @preference=NoBackslashEscapeS
```

Nonane Study Simulation M Files

C4_inhouse_inhal.m

```
%Robinson, P.J. and Merrill, E.A. 2008. A harmonized physiologically based
pharmacokinetic model
%     for nonane as a component of jet fuel. Wright-Patterson AFB, OH: Air Force
Research
%     Laboratory, Applied Biotechnology Branch. AFRL-RH-WP-TR-2008-0067, ADA502610.

resetdoses
rattus
nonanerat

%(t, cven, cfat, cliv, cslw)
ihl90d100 = [
 0.5    0.372   NaN     NaN    NaN
 0.5    0.427   NaN     NaN    NaN
 0.5    0.482   NaN     NaN       NaN
 1.0    0.370   NaN     NaN    NaN
 1.0    0.523   NaN     NaN    NaN
 1.0    0.676   NaN     NaN    NaN
 2.0    0.306   NaN     NaN    NaN
 2.0    0.516   NaN     NaN    NaN
 2.0    0.726   NaN     NaN    NaN
 3.0    0.496   NaN     NaN    NaN
 3.0    0.676   NaN     NaN    NaN
 3.0    0.856   NaN     NaN    NaN
 4.0    0.808   13.93   1.44   1.0
 4.0    0.891   27.24   3.83   2.76
 4.0    0.974   40.55   6.22   4.52
 4.08   0.292   NaN     NaN    NaN
 4.08   0.43    NaN     NaN    NaN
 4.08   0.568   NaN     NaN    NaN
 4.16   0.2251  NaN     NaN    NaN
 4.16   0.362   NaN     NaN    NaN
```

```
 4.16   0.498   NaN     NaN    NaN
 4.25   0.191   NaN     NaN    NaN
 4.25   0.304   NaN     NaN    NaN
 4.25   0.417   NaN     NaN    NaN
 4.5    0.097   NaN     NaN    NaN
 4.5    0.205   NaN     NaN    NaN
 4.5    0.313   NaN     NaN    NaN
 5.0    0.053   NaN     NaN    NaN
 5.0    0.114   NaN     NaN    NaN
 5.0    0.175   NaN     NaN    NaN
 6.0    0.004   NaN     NaN    NaN
 6.0    0.037   NaN     NaN    NaN
 6.0    0.07    NaN     NaN    NaN
 7.0    0.003   NaN     NaN    NaN
 7.0    0.03    NaN     NaN    NaN
 7.0    0.057   NaN     NaN    NaN
 8.0    0.0     8.29    0.0    0.0
 8.0    0.019   18.65   0.05   0.7
 8.0    0.042   29.01   0.22   1.65];

%(t, CV1, CF1, CL1, CS1)
ihl90d500 = [
 0.6    1.311   NaN     NaN    NaN
 0.6    2.051   NaN     NaN    NaN
 0.6    2.791   NaN     NaN    NaN
 1.1    1.406   NaN     NaN    NaN
 1.1    2.263   NaN     NaN    NaN
 1.1    3.12    NaN     NaN    NaN
 2.1    2.934   NaN     NaN    NaN
 2.1    3.736   NaN     NaN    NaN
 2.1    4.538   NaN     NaN    NaN
 3.1    2.201   NaN     NaN    NaN
 3.1    3.635   NaN     NaN    NaN
 3.1    5.069   NaN     NaN    NaN
 4.1    3.504   66.01   25.03  11.71
 4.1    4.43    131.11  39.63  17.33
 4.1    5.356   196.21  54.23  22.95
 4.18   3.0     NaN     NaN    NaN
 4.18   3.75    NaN     NaN    NaN
 4.18   4.5     NaN     NaN    NaN
 4.26   1.902   NaN     NaN    NaN
 4.26   2.785   NaN     NaN    NaN
 4.26   3.668   NaN     NaN    NaN
 4.35   1.322   NaN     NaN    NaN
 4.35   1.953   NaN     NaN    NaN
 4.35   2.584   NaN     NaN    NaN
 4.6    1.34    NaN     NaN    NaN
 4.6    1.768   NaN     NaN    NaN
 4.6    2.196   NaN     NaN    NaN
 5.1    0.811   NaN     NaN    NaN
 5.1    1.184   NaN     NaN    NaN
 5.1    1.557   NaN     NaN    NaN
 6.1    0.218   NaN     NaN    NaN
 6.1    0.41    NaN     NaN    NaN
 6.1    0.602   NaN     NaN    NaN
 7.1    0.195   NaN     NaN    NaN
 7.1    0.365   NaN     NaN    NaN
 7.1    0.535   NaN     NaN    NaN
 8.1    0.152   52.64   0.34   0.0
 8.1    0.251   82.2    0.48   4.96
 8.1    0.35    111.76  0.62   10.08];

%(t, CV1, CF1, CL1, CS1)
```

```
ihl90d1000 = [
 0.7    1.682   NaN     NaN    NaN
 0.7    6.933   NaN     NaN    NaN
 0.7    12.184  NaN     NaN    NaN
 1.2    3.385   NaN     NaN    NaN
 1.2    6.95    NaN     NaN    NaN
 1.2    10.515  NaN     NaN    NaN
 2.2    9.405   NaN     NaN    NaN
 2.2    15.211  NaN     NaN    NaN
 2.2    21.017  NaN     NaN    NaN
 3.2    7.789   NaN     NaN    NaN
 3.2    16.928  NaN     NaN    NaN
 3.2    26.067  NaN     NaN    NaN
 4.2    4.724   66.86   47.91  23.61
 4.2    16.467  360.28  99.9   45.0
 4.2    28.21   653.7   151.91 66.39
 4.28   6.904   NaN     NaN    NaN
 4.28   13.625  NaN     NaN    NaN
 4.28   20.346  NaN     NaN    NaN
 4.36   2.902   NaN     NaN    NaN
 4.36   10.88   NaN     NaN    NaN
 4.36   18.858  NaN     NaN    NaN
 4.45   3.02    NaN     NaN    NaN
 4.45   9.281   NaN     NaN    NaN
 4.45   15.542  NaN     NaN    NaN
 4.7    1.649   NaN     NaN    NaN
 4.7    5.073   NaN     NaN    NaN
 4.7    8.497   NaN     NaN    NaN
 5.2    0.888   NaN     NaN    NaN
 5.2    4.403   NaN     NaN    NaN
 5.2    7.918   NaN     NaN    NaN
 6.2    0.638   NaN     NaN    NaN
 6.2    2.378   NaN     NaN    NaN
 6.2    4.118   NaN     NaN    NaN
 7.2    0.514   NaN     NaN    NaN
 7.2    1.483   NaN     NaN    NaN
 7.2    2.452   NaN     NaN    NaN
 8.2    0.247   155.42  2.2    7.07
 8.2    0.687   316.26  7.15   21.11
 8.2    1.127   477.1   12.1   35.15];

BW=0.3;

CONC(4)=100.0, TCHNG=4.0;
TSTOP=10;
start @nocallback

plotcven = plot (0, ihl90d100(:,1), ihl90d100(:,2), '+b', _t, _cven(:,4), '-b');
plotcfat = plot (0, ihl90d100(:,1), ihl90d100(:,3), '+b', _t, _cfat(:,4), '-b');
plotcliv = plot (0, ihl90d100(:,1), ihl90d100(:,4), '+b', _t, _cliv(:,4), '-b');
plotcslw = plot (0, ihl90d100(:,1), ihl90d100(:,5), '+b', _t, _cslw(:,4), '-b');

CONC(4)=500.0, TCHNG(4)=4.1;
start @nocallback

plot (plotcven, 1, ihl90d500(:,1), ihl90d500(:,2), '+k', _t, _cven(:,4), '-k');
plot (plotcfat, 1, ihl90d500(:,1), ihl90d500(:,3), '+k', _t, _cfat(:,4), '-k');
plot (plotcliv, 1, ihl90d500(:,1), ihl90d500(:,4), '+k', _t, _cliv(:,4), '-k');
plot (plotcslw, 1, ihl90d500(:,1), ihl90d500(:,5), '+k', _t, _cslw(:,4), '-k');

CONC(4)=1000.0, TCHNG(4)=4.2;
start @nocallback
```

```
plot (plotcven, 1, ihl90d500(:,1), ihl90d1000(:,2), '+g', _t, _cven(:,4), '-g');
plot (plotcfat, 1, ihl90d500(:,1), ihl90d1000(:,3), '+g', _t, _cfat(:,4), '-g');
plot (plotcliv, 1, ihl90d500(:,1), ihl90d1000(:,4), '+g', _t, _cliv(:,4), '-g');
plot (plotcslw, 1, ihl90d500(:,1), ihl90d1000(:,5), '+g', _t, _cslw(:,4), '-g');


set @preference=BackslashEscapeS

    pltscript(plotcven, "Chart.Header.Text = \"In-House Nonane Inhalation Study\";")
    pltscript(plotcven, "Chart.SubHeader.Text = \"100, 500, 1000 ppm Inhalation for 4
Hours\";")
    pltscript(plotcven, "Chart.SubHeader.Visible=true;")
    pltscript(plotcven, "Chart.Axes.Left.Title.Text=\"Nonane in Venous Blood
[mg/L]\";")
    pltscript(plotcven, "Chart.Axes.Bottom.Title.Text=\"Hours\";")
    pltscript(plotcven, "Chart.Series[0].Title=\"100 ppm\";")
    pltscript(plotcven, "Chart.Series[1].Title=\"Simulation 100 ppm\";")
    pltscript(plotcven, "Chart.Series[2].Title=\"500 ppm\";")
    pltscript(plotcven, "Chart.Series[3].Title=\"Simulation 500 ppm\";")
    pltscript(plotcven, "Chart.Series[4].Title=\"1000 ppm\";")
    pltscript(plotcven, "Chart.Series[5].Title=\"Simulation 1000 ppm\";")

    pltscript(plotcfat, "Chart.Header.Text = \"In-House Nonane Inhalation Study\";")
    pltscript(plotcfat, "Chart.SubHeader.Text = \"100, 500, 1000 ppm Inhalation for 4
Hours\";")
    pltscript(plotcfat, "Chart.SubHeader.Visible=true;")
    pltscript(plotcfat, "Chart.Axes.Left.Title.Text=\"Nonane in Fat [mg/L]\";")
    pltscript(plotcfat, "Chart.Axes.Bottom.Title.Text=\"Hours\";")
    pltscript(plotcfat, "Chart.Series[0].Title=\"100 ppm\";")
    pltscript(plotcfat, "Chart.Series[1].Title=\"Simulation 100 ppm\";")
    pltscript(plotcfat, "Chart.Series[2].Title=\"500 ppm\";")
    pltscript(plotcfat, "Chart.Series[3].Title=\"Simulation 500 ppm\";")
    pltscript(plotcfat, "Chart.Series[4].Title=\"1000 ppm\";")
    pltscript(plotcfat, "Chart.Series[5].Title=\"Simulation 1000 ppm\";")

    pltscript(plotcliv, "Chart.Header.Text = \"In-House Nonane Inhalation Study\";")
    pltscript(plotcliv, "Chart.SubHeader.Text = \"100, 500, 1000 ppm Inhalation for 4
Hours\";")
    pltscript(plotcliv, "Chart.SubHeader.Visible=true;")
    pltscript(plotcliv, "Chart.Axes.Left.Title.Text=\"Nonane in Liver [mg/L]\";")
    pltscript(plotcliv, "Chart.Axes.Bottom.Title.Text=\"Hours\";")
    pltscript(plotcliv, "Chart.Series[0].Title=\"100 ppm\";")
    pltscript(plotcliv, "Chart.Series[1].Title=\"Simulation 100 ppm\";")
    pltscript(plotcliv, "Chart.Series[2].Title=\"500 ppm\";")
    pltscript(plotcliv, "Chart.Series[3].Title=\"Simulation 500 ppm\";")
    pltscript(plotcliv, "Chart.Series[4].Title=\"1000 ppm\";")
    pltscript(plotcliv, "Chart.Series[5].Title=\"Simulation 1000 ppm\";")

    pltscript(plotcslw, "Chart.Header.Text = \"In-House Nonane Inhalation Study\";")
    pltscript(plotcslw, "Chart.SubHeader.Text = \"100, 500, 1000 ppm Inhalation for 4
Hours\";")
    pltscript(plotcslw, "Chart.SubHeader.Visible=true;")
    pltscript(plotcslw, "Chart.Axes.Left.Title.Text=\"Nonane in Slowly Perfused
Tissues [mg/L]\";")
    pltscript(plotcslw, "Chart.Axes.Bottom.Title.Text=\"Hours\";")
    pltscript(plotcslw, "Chart.Series[0].Title=\"100 ppm\";")
    pltscript(plotcslw, "Chart.Series[1].Title=\"Simulation 100 ppm\";")
    pltscript(plotcslw, "Chart.Series[2].Title=\"500 ppm\";")
    pltscript(plotcslw, "Chart.Series[3].Title=\"Simulation 500 ppm\";")
    pltscript(plotcslw, "Chart.Series[4].Title=\"1000 ppm\";")
    pltscript(plotcslw, "Chart.Series[5].Title=\"Simulation 1000 ppm\";")

set @preference=NoBackslashEscapeS
```

C4_Lof99.m

```
%Lof, A., Lam, H.R., Gullstrand, E., Ostergaard, G. and Ladefoged, O. 1999.
Distribution of
%     dearomatised white spirit in brain, blood, and fat tissue after repeated
exposure of
%     rats. Pharmacol.Toxicol. 85(2): 92-97.

% Rats dosed with 400 and 800 ppm white spirits; 3.6% n-nonane = 14.4 and 28.8 ppm
nonane, respectively

resetdoses
rattus
nonanerat

 %(T, CVen, CBrnTot, CFat)
 lof99lo = [
 102.  0.1        0.73   27.26
 102.  0.14       1.17   32.
 102.  0.06       0.29   22.52
 270.  0.09       0.65   32.5
 270.  0.15       0.85   39.7
 270.  0.03       0.45   25.3
 438.  0.1        0.54   29.06
 438.  0.13       0.62   34.41
 438.  0.07       0.46   23.71
 440.  0.03       0.24   33.85
 440.  0.04       0.27   41.22
 440.  0.02       0.21   26.48
 442.  0.02       0.19   29.75
 442.  0.03       0.24   35.48
 442.  0.01       0.14   24.02
 444.  0.02       0.14   28.54
 444.  0.03       0.18   32.46
 444.  0.01       0.1    24.62
 462.  0.01       0.18   23.75
 462.  0.01       0.24   24.58
 462.  0.01       0.12   22.92];

%(T, CVen, CBrnTot, CFat)
 lof99hi = [
 102.   0.26       1.2    69.82
 102.   0.41       1.58   81.94
 102.   0.11       0.82   57.7
 270.   0.21       1.31   90.39
 270.   0.31       1.54   111.72
 270.   0.11       1.08   69.06
 438.   0.32       1.27   99.51
 438.   0.44       1.4    127.56
 438.   0.2        1.14   71.46
 440.   0.06       0.32   88.96
 440.   0.08       0.4    101.56
 440.   0.04       0.24   76.36
 442.   0.03       0.34   74.76
 442.   0.04       0.51   82.
 442.   0.02       0.17   67.52
 444.   0.02       0.2    69.3
 444.   0.03       0.23   75.36
 444.   0.01       0.17   63.24
 462.   0.02       0.18   50.07
 462.   0.02       0.25   58.5
 462.   0.02       0.11   41.64];
```

```
BW=0.3;

CONC(4)=14.4;
TCHNG=6.0; DOSEINT=24.0; DAYSWK=5.0; TMAX=504.0;
CINT=0.1;
TSTOP=525.0; %not sure why it was 529 before - this is the next interval of 25 higher
than last dosing
start @nocallback

plotcven = plot (0, lof99lo(:,1), lof99lo(:,2), '+b', _t, _cven(:,4), '-b');
plotcbrntot = plot (0, lof99lo(:,1), lof99lo(:,3), '+b', _t, _cbrntot(:,4), '-b');
plotcfat = plot (0, lof99lo(:,1), lof99lo(:,4), '+b', _t, _cfat(:,4), '-b');

CONC(4)=28.8;
start @nocallback

plot (plotcven, 1, lof99hi(:,1), lof99hi(:,2), '+k', _t, _cven(:,4), '-k');
plot (plotcbrntot, 1, lof99hi(:,1), lof99hi(:,3), '+k', _t, _cbrntot(:,4), '-k');
plot (plotcfat, 1, lof99hi(:,1), lof99hi(:,4), '+k', _t, _cfat(:,4), '-k');


set @preference=BackslashEscapeS

    pltscript(plotcven, "Chart.Header.Text = \"Lof et al. (1999) White Spirits
Inhalation Study\";")
    pltscript(plotcven, "Chart.SubHeader.Text = \"14.4 and 28.8 ppm for 6 Hours\";")
    pltscript(plotcven, "Chart.SubHeader.Visible=true;")
    pltscript(plotcven, "Chart.Axes.Left.Title.Text=\"Nonane in Venous Blood
[mg/L]\";")
    pltscript(plotcven, "Chart.Axes.Bottom.Title.Text=\"Hours\";")
    pltscript(plotcven, "Chart.Series[0].Title=\"14.4 ppm\";")
    pltscript(plotcven, "Chart.Series[1].Title=\"Simulation 14.4 ppm\";")
    pltscript(plotcven, "Chart.Series[2].Title=\"28.8 ppm\";")
    pltscript(plotcven, "Chart.Series[3].Title=\"Simulation 28.8 ppm\";")

    pltscript(plotcbrntot, "Chart.Header.Text = \"Lof et al. (1999) White Spirits
Inhalation Study\";")
    pltscript(plotcbrntot, "Chart.SubHeader.Text = \"14.4 and 28.8 ppm for 6
Hours\";")
    pltscript(plotcbrntot, "Chart.SubHeader.Visible=true;")
    pltscript(plotcbrntot, "Chart.Axes.Left.Title.Text=\"Nonane in Total Brain
[mg/L]\";")
    pltscript(plotcbrntot, "Chart.Axes.Bottom.Title.Text=\"Hours\";")
    pltscript(plotcbrntot, "Chart.Series[0].Title=\"14.4 ppm\";")
    pltscript(plotcbrntot, "Chart.Series[1].Title=\"Simulation 14.4 ppm\";")
    pltscript(plotcbrntot, "Chart.Series[2].Title=\"28.8 ppm\";")
    pltscript(plotcbrntot, "Chart.Series[3].Title=\"Simulation 28.8 ppm\";")

    pltscript(plotcfat, "Chart.Header.Text = \"Lof et al. (1999) White Spirits
Inhalation Study\";")
    pltscript(plotcfat, "Chart.SubHeader.Text = \"14.4 and 28.8 ppm for 6 Hours\";")
    pltscript(plotcfat, "Chart.SubHeader.Visible=true;")
    pltscript(plotcfat, "Chart.Axes.Left.Title.Text=\"Nonane in Fat [mg/L]\";")
    pltscript(plotcfat, "Chart.Axes.Bottom.Title.Text=\"Hours\";")
    pltscript(plotcfat, "Chart.Series[0].Title=\"14.4 ppm\";")
    pltscript(plotcfat, "Chart.Series[1].Title=\"Simulation 14.4 ppm\";")
    pltscript(plotcfat, "Chart.Series[2].Title=\"28.8 ppm\";")
    pltscript(plotcfat, "Chart.Series[3].Title=\"Simulation 28.8 ppm\";")

set @preference=NoBackslashEscapeS
```

C4_Zahlsen90.m

```
%Zahlsen, K., Nilsen, A.M., Eide, I. and Nilsen, O.G. 1990. Accumulation and
distribution of
%     aliphatic (n-nonane), aromatic (1,2,4-trimethylbenzene) and naphthenic
%     (1,2,4-trimethylcyclohexane) hydrocarbons in the rat after repeated inhalation.
Pharmacol.
%     Toxicol. 67(5): 436-440.


resetdoses
rattus
nonanerat

 %(T, CVen, CBrnTot)
 zahl90 = [
 12.      21.8     179.
 60.      17.3     153.
 156.     15.4     153.
 228.     11.5     132.
 348.     10.2     123.];

% At the start, the animals weighed 150-200 g; Assumed 200 g overall due to growth
BW=0.2;

CONC(4)=1025.2; %Target was 1000 ppm, measured on 5 days, average 1025.2 ppm
TCHNG=12.0; DOSEINT=24.0; DAYSWK=7.0; TMAX=360.0; %TMAX=336.0 depending on how you
read it
CINT=0.1;
TSTOP=360.0;

start @nocallback

plotcven = plot (0, zahl90(:,1), zahl90(:,2), '+b', _t, _cven(:,4), '-b');
plotcbrntot = plot (0, zahl90(:,1), zahl90(:,3), '+b', _t, _cbrntot(:,4), '-b');


set @preference=BackslashEscapeS

    pltscript(plotcven, "Chart.Header.Text = \"Zahlsen et al. (1990) Nonane Inhalation
Study\";")
    pltscript(plotcven, "Chart.SubHeader.Text = \"1000 ppm for 12 Hours\";")
    pltscript(plotcven, "Chart.SubHeader.Visible=true;")
    pltscript(plotcven, "Chart.Axes.Left.Title.Text=\"Nonane in Venous Blood
[mg/L]\";")
    pltscript(plotcven, "Chart.Axes.Bottom.Title.Text=\"Hours\";")
    pltscript(plotcven, "Chart.Series[0].Title=\"1000 ppm\";")
    pltscript(plotcven, "Chart.Series[1].Title=\"Simulation 1000 ppm\";")

    pltscript(plotcbrntot, "Chart.Header.Text = \"Zahlsen et al. (1990) Nonane
Inhalation Study\";")
    pltscript(plotcbrntot, "Chart.SubHeader.Text = \"1000 ppm for 12 Hours\";")
    pltscript(plotcbrntot, "Chart.SubHeader.Visible=true;")
    pltscript(plotcbrntot, "Chart.Axes.Left.Title.Text=\"Nonane in Total Brain
[mg/L]\";")
    pltscript(plotcbrntot, "Chart.Axes.Bottom.Title.Text=\"Hours\";")
    pltscript(plotcbrntot, "Chart.Series[0].Title=\"1000 ppm\";")
    pltscript(plotcbrntot, "Chart.Series[1].Title=\"Simulation 1000 ppm\";")

set @preference=NoBackslashEscapeS
```

Decane Study Simulation M Files

C5_Lof99.m

```
%Lof, A., Lam, H.R., Gullstrand, E., Ostergaard, G. and Ladefoged, O. 1999.
Distribution of
%     dearomatised white spirit in brain, blood, and fat tissue after repeated
exposure of
%     rats. Pharmacol.Toxicol. 85(2): 92-97.

% Rats dosed with 400 and 800 ppm white spirits; 16.6% n-decane = 106.4 and 212 ppm
decane, respectively

resetdoses
rattus
decanerat

 %(T, CVen, CBrnTot, CFat)
 %Additional data are present in the original cmd file, but commented out
 lof99lo = [
 102.    0.7  3.35   150.3
 102.    0.86 4.99   178.94
 102.    0.54 1.71   121.66
 270.    0.88 2.64   182.8
 270.    1.1  3.27   222.1
 270.    0.66 2.01   143.5
 438.    0.7  2.34   172.1
 438.    0.81 2.89   198.4
 438.    0.59 1.79   145.8
 440.    0.3  1.24   202.8
 440.    0.35 1.34   256.19
 440.    0.25 1.14   149.41
 442.    0.24 0.78   190.8
 442.    0.29 0.93   218.12
 442.    0.19 0.63   163.48
 444.    0.21 0.54   191.7
 444.    0.25 0.72   228.18
 444.    0.17 0.36   155.22
 462.    0.13 0.45   166.5
 462.    0.16 0.88   187.19
 462.    0.1  0.02   145.81];

%(T, CVen, CBrnTot, CFat)
 lof99hi = [
 102.         2.09  6.08   440.2
 102.    2.78 7.62   493.34
 102.    1.4  4.54   387.06
 270.    1.73 6.24   537.7
 270.    2.12 6.96   642.8
 270.    1.34 5.52   432.6
 438.    2.21 5.95   590.5
 438.    2.75 7.19   770.5
 438.    1.67 4.71   410.5
 440.    0.57 2.91   547.3
 440.    0.64 3.24   616.49
 440.    0.5  2.58   478.11
 442.    0.44 1.96   511.9
 442.    0.48 2.8     571.78
 442.    0.4  1.12   452.02
 444.    0.36 1.14   489.6
```

```
 444.    0.42 1.37   534.2
 444.    0.3  0.91   445.
 462.    0.16 0.57   426.
 462.    0.18 0.97   462.76
 462.    0.14 0.17   389.24];

BW=0.3;

CONC(5)=106.4;
TCHNG=6.0; DOSEINT=24.0; DAYSWK=5.0; TMAX=504.0;
CINT=0.1;
TSTOP=525.0; %not sure why it was 529 before - this is the next interval of 25 higher
than last dosing
start @nocallback

plotcven = plot (0, lof99lo(:,1), lof99lo(:,2), '+b', _t, _cven(:,5), '-b');
plotcbrntot = plot (0, lof99lo(:,1), lof99lo(:,3), '+b', _t, _cbrntot(:,5), '-b');
plotcfat = plot (0, lof99lo(:,1), lof99lo(:,4), '+b', _t, _cfat(:,5), '-b');

CONC(5)=212.0;
start @nocallback

plot (plotcven, 1, lof99hi(:,1), lof99hi(:,2), '+k', _t, _cven(:,5), '-k');
plot (plotcbrntot, 1, lof99hi(:,1), lof99hi(:,3), '+k', _t, _cbrntot(:,5), '-k');
plot (plotcfat, 1, lof99hi(:,1), lof99hi(:,4), '+k', _t, _cfat(:,5), '-k');


set @preference=BackslashEscapeS

    pltscript(plotcven, "Chart.Header.Text = \"Lof et al. (1999) White Spirits
Inhalation Study\";")
    pltscript(plotcven, "Chart.SubHeader.Text = \"106.4 and 212 ppm for 6 Hours\";")
    pltscript(plotcven, "Chart.SubHeader.Visible=true;")
    pltscript(plotcven, "Chart.Axes.Left.Title.Text=\"Decane in Venous Blood
[mg/L]\";")
    pltscript(plotcven, "Chart.Axes.Bottom.Title.Text=\"Hours\";")
    pltscript(plotcven, "Chart.Series[0].Title=\"106.4 ppm\";")
    pltscript(plotcven, "Chart.Series[1].Title=\"Simulation 106.4 ppm\";")
    pltscript(plotcven, "Chart.Series[2].Title=\"212 ppm\";")
    pltscript(plotcven, "Chart.Series[3].Title=\"Simulation 212 ppm\";")

    pltscript(plotcbrntot, "Chart.Header.Text = \"Lof et al. (1999) White Spirits
Inhalation Study\";")
    pltscript(plotcbrntot, "Chart.SubHeader.Text = \"106.4 and 212 ppm for 6
Hours\";")
    pltscript(plotcbrntot, "Chart.SubHeader.Visible=true;")
    pltscript(plotcbrntot, "Chart.Axes.Left.Title.Text=\"Decane in Total Brain
[mg/L]\";")
    pltscript(plotcbrntot, "Chart.Axes.Bottom.Title.Text=\"Hours\";")
    pltscript(plotcbrntot, "Chart.Series[0].Title=\"106.4 ppm\";")
    pltscript(plotcbrntot, "Chart.Series[1].Title=\"Simulation 106.4 ppm\";")
    pltscript(plotcbrntot, "Chart.Series[2].Title=\"212 ppm\";")
    pltscript(plotcbrntot, "Chart.Series[3].Title=\"Simulation 212 ppm\";")

    pltscript(plotcfat, "Chart.Header.Text = \"Lof et al. (1999) White Spirits
Inhalation Study\";")
    pltscript(plotcfat, "Chart.SubHeader.Text = \"106.4 and 212 ppm for 6 Hours\";")
    pltscript(plotcfat, "Chart.SubHeader.Visible=true;")
    pltscript(plotcfat, "Chart.Axes.Left.Title.Text=\"Decane in Fat [mg/L]\";")
    pltscript(plotcfat, "Chart.Axes.Bottom.Title.Text=\"Hours\";")
    pltscript(plotcfat, "Chart.Series[0].Title=\"106.4 ppm\";")
    pltscript(plotcfat, "Chart.Series[1].Title=\"Simulation 106.4 ppm\";")
    pltscript(plotcfat, "Chart.Series[2].Title=\"212 ppm\";")
```

```
    pltscript(plotcfat, "Chart.Series[3].Title=\"Simulation 212 ppm\";")

set @preference=NoBackslashEscapeS
```

C5_Perleberg04.m

```
%Perleberg, U.R., Keys, D.A. and Fisher, J.W. 2004. Development of a physiologically
%     based pharmacokinetic model for decane, a constituent of Jet Propellent-8.
%     Inhal.Toxicol. 16(11-12): 771-783.

resetdoses
rattus
decanerat

 %(1-T, 2-CArt, 3-CLiv, 4-CBrnTot, 5-CRap, 6-CFat, 7-conc-bone-marrow, 8-conc-skin)
 perl1200 = [
 4.08  4.34   33.74  120.38 11.09  104.91 260.89 8.18
 4.08  4.79   37.96  131.21 13.08  122.68 315.37 9.83
 4.08  3.89   29.52  109.55 9.10   87.15  206.42 6.53
 4.50  0.63   17.48  94.85  11.02  60.51  195.57 8.72
 4.50  0.82   23.02  108.64 13.91  81.42  272.81 10.82
 4.50  0.44   11.94  81.07  8.12   39.60  118.33 6.622
 5.00  0.58   5.17   73.29  5.84   112.89 NaN    24.12
 5.00  0.72   6.15   75.55  7.44   142.72 NaN    37.15
 5.00  0.45   4.18   71.04  4.23   83.05  NaN    11.09
 6.00  0.26   1.16   45.37  4.97   88.52  158.30 10.43
 6.00  0.32   1.64   48.94  6.32   107.13 200.46 13.81
 6.00  0.20   0.69   41.80  3.62   69.91  116.14 7.050
 8.00  0.15   0.55   14.76  3.23   94.43  NaN    8.363
 8.00  0.19   0.74   15.76  3.76   118.91 NaN    13.45
 8.00  0.10   0.37   13.76  2.71   69.94  NaN    3.277
 10.00 NaN    NaN    6.90   3.82   101.23 57.139 20.98
 10.00 NaN    NaN    7.77   5.48   123.56 66.751 29.04
 10.00 NaN    NaN    6.02   2.17   78.89  47.528 12.93
 16.00 NaN    NaN    2.09   2.85   74.96  6.140  0.861
 16.00 NaN    NaN    2.28   4.15   83.96  6.911  1.463
 16.00 NaN    NaN    1.90   1.55   65.96  5.370  0.259
 28.00 NaN    NaN    0.36   2.45   55.34  1.348  1.004
 28.00 NaN    NaN    0.45   3.66   64.11  1.672  1.572
 28.00 NaN    NaN    0.27   1.24   46.57  1.025  0.435];

 %(1-T, 2-CArt, 3-CLiv, 4-CBrnTot, 5-CRap, 6-CFat, 7-conc-bone-marrow, 8-conc-skin)
 perl781 = [
 4.00  2.68   34.8   61.1   12.1   51.1   109.64 NaN
 4.00  3.58   45.1   65.9   16.7   72.3   163.83 NaN
 4.00  1.78   24.5   56.2   7.42   29.7   55.469 NaN];

 %(1-T, 2-CArt, 3-CLiv, 4-CBrnTot, 5-CRap, 6-CFat, 7-conc-bone-marrow, 8-conc-skin)
 perl273 = [
 4.00  0.49   4.39   18.3   2.14   14.3   52.479 1.45
 4.00  0.65   5.30   21.1   2.76   23.3   66.393 1.45
 4.00  0.34   3.49   16.1   1.53   5.34   38.565 0.79];

BW=0.211;

CONC(5)=1200.0;
TCHNG=4.0; DOSEINT=24.0; DAYSWK=5.0; TMAX=24.0;
CINT=0.1;
TSTOP=30.0;
start @nocallback
```

```
plotcart = plot (0, perl1200(:,1), perl1200(:,2), '+b', _t, _cart(:,5), '-b');
plotcliv = plot (0, perl1200(:,1), perl1200(:,3), '+b', _t, _cliv(:,5), '-b');
plotcbrntot = plot (0, perl1200(:,1), perl1200(:,4), '+b', _t, _cbrntot(:,5), '-b');
plotcrap = plot (0, perl1200(:,1), perl1200(:,5), '+b', _t, _crap(:,5), '-b');
plotcfat = plot (0, perl1200(:,1), perl1200(:,6), '+b', _t, _cfat(:,5), '-b');

CONC(5)=781.0;
TSTOP=5.0;
start @nocallback

plot (plotcart, 1, perl781(:,1), perl781(:,2), '+k', _t, _cart(:,5), '-k');
plot (plotcliv, 1, perl781(:,1), perl781(:,3), '+k', _t, _cliv(:,5), '-k');
plot (plotcbrntot, 1, perl781(:,1), perl781(:,4), '+k', _t, _cbrntot(:,5), '-k');
plot (plotcrap, 1, perl781(:,1), perl781(:,5), '+k', _t, _crap(:,5), '-k');
plot (plotcfat, 1, perl781(:,1), perl781(:,6), '+k', _t, _cfat(:,5), '-k');

CONC(5)=273.0;
start @nocallback

plot (plotcart, 1, perl273(:,1), perl273(:,2), '+g', _t, _cart(:,5), '-g');
plot (plotcliv, 1, perl273(:,1), perl273(:,3), '+g', _t, _cliv(:,5), '-g');
plot (plotcbrntot, 1, perl273(:,1), perl273(:,4), '+g', _t, _cbrntot(:,5), '-g');
plot (plotcrap, 1, perl273(:,1), perl273(:,5), '+g', _t, _crap(:,5), '-g');
plot (plotcfat, 1, perl273(:,1), perl273(:,6), '+g', _t, _cfat(:,5), '-g');


set @preference=BackslashEscapeS

    pltscript(plotcart, "Chart.Header.Text = \"Perleberg et al. (2004) n-Decane
Inhalation Study\";")
    pltscript(plotcart, "Chart.SubHeader.Text = \"273, 781 or 1200 ppm for 4
Hours\";")
    pltscript(plotcart, "Chart.SubHeader.Visible=true;")
    pltscript(plotcart, "Chart.Axes.Left.Automatic=false;")
    pltscript(plotcart, "Chart.Axes.Left.Minimum=0.01;")
    pltscript(plotcart, "Chart.Axes.Left.Maximum=100.0;")
    pltscript(plotcart, "Chart.Axes.Left.Logarithmic = true;")
    pltscript(plotcart, "Chart.Axes.Left.Title.Text=\"Decane in Arterial Blood
[mg/L]\";")
    pltscript(plotcart, "Chart.Axes.Bottom.Title.Text=\"Hours\";")
    pltscript(plotcart, "Chart.Series[0].Title=\"1200 ppm\";")
    pltscript(plotcart, "Chart.Series[1].Title=\"Simulation 1200 ppm\";")
    pltscript(plotcart, "Chart.Series[2].Title=\"781 ppm\";")
    pltscript(plotcart, "Chart.Series[3].Title=\"Simulation 781 ppm\";")
    pltscript(plotcart, "Chart.Series[4].Title=\"273 ppm\";")
    pltscript(plotcart, "Chart.Series[5].Title=\"Simulation 273 ppm\";")

    pltscript(plotcliv, "Chart.Header.Text = \"Perleberg et al. (2004) n-Decane
Inhalation Study\";")
    pltscript(plotcliv, "Chart.SubHeader.Text = \"273, 781 or 1200 ppm for 4
Hours\";")
    pltscript(plotcliv, "Chart.SubHeader.Visible=true;")
    pltscript(plotcliv, "Chart.Axes.Left.Automatic=false;")
    pltscript(plotcliv, "Chart.Axes.Left.Minimum=0.01;")
    pltscript(plotcliv, "Chart.Axes.Left.Maximum=100.0;")
    pltscript(plotcliv, "Chart.Axes.Left.Logarithmic = true;")
    pltscript(plotcliv, "Chart.Axes.Left.Title.Text=\"Decane in Liver [mg/L]\";")
    pltscript(plotcliv, "Chart.Axes.Bottom.Title.Text=\"Hours\";")
    pltscript(plotcliv, "Chart.Series[0].Title=\"1200 ppm\";")
    pltscript(plotcliv, "Chart.Series[1].Title=\"Simulation 1200 ppm\";")
    pltscript(plotcliv, "Chart.Series[2].Title=\"781 ppm\";")
    pltscript(plotcliv, "Chart.Series[3].Title=\"Simulation 781 ppm\";")
    pltscript(plotcliv, "Chart.Series[4].Title=\"273 ppm\";")
```

```
    pltscript(plotcliv, "Chart.Series[5].Title=\"Simulation 273 ppm\";")

    pltscript(plotcbrntot, "Chart.Header.Text = \"Perleberg et al. (2004) n-Decane
Inhalation Study\";")
    pltscript(plotcbrntot, "Chart.SubHeader.Text = \"273, 781 or 1200 ppm for 4
Hours\";")
    pltscript(plotcbrntot, "Chart.SubHeader.Visible=true;")
    pltscript(plotcbrntot, "Chart.Axes.Left.Automatic=false;")
    pltscript(plotcbrntot, "Chart.Axes.Left.Minimum=0.01;")
    pltscript(plotcbrntot, "Chart.Axes.Left.Maximum=200.0;")
    pltscript(plotcbrntot, "Chart.Axes.Left.Logarithmic = true;")
    pltscript(plotcbrntot, "Chart.Axes.Left.Title.Text=\"Decane in Total Brain
[mg/L]\";")
    pltscript(plotcbrntot, "Chart.Axes.Bottom.Title.Text=\"Hours\";")
    pltscript(plotcbrntot, "Chart.Series[0].Title=\"1200 ppm\";")
    pltscript(plotcbrntot, "Chart.Series[1].Title=\"Simulation 1200 ppm\";")
    pltscript(plotcbrntot, "Chart.Series[2].Title=\"781 ppm\";")
    pltscript(plotcbrntot, "Chart.Series[3].Title=\"Simulation 781 ppm\";")
    pltscript(plotcbrntot, "Chart.Series[4].Title=\"273 ppm\";")
    pltscript(plotcbrntot, "Chart.Series[5].Title=\"Simulation 273 ppm\";")

    pltscript(plotcrap, "Chart.Header.Text = \"Perleberg et al. (2004) n-Decane
Inhalation Study\";")
    pltscript(plotcrap, "Chart.SubHeader.Text = \"273, 781 or 1200 ppm for 4
Hours\";")
    pltscript(plotcrap, "Chart.SubHeader.Visible=true;")
    pltscript(plotcrap, "Chart.Axes.Left.Automatic=false;")
    pltscript(plotcrap, "Chart.Axes.Left.Minimum=0.01;")
    pltscript(plotcrap, "Chart.Axes.Left.Maximum=100.0;")
    pltscript(plotcrap, "Chart.Axes.Left.Logarithmic = true;")
    pltscript(plotcrap, "Chart.Axes.Left.Title.Text=\"Decane in Rapidly Perfused
Tissues [mg/L]\";")
    pltscript(plotcrap, "Chart.Axes.Bottom.Title.Text=\"Hours\";")
    pltscript(plotcrap, "Chart.Series[0].Title=\"1200 ppm\";")
    pltscript(plotcrap, "Chart.Series[1].Title=\"Simulation 1200 ppm\";")
    pltscript(plotcrap, "Chart.Series[2].Title=\"781 ppm\";")
    pltscript(plotcrap, "Chart.Series[3].Title=\"Simulation 781 ppm\";")
    pltscript(plotcrap, "Chart.Series[4].Title=\"273 ppm\";")
    pltscript(plotcrap, "Chart.Series[5].Title=\"Simulation 273 ppm\";")

    pltscript(plotcfat, "Chart.Header.Text = \"Perleberg et al. (2004) n-Decane
Inhalation Study\";")
    pltscript(plotcfat, "Chart.SubHeader.Text = \"273, 781 or 1200 ppm for 4
Hours\";")
    pltscript(plotcfat, "Chart.SubHeader.Visible=true;")
    pltscript(plotcfat, "Chart.Axes.Left.Logarithmic = true;")
    pltscript(plotcfat, "Chart.Axes.Left.Title.Text=\"Decane in Fat [mg/L]\";")
    pltscript(plotcfat, "Chart.Axes.Bottom.Title.Text=\"Hours\";")
    pltscript(plotcfat, "Chart.Series[0].Title=\"1200 ppm\";")
    pltscript(plotcfat, "Chart.Series[1].Title=\"Simulation 1200 ppm\";")
    pltscript(plotcfat, "Chart.Series[2].Title=\"781 ppm\";")
    pltscript(plotcfat, "Chart.Series[3].Title=\"Simulation 781 ppm\";")
    pltscript(plotcfat, "Chart.Series[4].Title=\"273 ppm\";")
    pltscript(plotcfat, "Chart.Series[5].Title=\"Simulation 273 ppm\";")

set @preference=NoBackslashEscapeS
```

C5_Zahlsen92.m

```
%Zahlsen, K., Eide, I., Nilsen, A.M. and Nilsen, O.G. 1992. Inhalation kinetics of C6
%     to C10 aliphatic, aromatic and naphthenic hydrocarbons in rat after repeated
%     exposures. Pharmacol.Toxicol. 71(2): 144-149.

resetdoses
rattus
decanerat

 %(1-T, 2-CArt, 3-CBrnTot, 4-CLiv, 5-CRap, 6-CFat)
 zahl = [
 12.0  0.83957       12.73585   5.49278   4.76705   119.6743
 12.0  0.93918       13.71772   6.95847   5.53547   167.2025
 12.0  0.73996       11.75398   4.02709   3.99863   72.1461
 36.0  0.91072       8.28186    6.48888   8.09687   188.4052
 36.0  1.01033       10.08907   7.31422   9.07874   208.0426
 36.0  0.81111       6.47465    5.66354   7.115     168.7678
 60.0  0.96764       8.56646    6.53157   11.05671   175.029
 60.0  1.03879       10.37367   7.08654   14.9415   183.9939
 60.0  0.89649       6.75925    5.9766    7.17192   166.0641
 72.0  0.01423       0.24191    NaN       0.24191   131.6275
 72.0  0.02846       0.25614    NaN       0.32729   145.9998
 72.0  0.001    0.22768    NaN       0.15653   117.2552];

BW=0.175;
SCRUB(5)=0.4;

CONC(5)=100.0;
TCHNG=12.0; DOSEINT=24.0; DAYSWK=5.0; TMAX=72.0;
CINT=0.1;
TSTOP=80.0;
start @nocallback

plotcart = plot (0, zahl(:,1), zahl(:,2), '+b', _t, _cart(:,5), '-b');
plotcbrntot = plot (0, zahl(:,1), zahl(:,3), '+b', _t, _cbrntot(:,5), '-b');
plotcliv = plot (0, zahl(:,1), zahl(:,4), '+b', _t, _cliv(:,5), '-b');
plotcrap = plot (0, zahl(:,1), zahl(:,5), '+b', _t, _crap(:,5), '-b');
plotcfat = plot (0, zahl(:,1), zahl(:,6), '+b', _t, _cfat(:,5), '-b');


set @preference=BackslashEscapeS

    pltscript(plotcart, "Chart.Header.Text = \"Zahlsen et al. (1992) n-Decane
Inhalation Study\";")
    pltscript(plotcart, "Chart.SubHeader.Text = \"100 ppm for 12 Hours\";")
    pltscript(plotcart, "Chart.SubHeader.Visible=true;")
    pltscript(plotcart, "Chart.Axes.Left.Title.Text=\"Decane in Arterial Blood
[mg/L]\";")
    pltscript(plotcart, "Chart.Axes.Bottom.Title.Text=\"Hours\";")
    pltscript(plotcart, "Chart.Series[0].Title=\"100 ppm\";")
    pltscript(plotcart, "Chart.Series[1].Title=\"Simulation 100 ppm\";")

    pltscript(plotcbrntot, "Chart.Header.Text = \"Zahlsen et al. (1992) n-Decane
Inhalation Study\";")
    pltscript(plotcbrntot, "Chart.SubHeader.Text = \"100 ppm for 12 Hours\";")
    pltscript(plotcbrntot, "Chart.SubHeader.Visible=true;")
    pltscript(plotcbrntot, "Chart.Axes.Left.Title.Text=\"Decane in Total Brain
[mg/L]\";")
    pltscript(plotcbrntot, "Chart.Axes.Bottom.Title.Text=\"Hours\";")
    pltscript(plotcbrntot, "Chart.Series[0].Title=\"100 ppm\";")
    pltscript(plotcbrntot, "Chart.Series[1].Title=\"Simulation 100 ppm\";")
```

```
    pltscript(plotcliv, "Chart.Header.Text = \"Zahlsen et al. (1992) n-Decane
Inhalation Study\";")
    pltscript(plotcliv, "Chart.SubHeader.Text = \"100 ppm for 12 Hours\";")
    pltscript(plotcliv, "Chart.SubHeader.Visible=true;")
    pltscript(plotcliv, "Chart.Axes.Left.Automatic=false;")
    pltscript(plotcliv, "Chart.Axes.Left.Minimum=0.01;")
    pltscript(plotcliv, "Chart.Axes.Left.Maximum=100.0;")
    pltscript(plotcliv, "Chart.Axes.Left.Logarithmic = true;")
    pltscript(plotcliv, "Chart.Axes.Left.Title.Text=\"Decane in Liver [mg/L]\";")
    pltscript(plotcliv, "Chart.Axes.Bottom.Title.Text=\"Hours\";")
    pltscript(plotcliv, "Chart.Series[0].Title=\"100 ppm\";")
    pltscript(plotcliv, "Chart.Series[1].Title=\"Simulation 100 ppm\";")

    pltscript(plotcrap, "Chart.Header.Text = \"Zahlsen et al. (1992) n-Decane
Inhalation Study\";")
    pltscript(plotcrap, "Chart.SubHeader.Text = \"100 ppm for 12 Hours\";")
    pltscript(plotcrap, "Chart.SubHeader.Visible=true;")
    pltscript(plotcrap, "Chart.Axes.Left.Automatic=false;")
    pltscript(plotcrap, "Chart.Axes.Left.Minimum=0.01;")
    pltscript(plotcrap, "Chart.Axes.Left.Maximum=100.0;")
    pltscript(plotcrap, "Chart.Axes.Left.Logarithmic = true;")
    pltscript(plotcrap, "Chart.Axes.Left.Title.Text=\"Decane in Kidney (Rapidly
Perfused Tissues) [mg/L]\";")
    pltscript(plotcrap, "Chart.Axes.Bottom.Title.Text=\"Hours\";")
    pltscript(plotcrap, "Chart.Series[0].Title=\"100 ppm\";")
    pltscript(plotcrap, "Chart.Series[1].Title=\"Simulation 100 ppm\";")

    pltscript(plotcfat, "Chart.Header.Text = \"Zahlsen et al. (1992) n-Decane
Inhalation Study\";")
    pltscript(plotcfat, "Chart.SubHeader.Text = \"100 ppm for 12 Hours\";")
    pltscript(plotcfat, "Chart.SubHeader.Visible=true;")
    pltscript(plotcfat, "Chart.Axes.Left.Title.Text=\"Decane in Fat [mg/L]\";")
    pltscript(plotcfat, "Chart.Axes.Bottom.Title.Text=\"Hours\";")
    pltscript(plotcfat, "Chart.Series[0].Title=\"100 ppm\";")
    pltscript(plotcfat, "Chart.Series[1].Title=\"Simulation 100 ppm\";")

set @preference=NoBackslashEscapeS
```

APPENDIX C: MODEL SIMULATIONS FOR INDIVIDUAL KEY COMPONENTS

These simulations are organized by key component and then by study. The section titles correspond to the m file names seen in Appendix B. The study reference is cited in the first bullet. The citation is followed by a list of study conditions necessary to simulate the kinetics of the chemical.

TOLUENE RAT EXPOSURE SIMULATIONS

C1_Haddad.m

- Haddad, S., Tardif, R., Charest-Tardif, G. and Krishnan, K. 1999. Physiological modeling of the toxicokinetic interactions in a quaternary mixture of aromatic hydrocarbons. Toxicol.Appl.Pharmacol. 161(3): 249-257.
- Male Sprague-Dawley rats
- Body weight = 0.235 kg
- 4-hour inhalation exposure
- 50, 100, or 200 ppm
- Data points = mean ± 1 SD

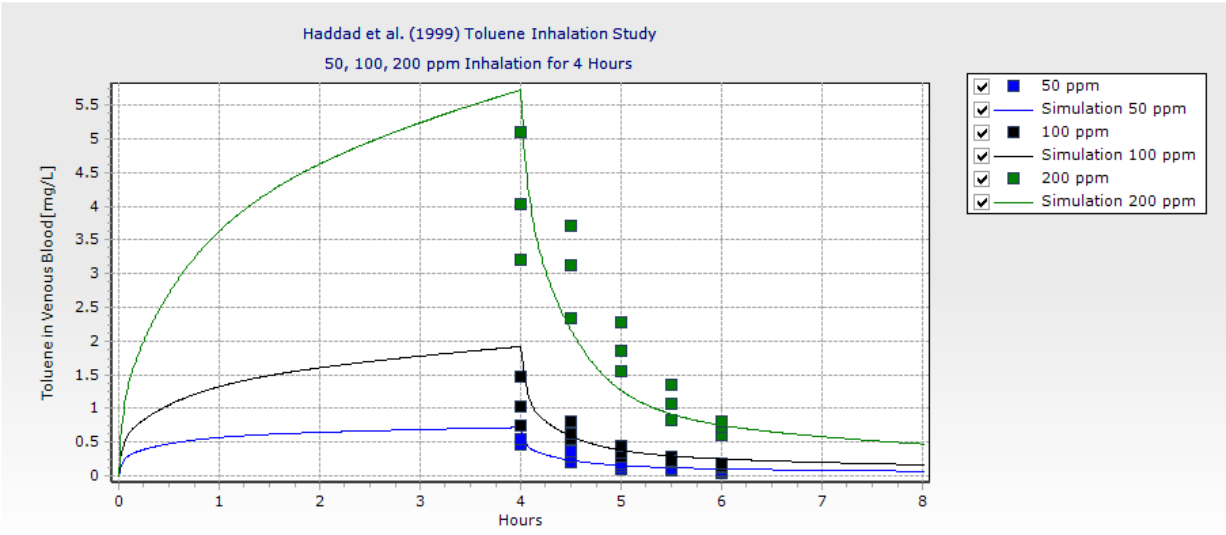

C1_Lam.m

- Lam, C.W., Galen, T.J., Boyd, J.F. and Pierson, D.L. 1990. Mechanism of transport and distribution of organic solvents in blood. Toxicol.Appl.Pharmacol. 104(1): 117-129.
- Male Sprague-Dawley rats
- Body weight = estimated 0.3 kg

- 2-hour inhalation exposure
- 488 ± 24 ppm
- Data points = individual values, n =5

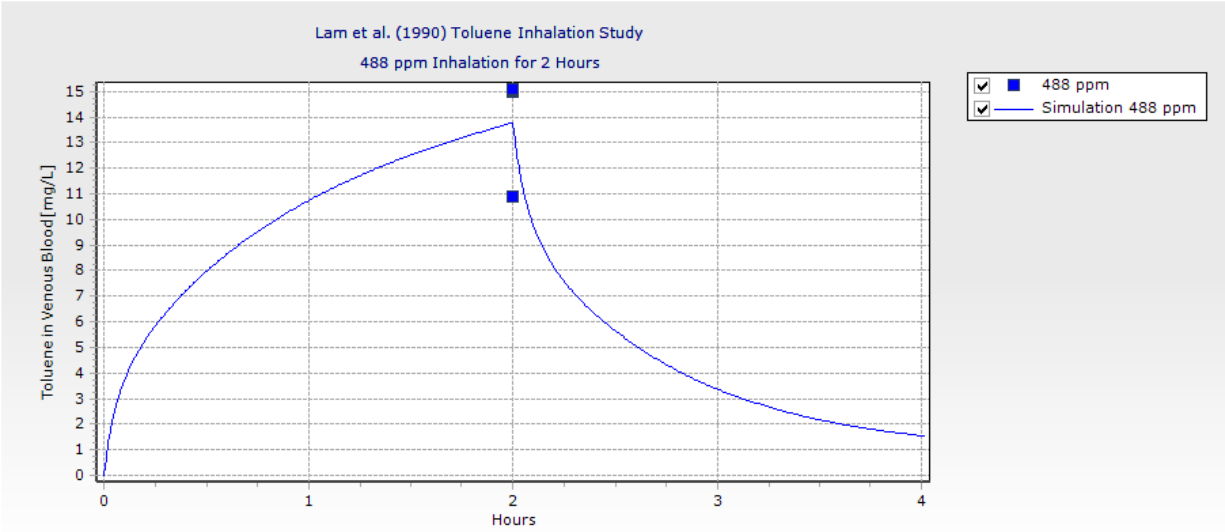

C1_Romer.m

- Romer, K.G., Federsel, R.J. and Freundt, K.J. 1986. Rise of inhaled toluene, ethyl benzene, m-xylene, or mesitylene in rat blood after treatment with ethanol. Bull Environ Contam Toxicol 37(6): 874-876.
- Female Sprague-Dawley rats
- Body weight = 0.210 kg (range: 0.200 – 0.220)
- 2-hour inhalation exposure
- 220 ppm
- Data points = mean ± 1 SD

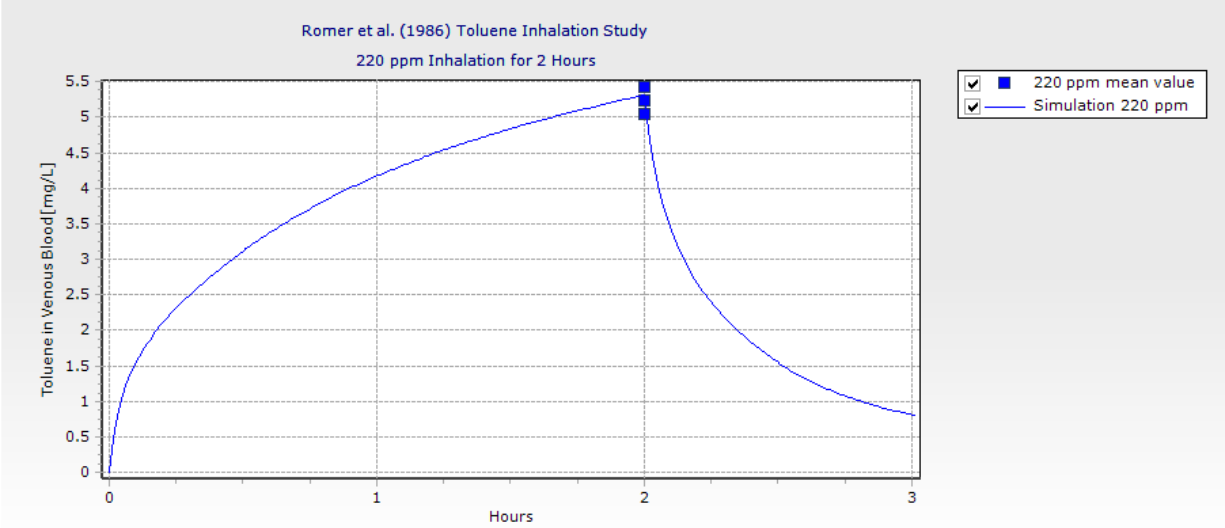

C1_Tardif.m

- Tardif, R., Charest-Tardif, G. and Brodeur, J. 1996. Comparison of the influence of binary mixtures versus a ternary mixture of inhaled aromatic hydrocarbons on their blood kinetics in the rat. Arch Toxicol 70(7): 405-413.
- Male Sprague-Dawley rats
- Body weight = 0.240 kg (range: 0.235 – 0.245)
- 4-hour inhalation exposure
- 100 or 200 ppm
- Data points = mean ± 1 SD

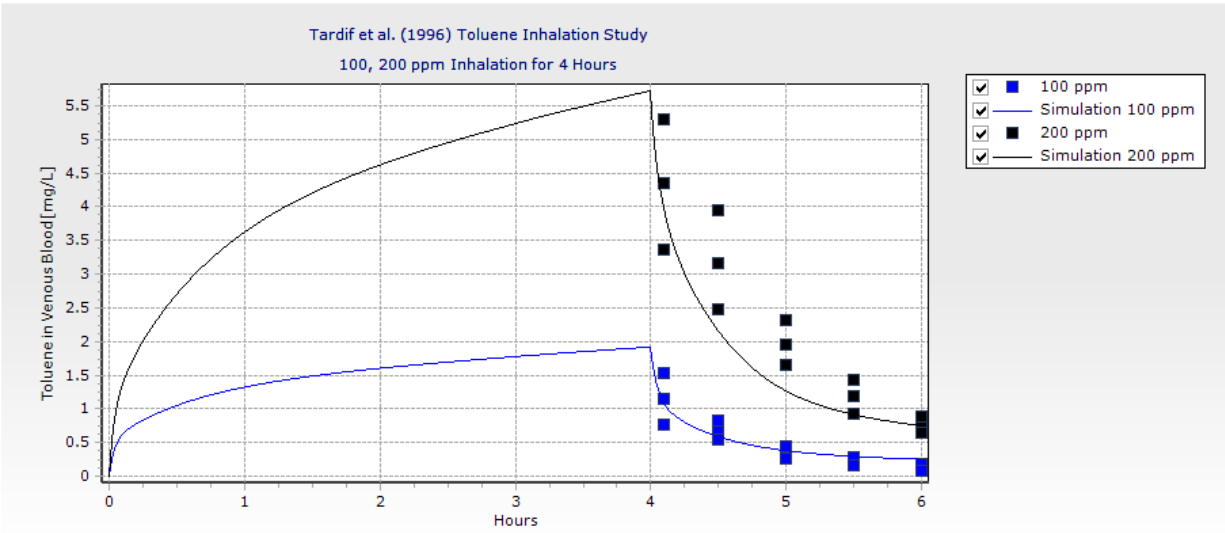

ETHYLBENZENE RAT EXPOSURE SIMULATIONS

C2_Haddad.m

- Haddad et al. (1999)
- Male Sprague-Dawley rats
- Body weight = 0.235 kg
- 4-hour inhalation exposure
- 50, 100, or 200 ppm
- Data points = mean ± 1 SD

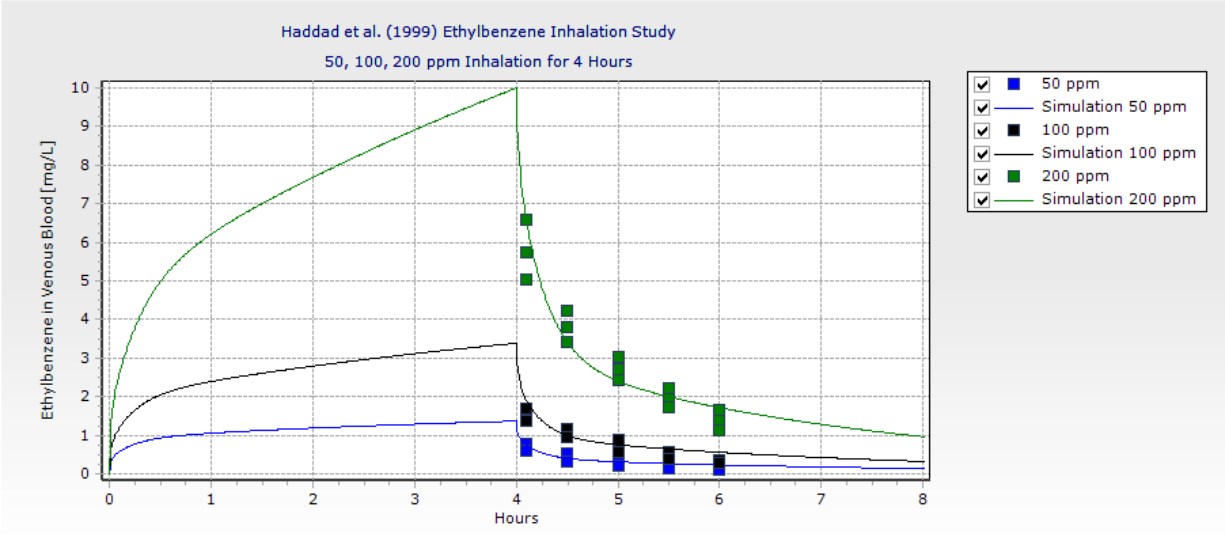

C2_Tardif.m

- Tardif et al. (1996)
- Male Sprague-Dawley rats
- Body weight = 0.240 kg (range: 0.235 – 0.245)
- 4-hour inhalation exposure
- 100 or 200 ppm
- Data points = mean ± 1 SD

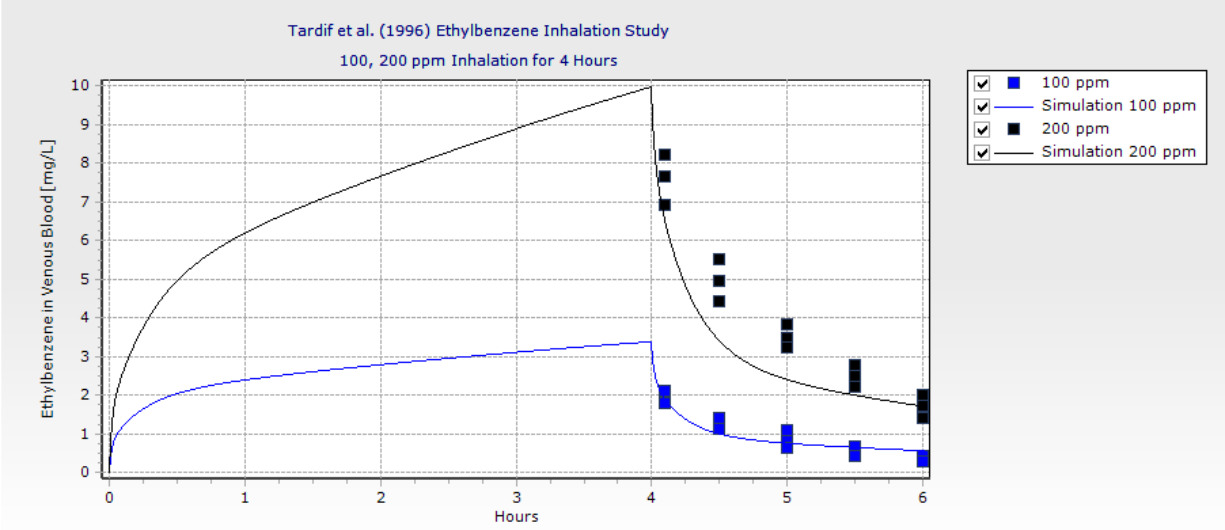

XYLENES RAT EXPOSURE SIMULATIONS

C3_Haddad.m

- Haddad et al. (1999)
- Male Sprague-Dawley rats
- Body weight = 0.235 kg
- 4-hour inhalation exposure
- 50, 100, or 200 ppm
- Data points = mean ± 1 SD

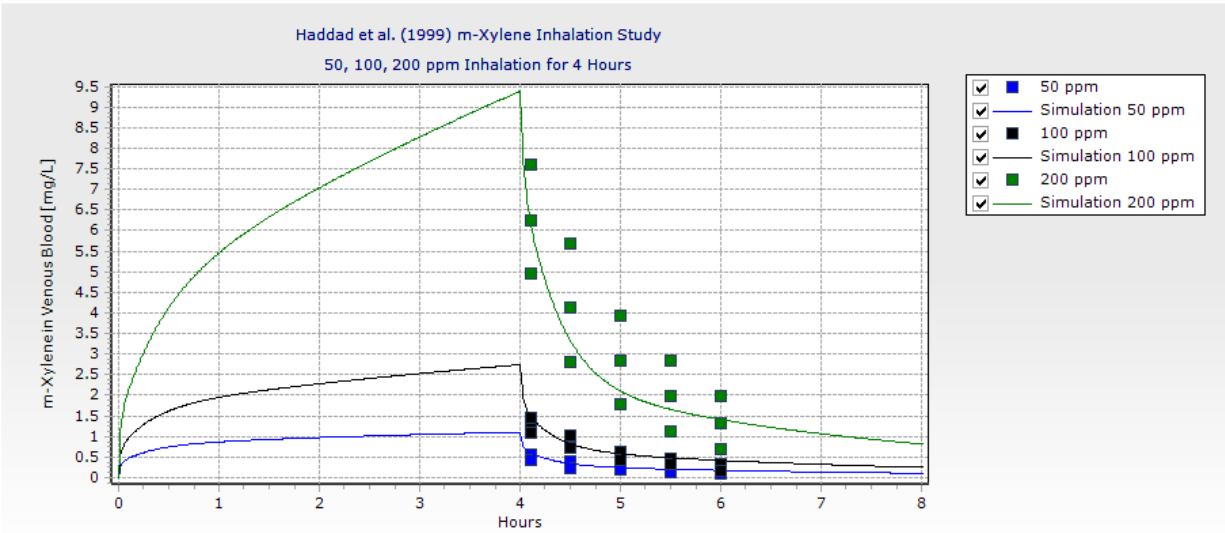

C3_Tardif.m

- Tardif et al. (1996)
- Male Sprague-Dawley rats
- Body weight = 0.240 kg (range: 0.235 – 0.245)
- 4-hour inhalation exposure
- 100 or 200 ppm
- Data points = mean ± 1 SD

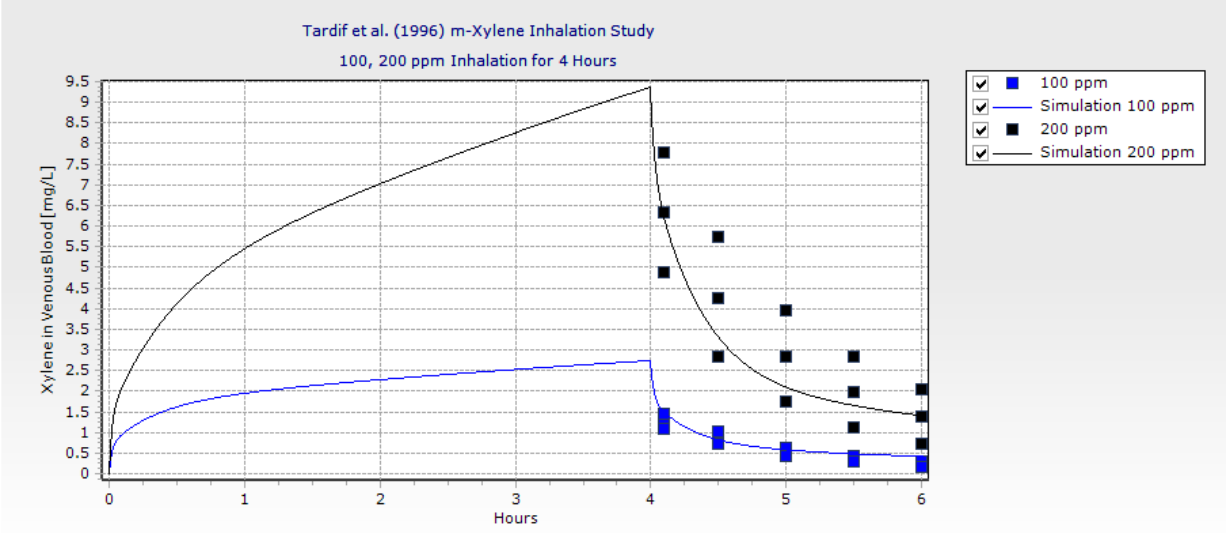

NONANE RAT EXPOSURE SIMULATIONS

C4_inhouse_inhal.m

- Robinson, P.J. and Merrill, E.A. 2008. A harmonized physiologically based pharmacokinetic model for nonane as a component of jet fuel. Wright-Patterson AFB, OH: Air Force Research Laboratory, Applied Biotechnology Branch. AFRL-RH-WP-TR-2008-0067, ADA502610.
- Female Fischer F344 rats
- Body weight = estimated 0.3 kg
- 4-hour inhalation exposure
- 100, 500 or 1000 ppm
- Data points = mean ± 1 SD

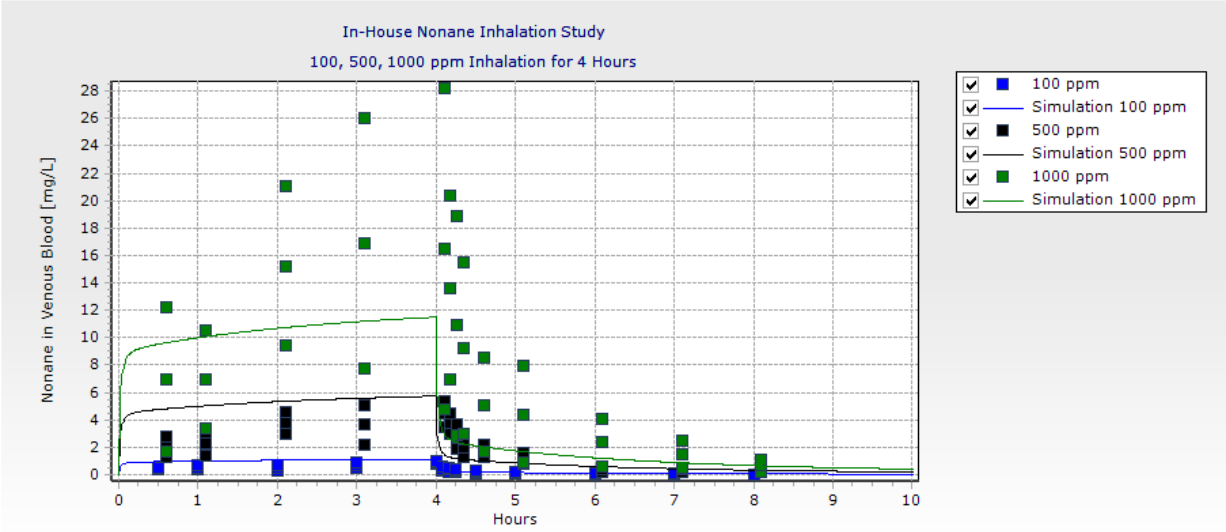

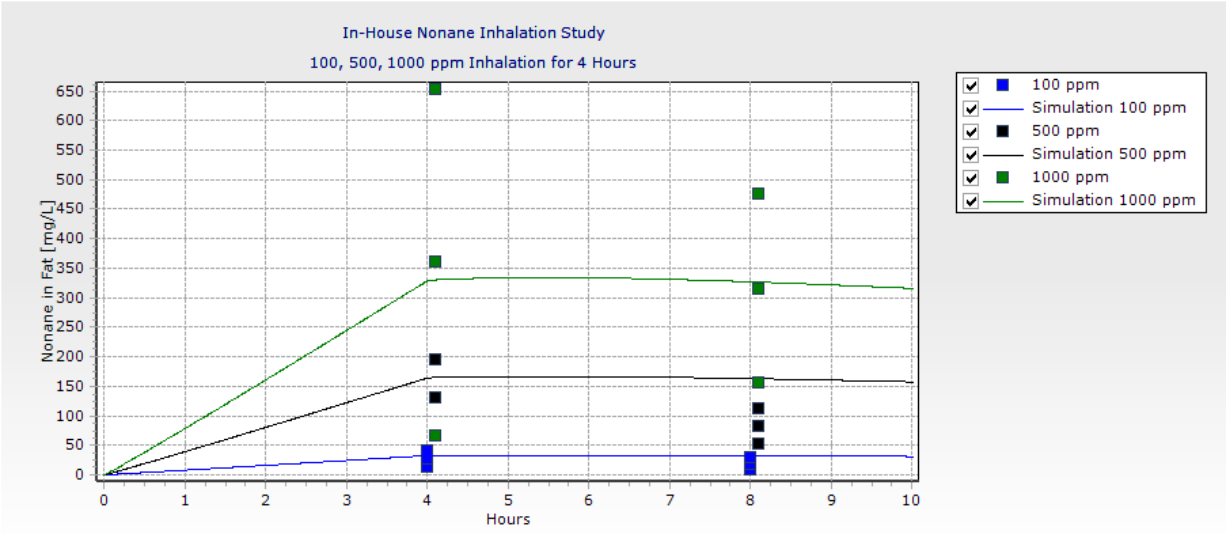

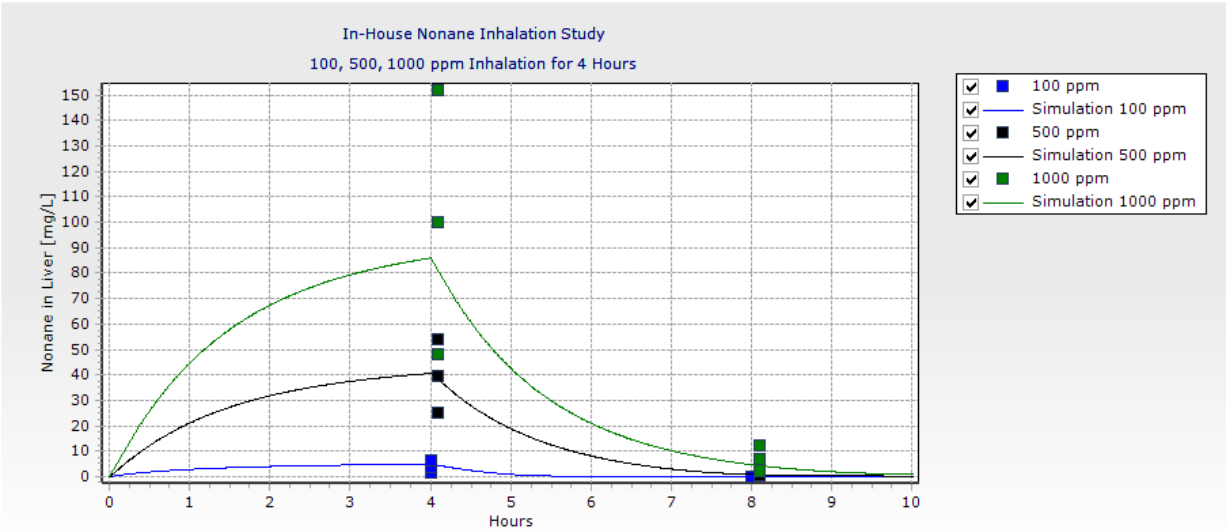

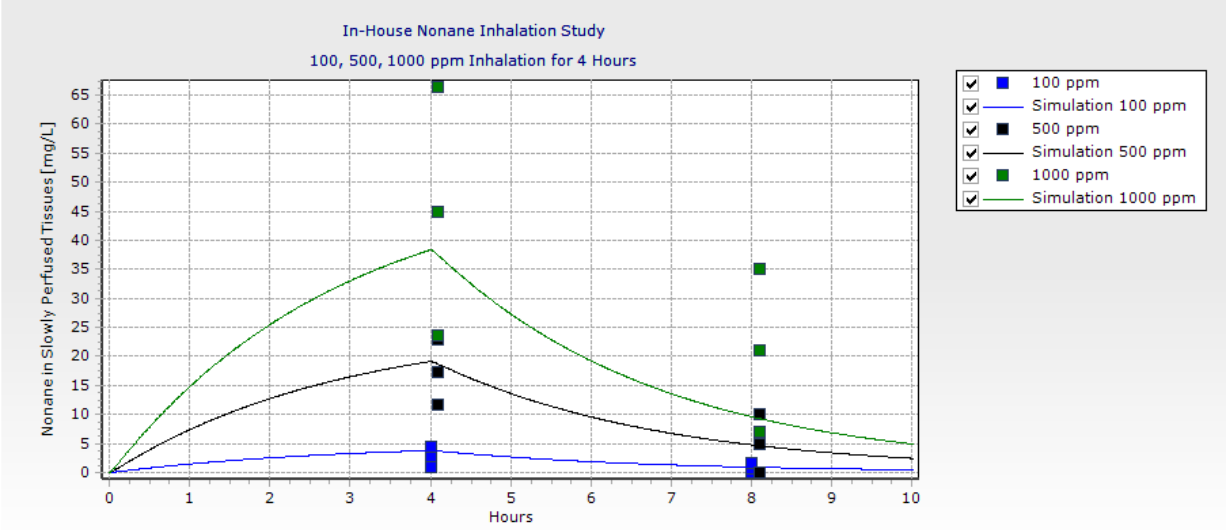

C4_Lof99.m

- Lof, A., Lam, H.R., Gullstrand, E., Ostergaard, G. and Ladefoged, O. 1999. Distribution of dearomatised white spirit in brain, blood, and fat tissue after repeated exposure of rats. Pharmacol.Toxicol. 85(2): 92-97.
- Male Wistar rats
- Body weight = estimated 0.3 kg
- 6-hour inhalation exposure
- 400 or 800 ppm white spirits
    - 3.6% n-nonane
    - = 14.4 or 28.8 ppm nonane
- Data points = mean ± 1 SD

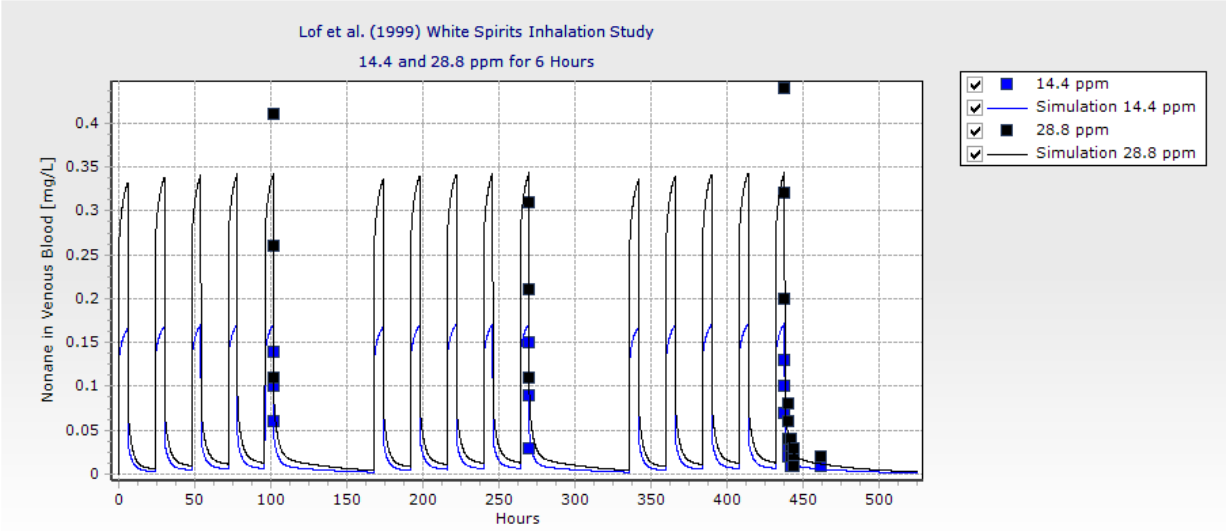

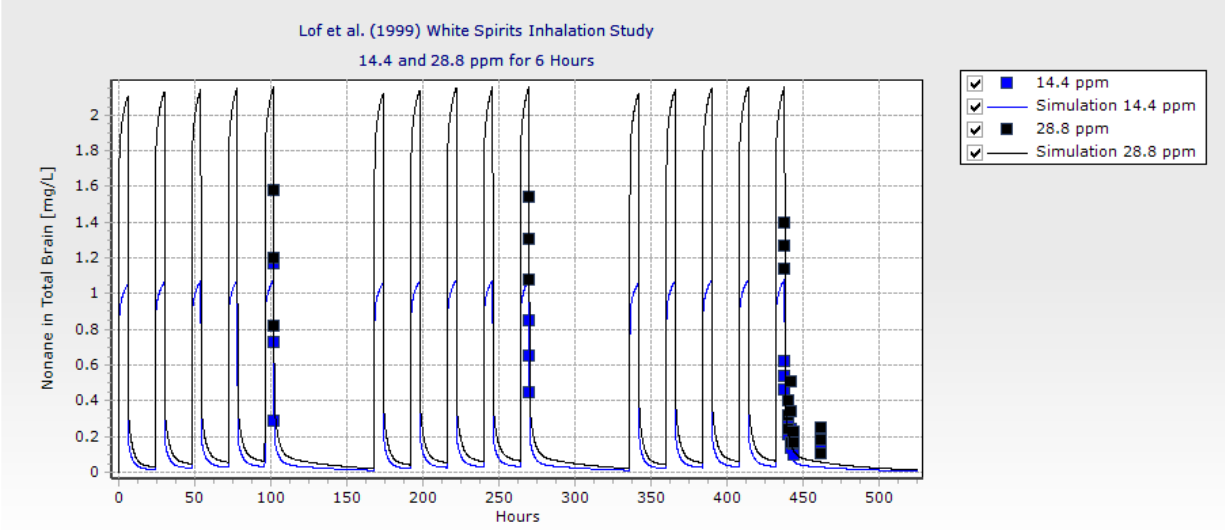

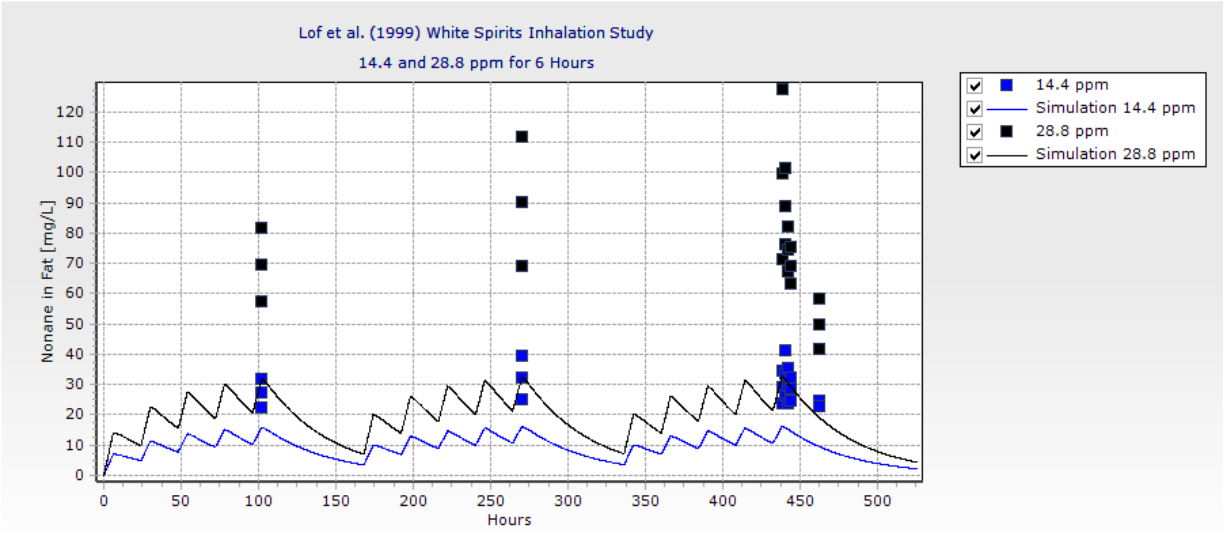

C4_Zahlsen90.m

- Zahlsen, K., Nilsen, A.M., Eide, I. and Nilsen, O.G. 1990. Accumulation and distribution of aliphatic (n-nonane), aromatic (1,2,4-trimethylbenzene) and naphthenic (1,2,4-trimethylcyclohexane) hydrocarbons in the rat after repeated inhalation. Pharmacol.Toxicol. 67(5): 436-440.
- Male Sprague-Dawley rats
- Body weight = 0.2 kg
- 12-hour inhalation exposure, 5 consecutive days
- 1025.2 ppm
    - Target concentration = 1000 ppm
    - Average over 5 days = 1025.2 ppm
- Data points = mean

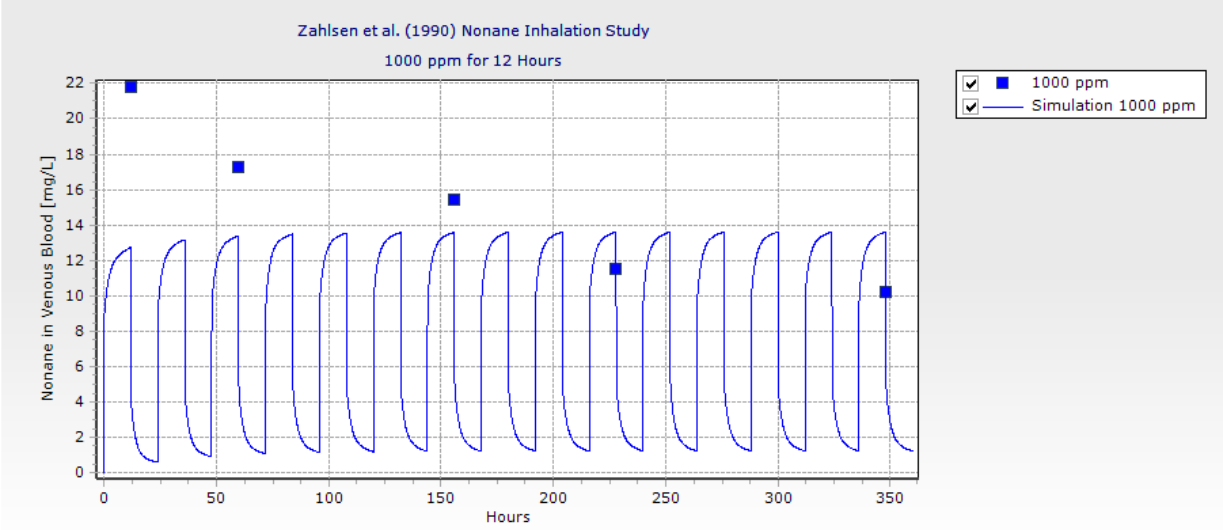

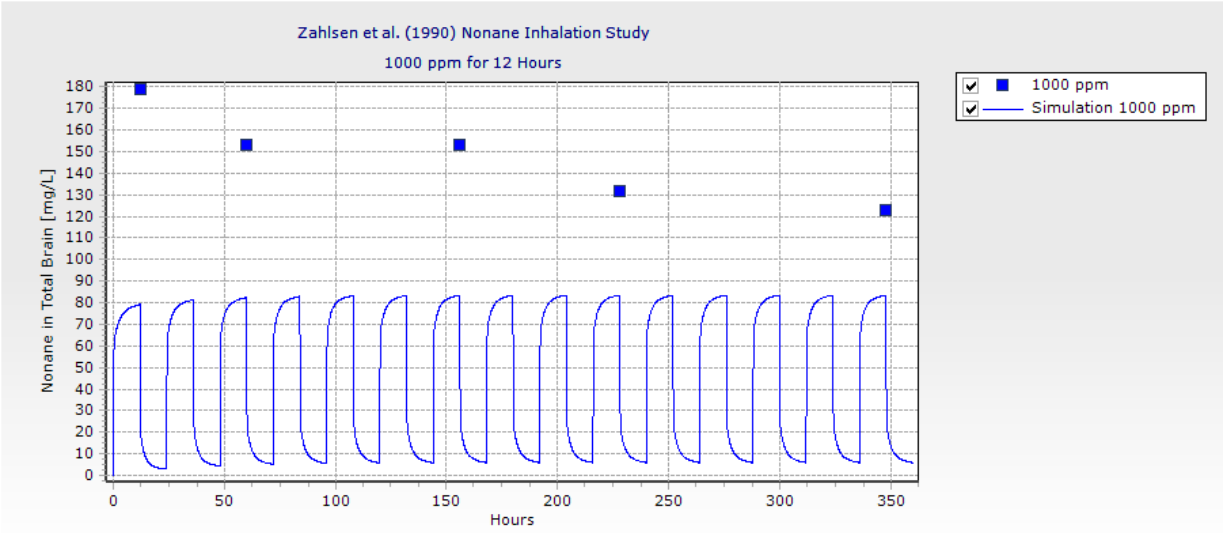

DECANE RAT EXPOSURE SIMULATIONS

C5_Lof99.m

- Lof et al. (1999)
- Male Wistar rats
- Body weight = estimated 0.3 kg
- 6-hour inhalation exposure
- 400 or 800 ppm white spirits
    - 16.6% n-nonane
    - = 106.4 or 212 ppm nonane
- Data points = mean ± 1 SD

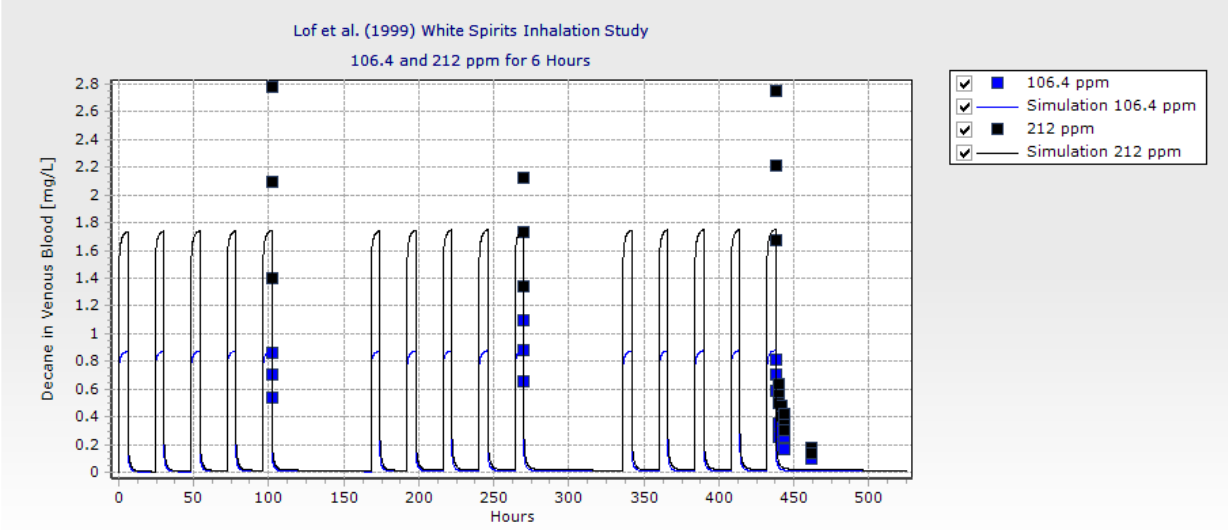

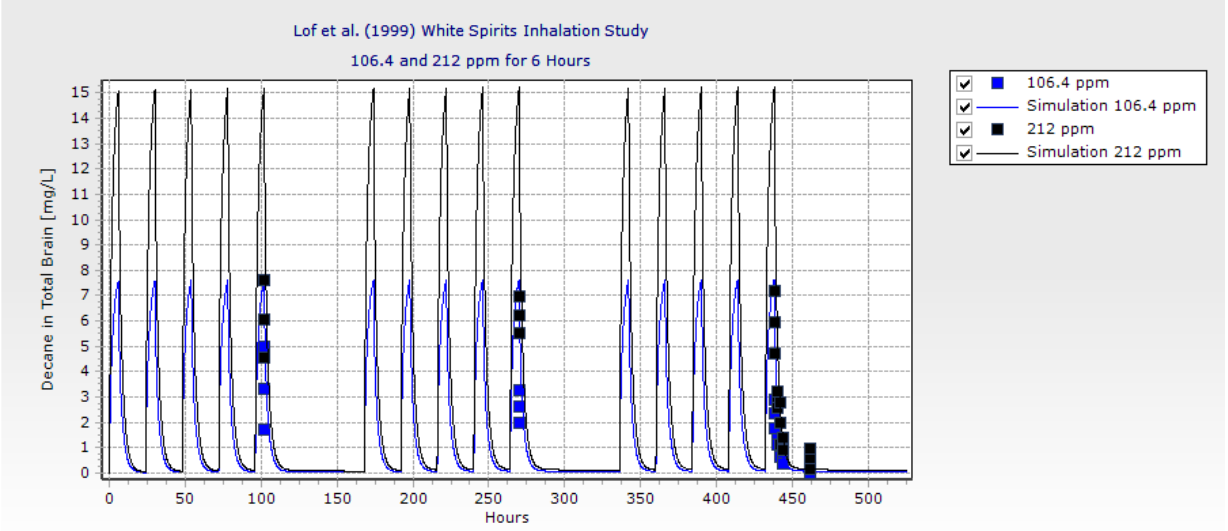

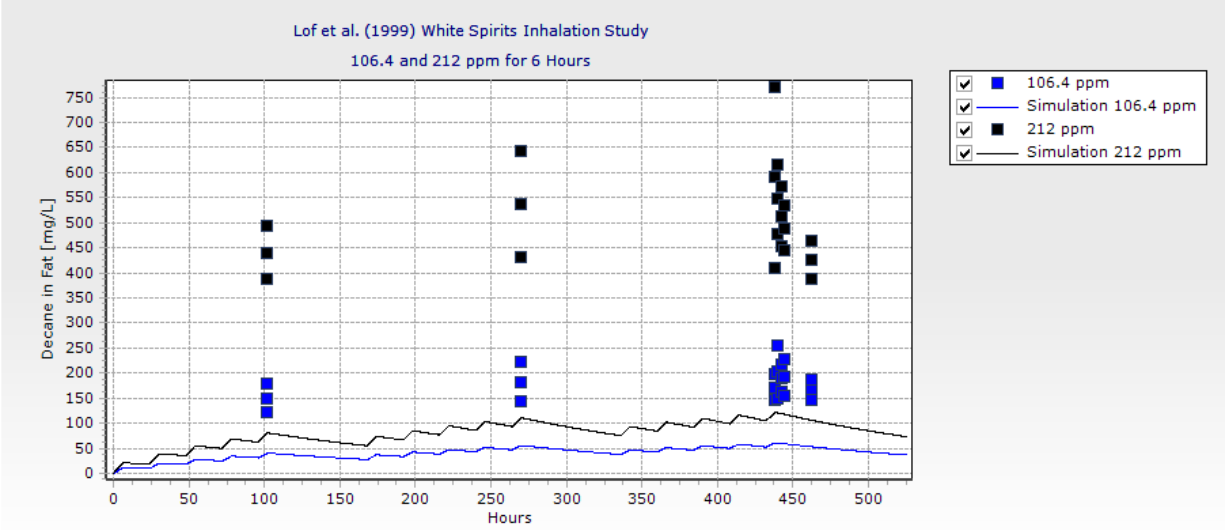

C5_Perleberg04.m

- Perleberg, U.R., Keys, D.A. and Fisher, J.W. 2004. Development of a physiologically based pharmacokinetic model for decane, a constituent of Jet Propellent-8. Inhal.Toxicol. 16(11-12): 771-783.
- Male Fischer F344 rats
- Body weight = 0.211 kg
- 4-hour inhalation exposure
- 273, 781 or 1200 ppm
- Data points = mean ± 1 SD

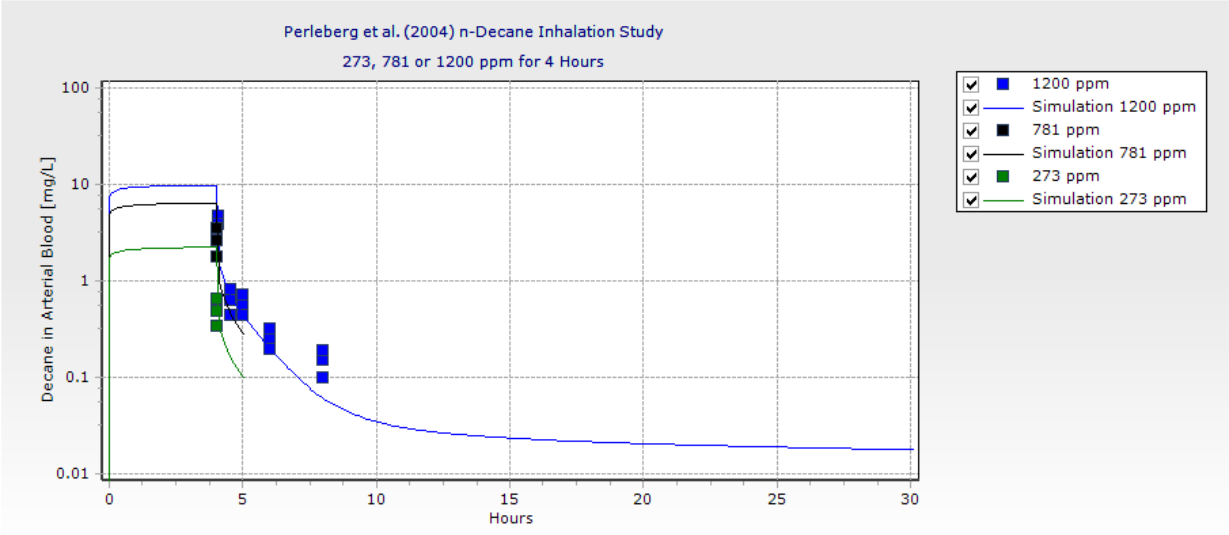

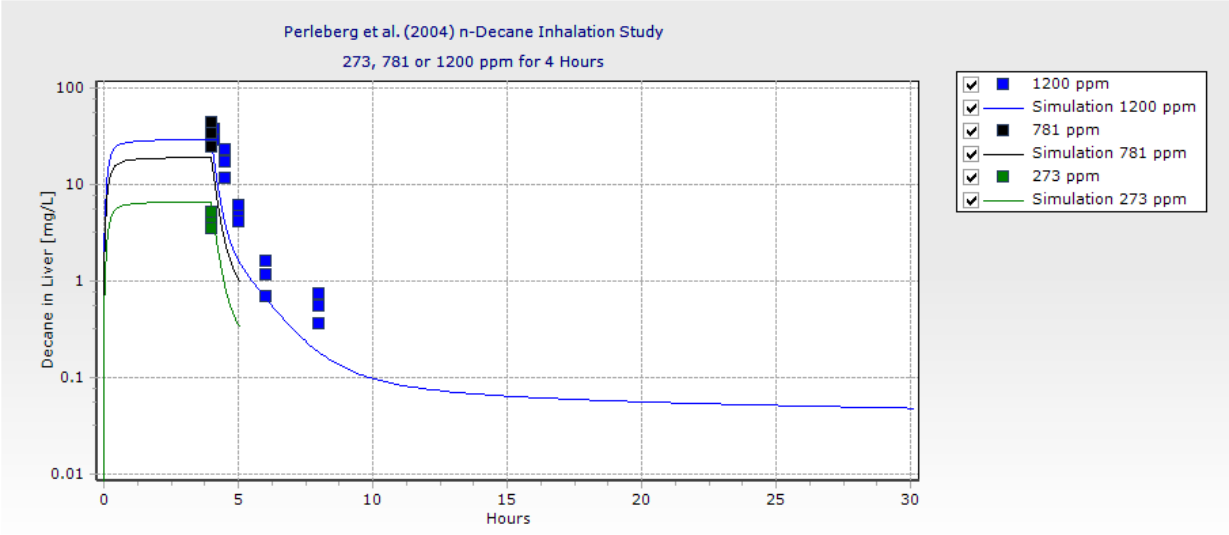

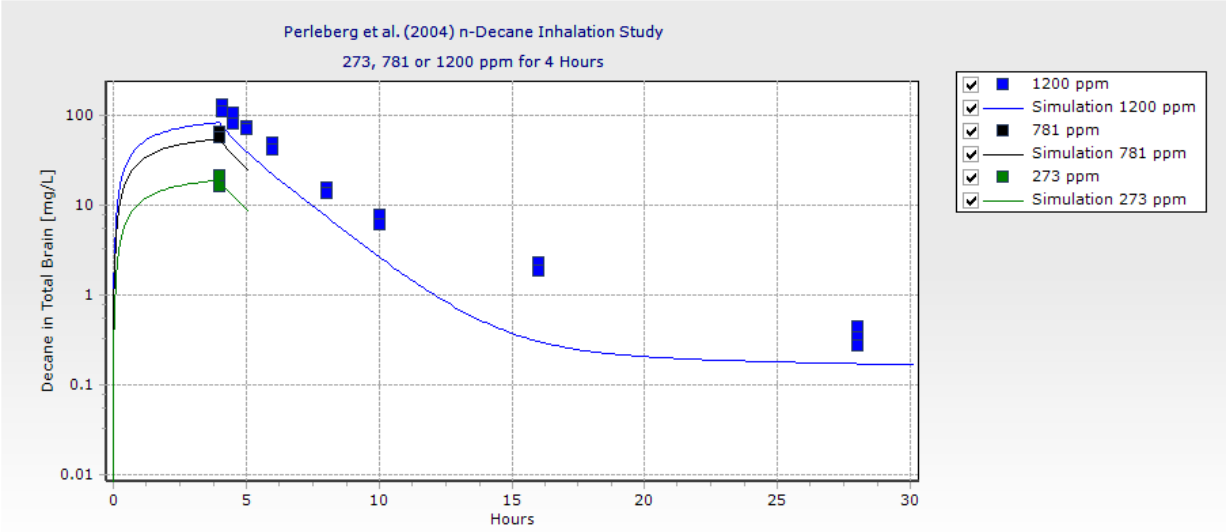

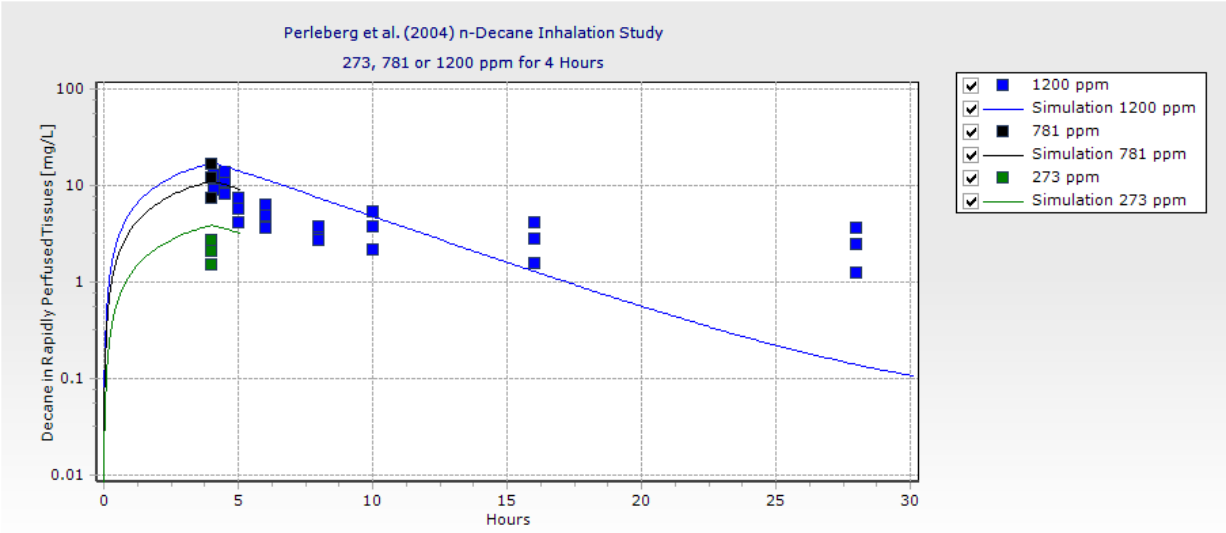

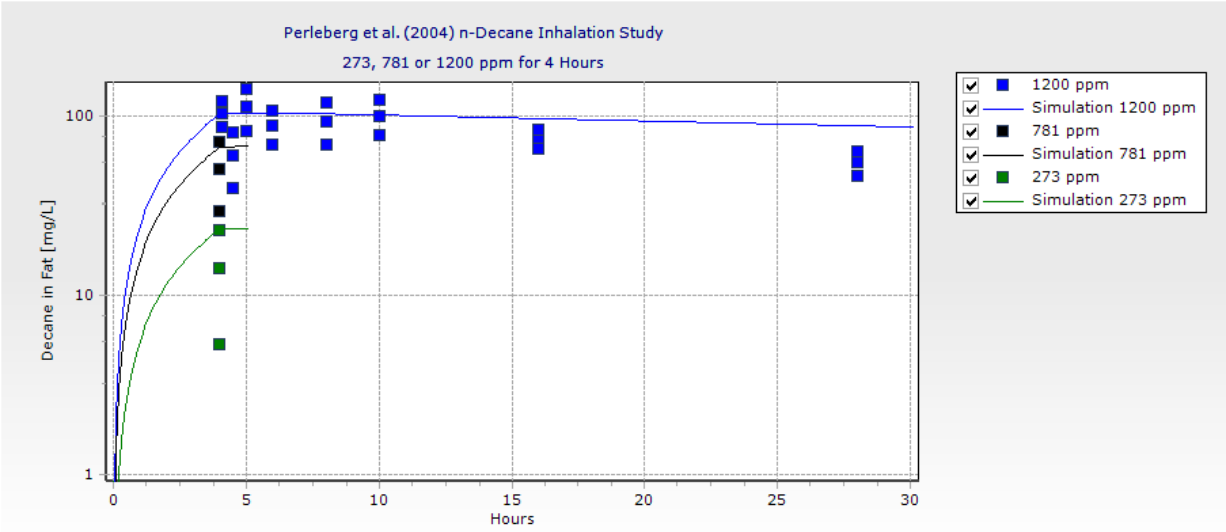

C5_Zahlsen92.m

- Zahlsen, K., Eide, I., Nilsen, A.M. and Nilsen, O.G. 1992. Inhalation kinetics of C6 to C10 aliphatic, aromatic and naphthenic hydrocarbons in rat after repeated exposures. Pharmacol.Toxicol. 71(2): 144-149.
- Male Sprague-Dawley rats
- Body weight = 0.175 kg
- 12-hour inhalation exposure, 5 consecutive days
- 100 ppm
- Data points = mean

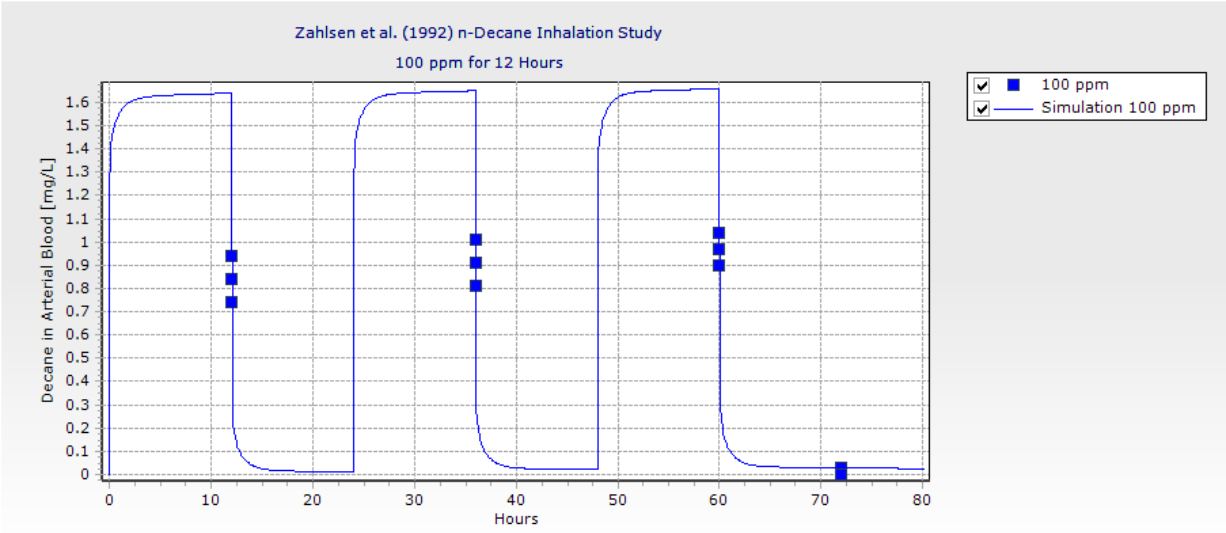

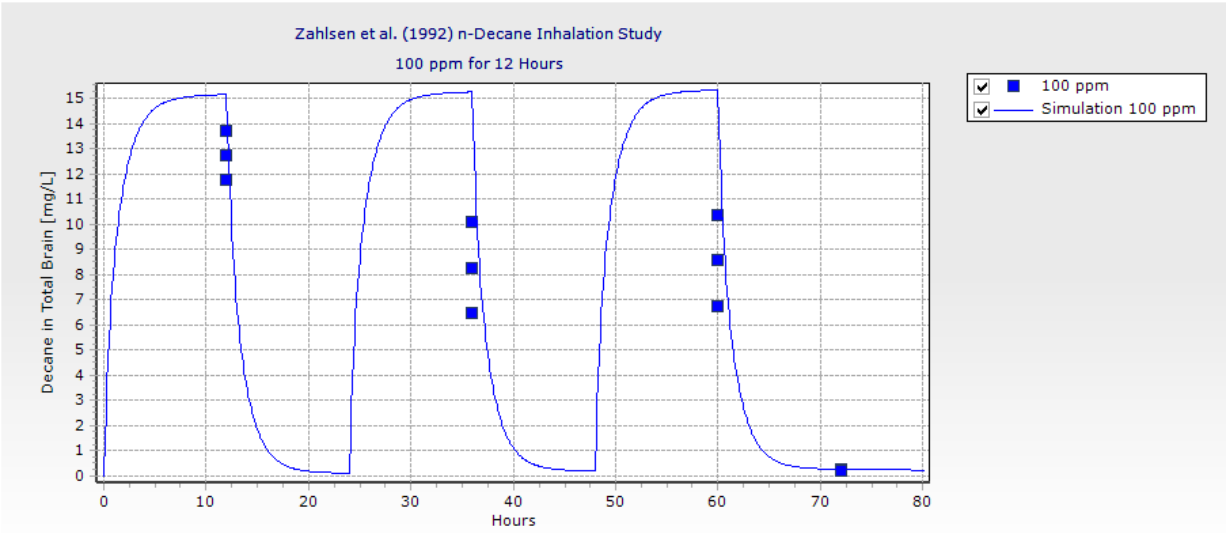

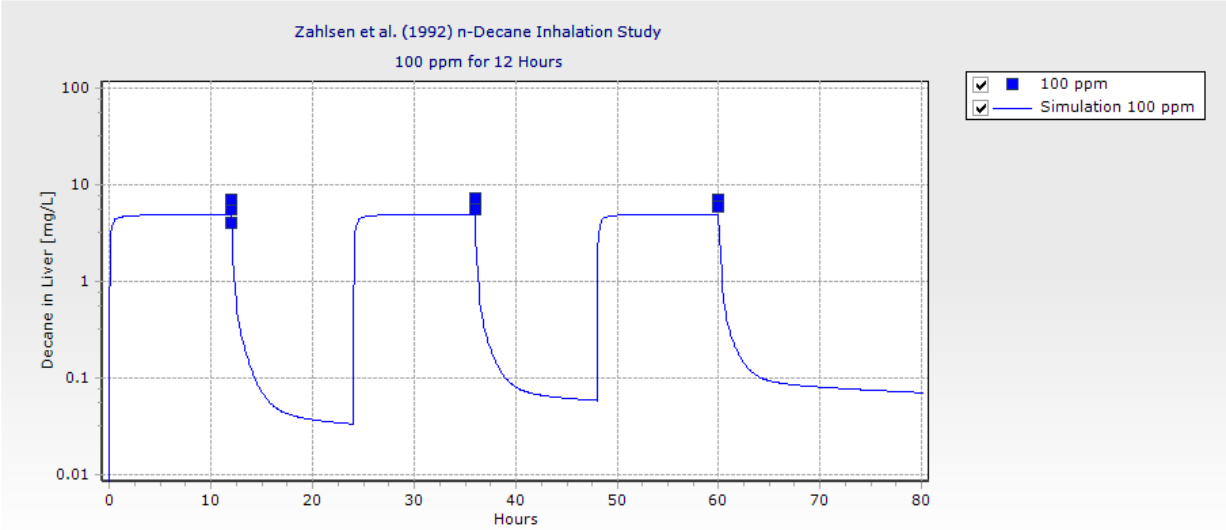

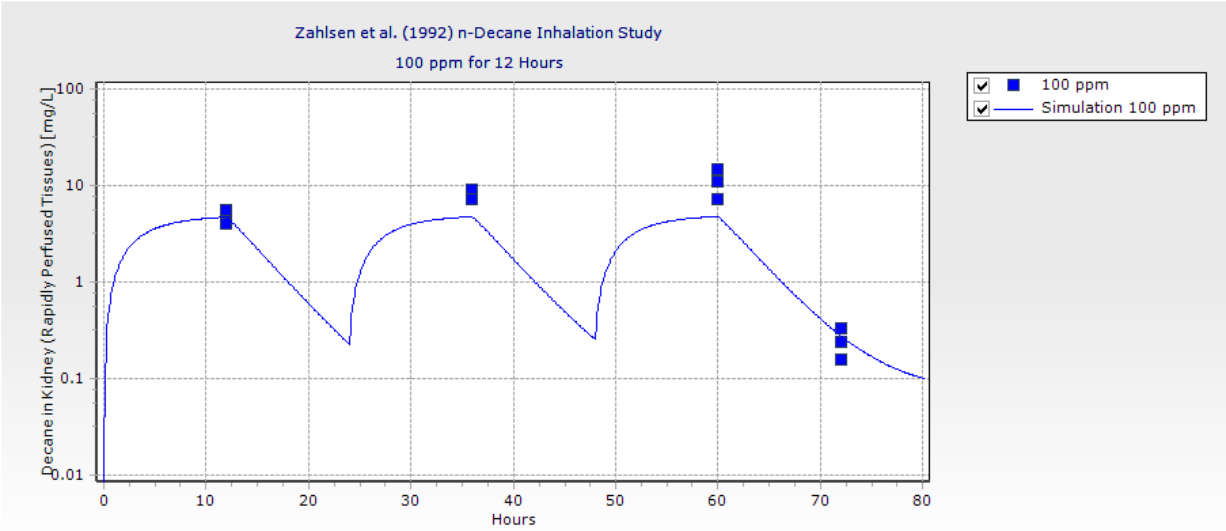

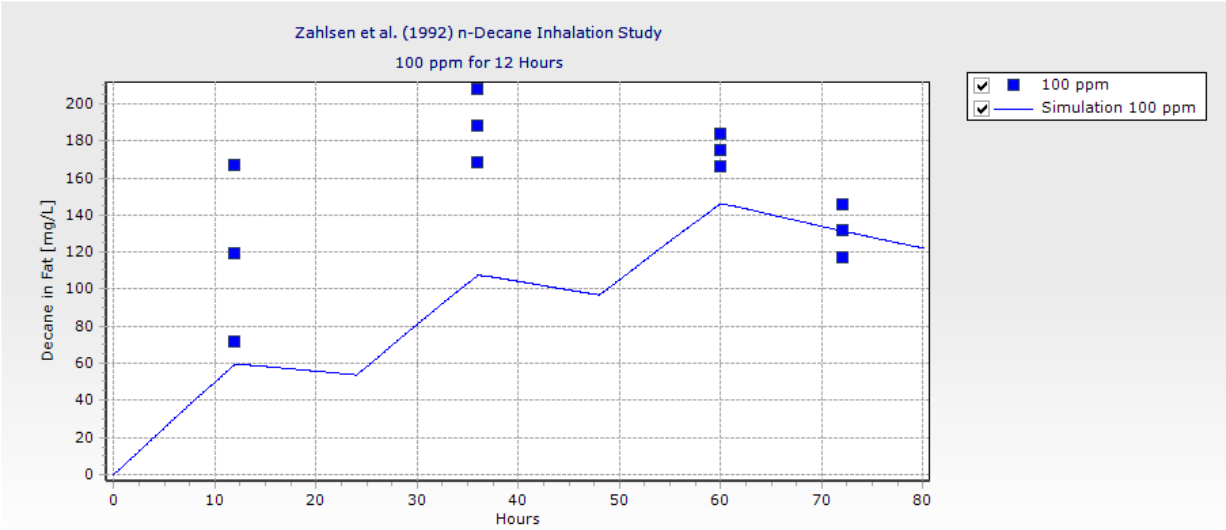

APPENDIX D. BERKELEY MADONNA CODE FOR PHARMACODYNAMIC MODELS

Model for Simple Neuron Circuit in the Dorsal Cochlear Nucleus of the CAP

```
METHOD RK4

STARTTIME = 0
STOPTIME = 5
DT = 0.02

Sf1 = Ref1*S0*time/(S0*time+Kef1)- Rif1*(Sc1+Sc2)/(Sc1+Sc2+Kif1)

; S represents signal strength
; f1 represents fusiform cell #1
; Sf1 is signal strength output from fusiform cell #1
; S0*time is input signal intensity (click strength)
; ”time” is a dummy variable to increase S0
; Ref1 is excitatory receptor density (at fusiform cell#1)
; Rif1 is inhibitory receptor density (at fusiform cell#1)
; Kef1, Kif1 are the “half saturation” signal strengths

Sc1 = Rec1*P0/(P0+Kec1)
Sc2 = Rec2*(P0)/(P0+Kec2)-Ric2*Sc1/(Sc1+Kic2)
; c represents cartwheel cell

limit Sc1>=0
limit Sc2>=0
limit Sf1>=0
; negative signal strengths are not permitted

S0=1
Ref1=1
Kef1=1
Rif1=1
Kif1=1
Rec1=1
P0=1
Kec1=1
Rec2=1
Kec2=1
Rec2=1
Kic2=1
Ric2=1
; most parameters are arbitrary at this point
```

Model for Neurotransmitter Accumulation in Synaptic Cleft

```
METHOD RK4

STARTTIME = 0
STOPTIME = 10
DT = 0.02

NT=STEP(NT0*exp(-k*(time-1)),1)+STEP(NT0*exp(-k*(time-2)),2)+STEP(NT0*exp(-k*(time-
3)),3)+STEP(NT0*exp(-k*(time-4)),4)+STEP(NT0*exp(-k*(time-5)),5)+STEP(NT0*exp(-
k*(time-6)),6)+STEP(NT0*exp(-k*(time-7)),7)+STEP(NT0*exp(-k*(time-8)),8)

NT0=1
k=0.5
```

APPENDIX E. THEORETICAL PREDICTION OF BRAIN REGIONAL PCS BASED ON WHITE TO GRAY MATTER RATIOS

In cases in which PCs are measured for a chemical in only two regions, PC values for other regions can be estimated, in theory, provided regional percentages of gray and white matter are known. The assumption is that the gray matter and white matter maintain the same PC values across different regions but the proportion of gray matter to white matter changes between regions. These different proportions of cell types can be used to predict the PC value for a region.

Let PC_1 and PC_2 be (measured) PC values for two brain regions, with (known) white matter fractions w_1 and w_2, respectively.

$$PC_1 = w_1.PC_w + (1 - w_1)PC_g$$

Equation 1

$$PC_2 = w_2.PC_w + (1 - w_2)PC_g$$

Equation 2

PC_w is the partition coefficient of the white matter, and PC_g is the partition coefficient for the gray matter. The rearrangement of Equation 2 yields:

$$PC_w = (PC_2 - (1 - w_2)PC_g)/w_2$$

Equation 3

Equation 1 is then substituted:

$$PC_1 = (w_1/w_2).\ (PC_2 - (1 - w_2)PC_g) + (1 - w_1)PC_g$$

$$= (w_1/w_2).\ PC_2 - (w_1/w_2)\ PC_g + w_1PC_g + PC_g - w_1PC_g$$

Equation 4

Rearranging Equation 4 gives PC_g in terms of the (measured) regional PC values and (known) white matter fractions:

$$PC_g = \frac{PC_1 - \frac{w_1}{w_2}PC_2}{1 - \frac{w_1}{w_2}}$$

Equation 5

And substituting Equation 5 into Equation 3 gives an expression for PC_w.

$$PC_w = \frac{1}{w_2}\left[PC_2 - (1 - w_2)\frac{PC_1 - \frac{w_1}{w_2}PC_2}{1 - \frac{w_1}{w_2}}\right]$$

Equation 6

A PC value (PC_x) for a different region of interest can then be calculated based on gray and white matter PCs (Equations 5 and 6) and the fraction of white matter in the region of interest:

$$PC_x = F_g.PC_g + F_w.PC_w$$

Equation 7

This algorithm can be used to:

- Validate PC measurements for a chemical from multiple brain regions, by checking for consistency with white and gray matter fractions, if known.
- Check measured gray and white matter PC measurements (since gray and white matter are difficult to separate out, particularly from small brains), or estimate measured gray and white matter PC values directly.
- Estimate gray and white-matter percentages of different brain regions by back-calculating from measured gray/white matter PC values from (at least) two different chemicals. Additional chemicals can be used to check for consistency.
- Combine with predictions (such as the modified Schmitt (2008) model, see Ruark et al. (2014)) based on lipid/protein content of regions and gray and white matter, as a further consistency check.

Separate white and gray matter blood flows can also be used in brain kinetic models (both regional and whole-brain). In humans, cerebral spinal fluid for whole brain is 55 to 60 mL/100 g brain tissue/minute, gray matter is 55 mL/100 g brain tissue/minute, and white matter is 45 mL/100 g brain tissue/minute (Rengachary and Ellenbogen, 2005).

LIST OF ACRONYMS

ABR	auditory brainstem response
ATP	adenosine triphosphate
BCA	bicinchoninic acid
CAP	central auditory pathway
CAPD	central auditory processing dysfunction
$CHCl_3$	chloroform
DMEM	Dulbecco's modified Eagle's medium
DMSO	dimethyl sulfoxide
D-PBS	Dulbecco's phosphate buffered saline
DPOAE	distortion product otoacoustic emissions
F-344	Fischer 344
FBS	fetal bovine serum
FR	free radical
f_{ub}	fraction unbound in plasma
GABA	gamma-aminobutyric acid
GAT-3	GABA transporter 3
GC-FID	gas chromatography with a flame ionization detector
GSH	glutathione
HEI-OC1	House Ear Institute-Organ of Corti 1
IACUC	Institutional Animal Care and Use Committee
K_{ow}	octanol:water partition coefficient
MEM	minimal essential medium
MTS	(3-(4,5-dimethylthiazol-2-yl)-5-(3-carboxymethoxyphenyl)-2-(4-sulfophenyl)-2H-tetrazolium
NIHL	noise-induced hearing loss
NT	neurotransmitter
OEL	occupational exposure limit
PBPK	physiologically-based pharmacokinetic
PBS	phosphate buffered saline
PC	partition coefficient
PD	pharmacodynamic
PPUFAR	peroxy polyunsaturated fatty acid radical
PTFE	polytetrafluoroethylene
PUFAR	polyunsaturated fatty acid radical
QSPR	quantitative structure-property relationship
SD	standard deviation
SPL	sound pressure level
TWA	time weighted average
VDCC	voltage-dependent calcium channel
WPAFB	Wright-Patterson Air Force Base